

AN EXPERIMENTAL INVESTIGATION OF FREE CONVECTION
HEAT TRANSFER TO CARBON DIOXIDE IN THE REGION
OF ITS CRITICAL POINT

Thesis by
Karl K. Knapp

In Partial Fulfillment of the Requirements
For the Degree of
Doctor of Philosophy

California Institute of Technology
Pasadena, California

1965

(Submitted September 11, 1964)

ABSTRACT

Experimental results are presented for an investigation of free convection heat transfer to carbon dioxide in the region of its critical point. Shadowgraph images of the flow patterns accompanying the heat transfer have been recorded photographically. A horizontal 0.010-inch-diameter cylindrical Nichrome wire was used as the test section for the primary investigation. Tests were conducted in carbon dioxide with pressures from 1000 psia to 1500 psia and bulk temperatures from 49.0° to 137.0° F.

"Bubble-like" and oscillating flow conditions were observed in the experiments conducted with the cylindrical test section. The occurrence of "bubble-like" flow conditions, along with pronounced changes in the fluid properties, resulted in significant improvements in the heat transfer process, as compared to heat transfer resulting with laminar flow at lower heat fluxes. Additional experiments with a vertical wire and a horizontal strip indicated that the occurrence of the "bubble-like" flow depends on the shape and orientation of the heat transfer surface. The results of heat transfer with the "bubble-like" flow condition in supercritical carbon dioxide are compared with heat transfer results with boiling at subcritical pressures.

ACKNOWLEDGMENTS

My sincere thanks are extended to Professor R.H. Sabersky for his guidance, encouragement, and advice during the course of this research. I wish also to acknowledge the help afforded by Professor D. Morelli and Mr. H. Hartung in the design of the test apparatus.

Support for this research project provided by a National Science Foundation research grant and financial assistance offered the author by the Atomic Energy Commission's Special Fellowships in Nuclear Science and Engineering are most gratefully acknowledged.

My special appreciation is extended to Mrs. Ruth Toy and others on the California Institute of Technology staff for their generous donations of time and facilities.

TABLE OF CONTENTS

ABSTRACT	ii
ACKNOWLEDGMENTS	iii
LIST OF FIGURES	vi
LIST OF TABLES	xi
I INTRODUCTION	1
II FREE CONVECTION IN SUPERCRITICAL FLUIDS	12
A. Influence of Property Changes	12
B. Free Convection Experiments in Supercritical Fluids	18
III PROPERTIES OF SUPERCRITICAL CARBON DIOXIDE	23
A. Temperature-Dependent Properties	23
B. Property Variations with Heat Transfer	27
IV DESCRIPTION OF APPARATUS	29
A. General Description	29
B. Test Section	31
C. Test Chamber	34
D. Pressure and Temperature Control	36
E. Resistance-Measuring Bridge	39
F. Optical Flow Visualization	42
V EXPERIMENTAL PROCEDURES	43
A. Preparation	43
B. Test Procedure	46
C. Test Conditions	48

Contents (Continued)

VI	EXPERIMENTAL RESULTS	51
	A. Horizontal Wire in Supercritical Carbon Dioxide	51
	B. The Effect of Wire Diameter	57
	C. Horizontal Wire in Subcritical Carbon Dioxide	59
	D. Vertical Wire in Supercritical Carbon Dioxide	62
	E. Horizontal Strip in Supercritical Carbon Dioxide	65
VII	DISCUSSION OF EXPERIMENTAL RESULTS	68
	A. Laminar Free Convection in Supercritical Carbon Dioxide	68
	B. "Bubble-Like" Flow in Free Convection to Supercritical Carbon Dioxide	70
	C. Oscillating Flow Conditions in Free Convection to Supercritical Carbon Dioxide	79
VIII	SUMMARY AND CONCLUSIONS	82
	REFERENCES	85
	APPENDIX A PROPERTIES OF CARBON DIOXIDE	90
	APPENDIX B EXPERIMENTAL RESULTS	95
	APPENDIX C FLOW PATTERN PHOTOGRAPHS	116
	APPENDIX D APPARATUS	130
	APPENDIX E WHEATSTONE BRIDGE CIRCUIT	137
	APPENDIX F CALCULATIONS AND ERROR ANALYSIS	142
	APPENDIX G LIMIT CYCLE MODEL FOR OSCILLATING FLOW CONDITION	155
	APPENDIX H EXPERIMENTAL DATA	160

LIST OF FIGURES

Figure 1	Density of Carbon Dioxide	91
Figure 2	Thermal Conductivity of Carbon Dioxide	92
Figure 3	Dynamic Viscosity of Carbon Dioxide	93
Figure 4	Enthalpy of Carbon Dioxide	94
Figure 5	Free Convection Heat Transfer from a Horizontal Cylinder to Supercritical Carbon Dioxide at 1500 psia and 49.0 °F	96
Figure 6	Free Convection Heat Transfer from a Horizontal Cylinder to Supercritical Carbon Dioxide at 1300 psia and 49.0 °F	97
Figure 7	Free Convection Heat Transfer from a Horizontal Cylinder to Supercritical Carbon Dioxide at 1200 psia and 49.0 °F	98
Figure 8	Free Convection Heat Transfer from a Horizontal Cylinder to Supercritical Carbon Dioxide at 1100 psia and 49.0 °F	99
Figure 9	Free Convection Heat Transfer from a Horizontal Cylinder to Supercritical Carbon Dioxide at 1500 psia and 77.0 °F	100
Figure 10	Free Convection Heat Transfer from a Horizontal Cylinder to Supercritical Carbon Dioxide at 1300 psia and 77.0 °F	101
Figure 11	Free Convection Heat Transfer from a Horizontal Cylinder to Supercritical Carbon Dioxide at 1200 psia and 77.0 °F	102

Figures (Continued)

Figure 12	Free Convection Heat Transfer from a Horizontal Cylinder to Supercritical Carbon Dioxide at 1100 psia and 77.0 ^o F	103
Figure 13	Free Convection Heat Transfer from a Horizontal Cylinder to Supercritical Carbon Dioxide at 1500 psia and 107.0 ^o F	104
Figure 14	Free Convection Heat Transfer from a Horizontal Cylinder to Supercritical Carbon Dioxide at 1300 psia and 107.0 ^o F	105
Figure 15	Free Convection Heat Transfer from a Horizontal Cylinder to Supercritical Carbon Dioxide at 1200 psia and 107.0 ^o F	106
Figure 16	Free Convection Heat Transfer from a Horizontal Cylinder to Supercritical Carbon Dioxide at 1100 psia and 107.0 ^o F	107
Figure 17	Free Convection Heat Transfer from a Horizontal Cylinder to Supercritical Carbon Dioxide at 1500 psia and 137.0 ^o F	108
Figure 18	Free Convection Heat Transfer from a Horizontal Cylinder to Supercritical Carbon Dioxide at 1300 psia and 137.0 ^o F	109
Figure 19	Free Convection Heat Transfer from a Horizontal Cylinder to Supercritical Carbon Dioxide at 1200 psia and 137.0 ^o F	110
Figure 20	Film Boiling Heat Transfer from a Horizontal Cylinder to Subcritical Carbon Dioxide at 1000 psia, 49.0 ^o and 77.0 ^o F	111

Figures (Continued)

Figure 21	Free Convection Heat Transfer from a Vertical Cylinder to Supercritical Carbon Dioxide at 1200 psia and 77.0 ^o F	112
Figure 22	Free Convection Heat Transfer from a Horizontal Strip to Supercritical Carbon Dioxide at 1200 psia and 77.0 ^o F	113
Figure 23	Free Convection Heat Transfer from a Short Vertical Wall to Supercritical Carbon Dioxide at 1200 psia and 77.0 ^o F	114
Figure 24	The Influence of Wire Diameter and Heat Flux Rates on the Frequency of Flow Oscillations with Free Convection Heat Transfer to Supercritical Carbon Dioxide at 1300 psia and 77.0 ^o F	115
Figure 25	Laminar Free Convection from a Horizontal Cylinder in Supercritical Carbon Dioxide at 1200 psia and 77.0 ^o F	117
Figure 26	Oscillating Flow Condition with Free Convection from a Horizontal Cylinder in Supercritical Carbon Dioxide at 1200 psia and 77.0 ^o F	118
Figure 27	"Bubble-Like" Flow with Free Convection from a Horizontal Cylinder in Supercritical Carbon Dioxide at 1200 psia and 77.0 ^o F	119
Figure 28	"Bubble-Like" Flow with Free Convection from a Horizontal Cylinder in Supercritical Carbon Dioxide at 1200 psia and 77.0 ^o F	120

Figures (Continued)

Figure 29	"Bubble-Like" Flow with Free Convection from a Horizontal Cylinder in Supercritical Carbon Dioxide at 1500 psia and 49.0 ^o F	121
Figure 30	"Bubble-Like" Flow with Free Convection from a Horizontal Cylinder in Supercritical Carbon Dioxide at 1200 psia and 137.0 ^o F	122
Figure 31	"Bubble-Like" Flow with Free Convection from a Horizontal Cylinder in Supercritical Carbon Dioxide at 1200 psia and 77.0 ^o F	123
Figure 32	Film Boiling on a Horizontal Cylinder in Supercritical Carbon Dioxide at 1000 psia and 49.0 ^o F	124
Figure 33	Nucleate Boiling on a Horizontal Cylinder in Subcritical Carbon Dioxide	125
Figure 34	Free Convection along a Vertical Wire in Supercritical Carbon Dioxide at 1200 psia and 77.0 ^o F	126
Figure 35	Free Convection along a Vertical Wire in Supercritical Carbon Dioxide at 1200 psia and 77.0 ^o F	127
Figure 36	Free Convection from a Horizontal Strip in Supercritical Carbon Dioxide at 1200 psia and 77.0 ^o F	128

Figures (Concluded)

Figure 37	Free Convection from a Short Vertical Wall to Supercritical Carbon Dioxide at 1200 psia and 77.0 ^o F	129
Figure 38	Photographs of the Apparatus	
	A. Test Chamber, General View of Instrumentation	131
	B. Pressure Gauge and Gas Cylinders, Test Chamber on Optical Bench, Hydraulic Accumulator	132
Figure 39	Drawing of the Test Chamber	133
Figure 40	Schematic Drawing of the Apparatus	134
Figure 41	Schematic Drawing of the Shadowgraph Optics	135
Figure 42	Wheatstone Bridge Circuit	136

LIST OF TABLES

Table 1	Free Convection Heat Transfer Data for a Horizontal Cylinder in Supercritical Carbon Dioxide at 1500 psia and 49.0 ^o F	161
Table 2	Free Convection Heat Transfer Data for a Horizontal Cylinder in Supercritical Carbon Dioxide at 1300 psia and 49.0 ^o F	162
Table 3	Free Convection Heat Transfer Data for a Horizontal Cylinder in Supercritical Carbon Dioxide at 1200 psia and 49.0 ^o F	163
Table 4	Free Convection Heat Transfer Data for a Horizontal Cylinder in Supercritical Carbon Dioxide at 1100 psia and 49.0 ^o F	164
Table 5	Free Convection Heat Transfer Data for a Horizontal Cylinder in Supercritical Carbon Dioxide at 1500 psia and 77.0 ^o F	165
Table 6	Free Convection Heat Transfer Data for a Horizontal Cylinder in Supercritical Carbon Dioxide at 1300 psia and 77.0 ^o F	166
Table 7	Free Convection Heat Transfer Data for a Horizontal Cylinder in Supercritical Carbon Dioxide at 1200 psia and 77.0 ^o F	167
Table 8	Free Convection Heat Transfer Data for a Horizontal Cylinder in Supercritical Carbon Dioxide at 1100 psia and 77.0 ^o F	168
Table 9	Free Convection Heat Transfer Data for a Horizontal Cylinder in Supercritical Carbon Dioxide at 1500 psia and 107.0 ^o F	169

Tables (Concluded)

Table 10	Free Convection Heat Transfer Data for a Horizontal Cylinder in Supercritical Carbon Dioxide at 1300 psia and 107.0 ^o F	170
Table 11	Free Convection Heat Transfer Data for a Horizontal Cylinder in Supercritical Carbon Dioxide at 1200 psia and 107.0 ^o F	171
Table 12	Free Convection Heat Transfer Data for a Horizontal Cylinder in Supercritical Carbon Dioxide at 1100 psia and 107.0 ^o F	172
Table 13	Free Convection Heat Transfer Data for a Horizontal Cylinder in Supercritical Carbon Dioxide at 1500 psia and 137.0 ^o F	173
Table 14	Free Convection Heat Transfer Data for a Horizontal Cylinder in Supercritical Carbon Dioxide at 1300 psia and 137.0 ^o F	174
Table 15	Free Convection Heat Transfer Data for a Horizontal Cylinder in Supercritical Carbon Dioxide at 1200 psia and 137.0 ^o F	175
Table 16	Film Boiling Heat Transfer Data for a Horizontal Cylinder in Subcritical Carbon Dioxide at 1000 psia, 49.0 ^o and 77.0 ^o F	176
Table 17	Free Convection Heat Transfer Data for a Vertical Cylinder in Supercritical Carbon Dioxide at 1200 psia and 77.0 ^o F	177
Table 18	Free Convection Heat Transfer Data for a Horizontal Strip in Supercritical Carbon Dioxide at 1200 psia and 77.0 ^o F	178
Table 19	Free Convection Heat Transfer Data for a Short Vertical Wall in Supercritical Carbon Dioxide at 1200 psia and 77.0 ^o F	179

I INTRODUCTION

The process of heat transfer to fluids with highly temperature-dependent properties is becoming more important due to the increasing industrial use of fluids at supercritical pressures. Such fluids are used in a number of applications involving heat transfer: for example, nuclear power reactors, liquid propellant rocket motors, and high-pressure steam power plants. The case of heat transfer to a fluid at supercritical pressure is characterized mainly by the strong dependence of the fluid properties on temperature.

Critical state is defined first in terms of pressure: The critical pressure is that pressure above which the fluid cannot exist in a two-phase equilibrium. Second, critical state is defined in terms of temperature: The critical temperature is that temperature above which a fluid cannot be condensed by a change in pressure alone. Physically, the critical state is the upper limit--where the surface tension has diminished to zero--of the two-phase equilibrium region. Boiling, of the type experienced at subcritical fluid pressures, is not possible at pressures above the critical pressure.

Curves of the thermodynamic and transport properties of a fluid substance have inflections or singularities which are associated with the critical state. At pressures above the critical pressure the fluid shall be referred to as "supercritical." In general, this term will imply also that the temperature is at or below its critical value and thus bulk fluid properties are similar to those of a liquid at lower pressures.

Interest in the transfer of heat to a supercritical fluid was first expressed in Germany during the 1930's when Schmidt (1) proposed that the strong property changes--especially changes in density--accompanying temperature changes should enhance the effects of free convection. Since then, the efforts of Schmidt and his associates (2) have been concentrated primarily on the investigation of the equivalent conductivity of a tube of fluid, filled to critical density, which is heated at one end and cooled at the other. Their work has resulted in the successful design of gas turbine blades which are cooled internally by a supercritical fluid.

The major portion of the experimental investigations of heat transfer to supercritical fluids has been concerned with turbulent forced convection of fluids inside heated tubes. Dean and Thompson (3)

used nitrogen in heat transfer experiments conducted in an annular flow passage. Other investigators have used various fluids inside cylindrical tubes.¹

In several cases investigators have found that analytical results calculated on the basis of analyses by Goldmann (16) or Deissler (17) are in agreement with experimental heat transfer results if the fluid state conditions are relatively far removed from the critical state itself. Goldmann and Deissler, whose analyses are made on the basis of von Kármán's similarity theory, assume that, with variable fluid properties, the streamlines are basically the same as those for flow with constant fluid properties. In certain instances, however, these analyses do not predict, even approximately, the expected experimental results for the heat transfer process. Disagreement between the results of the analyses and the experiments occurs when the fluid states existing in the flow span the region of strong property changes near the critical temperature. Experimental results for heat transfer to fluids under this condition

¹For example, Bringer and Smith (4) used carbon dioxide, as did Koppel and Smith (5). Powell (6) used oxygen, nitrogen, and hydrogen; Dickinson and Welch (7) and Randall (8) used water; Del Bene and Barger (9) used Freon 12; Hines and Wolf (10) used

are as yet largely unexplained. There is a difference of opinion among workers in the field as to whether or not a change in the flow pattern occurs, or if the change in fluid properties can account for the observed results without postulating a change in streamlines. The large number of possible bulk state conditions and flow rates at the entrance to the heated tubes has prevented an accurate correlation of the data collected on experiments using different fluids in the supercritical region.

One of the more interesting investigations in this field was undertaken by Dean and Thompson (3) who studied heat transfer to nitrogen from a cylindrical heating element which formed the center of an annular flow passage. Dean and Thompson were able to compare the heat transfer to nitrogen at supercritical pressures with the heat transfer to nitrogen in the boiling region, with wide ranges of temperature differences in both cases. They found that, for the one flow rate and inlet bulk temperature used in their investigation, at large temperature differences heat transfer to the supercritical fluid was similar to heat transfer accomplished by film boiling.

RP-1 and diethylcyclohexane; Szetela (11) used hydrogen; Armand, Tarasova, and Conkov (12) and Miropolsky and Shitsman (13) used water; Petukhov, Krasnoschekov, and Protopopov (14) used carbon dioxide; Goldmann (15) also used water.

However, for any given temperature difference, the supercritical fluid transferred approximately twice as much heat as was transferred by film boiling. Their experimental data also indicate that, because of both this result and the observation that the heat flux to the supercritical fluid increased steadily with increasing wall temperature, higher heat flux rates were possible with supercritical nitrogen than were possible at subcritical pressures before the walls of the tube exceeded their melting temperatures.

Perhaps the best-known experimental results of heat transfer to a supercritical fluid flowing inside a heated tube are those of Dickinson and Welch (7) who investigated this problem using water inside an electrically heated tube. Their data, covering a very limited range of heat fluxes and flow rates and a wide range of bulk state conditions, show a distinct peak in the heat transfer coefficient when the wall temperature is near its critical point. This result corresponds to a strong increase in the heat flux as the temperature of the wall approaches the critical temperature, followed by a leveling off of the heat flux. Once the wall temperature exceeds the critical temperature, much larger increases in the temperature differences are required to increase the heat transfer rate. Heat transfer results predicted on the basis of Goldmann's

and Deissler's analyses exhibited from 20 to 100 percent variances from the actual experimental data. Disagreement was most marked when wall temperatures were near the critical temperature of the water: the analyses did not predict a peak in the heat transfer coefficient.

Recent data from an experimental investigation by Koppel and Smith (5) on heat transfer to supercritical carbon dioxide with forced convection inside an electrically heated tube indicate unusual axial variations in the heat transfer coefficient. These axial variations occurred with turbulent flow of carbon dioxide near its critical state when the temperature of the fluid entering the tube was below the critical temperature. Axial variations were found to depend on heat flux, wall temperature, and flow rate. Koppel and Smith observed that, when the carbon dioxide entering the tube was above the critical temperature, experimental results of heat transfer were similar to those of a constant property fluid and could be predicted on the basis of the analysis. The axial variations in the heat transfer coefficient became less predominant as the pressure was increased beyond the critical value.

The experience of other investigators, for instance, Powell (6) or Del Bene and Barger (9), confirms the general pattern of the experimental data: experimental results for conditions where the supercritical fluids pass through the region of strong property changes are very complicated and are usually not susceptible to prediction by existing methods. A summary of the results would seem to indicate that one or more of the following situations exists: (1) The analyses of Goldmann and Deissler do not adequately take into account the effect of property variations, although the streamlines of the flow are still substantially the same as are generally observed in the flow of fluids with constant properties. (2) The strong property variations, primarily changes in density, cause free convection, in addition to the forced convection, which noticeably affects the heat transfer. (3) The streamlines of the flow are significantly different from those in flows observed under conditions of negligible property changes.

These three explanations are not necessarily independent. The first explanation is difficult to assess, although it is definitely subject to the following criticism: The present analyses do predict accurately the experimental results for conditions where property changes vary moderately, such as in air or in a supercritical fluid

out of the region of strongest property changes; however, with strong property changes in a fluid near the critical state, predictions based on existing techniques not only differ in magnitude from the experimental results, but also fail to predict the trends of the experimental data.

The second explanation deserves serious consideration, particularly in experiments where the test section was mounted vertically, as in the work of Powell (6). Powell observed minimums in the heat transfer coefficient associated with the critical temperature for supercritical oxygen, nitrogen, and hydrogen. There are serious difficulties, of course, in analyzing the effects of strong buoyancy forces added to the turbulent flow of the forced convection.

The third explanation suggests that the property variations cause a fundamental change in the structure of the flow field, as does boiling at lower pressures. Goldmann (20) originally suggested the possibility of a "boiling-like" mechanism similar to nucleate boiling, with the growth and collapse of low-density regions near the heating surface aiding the transfer of heat. The possibility of boundary layer instabilities or similar changes in the structure of the flow has also been discussed by Goldmann. Steep gradients of

density, viscosity, and thermal conductivity, which must exist if the supercritical bulk fluid is below the critical temperature while the wall temperature is above the critical temperature, suggest that there are several types of mechanisms which might be responsible for flow instabilities.

The inability of present techniques to predict experimental results for the transfer of heat to supercritical fluids in the region of strong property changes points out the need to obtain additional information regarding the structure of the flows. It appears that additional attempts to analyze the heat transfer process will not be fruitful until there is a body of accurate empirical knowledge of the mechanisms of heat transfer and momentum transfer for this region.

Preliminary visual investigation by Griffith and Sabersky (18), using a Schlieren system to illuminate a heated horizontal wire immersed in supercritical Freon 114A, revealed the existence of a bubble-like flow pattern on the underside of the wire. The quantitative results of this free convection experiment do not show any marked effects associated with the bubble-like flow.

The primary purpose of the present investigation is to examine visually the flow conditions existing under the free convection of heat and mass in a supercritical fluid adjacent to a heated surface. In what must be considered the starting point in the exploration of the large number of flow situations possible for heat transfer to a supercritical fluid, both a photographic record of the flow conditions and a quantitative record of the heat transfer process are desired.

The particular case of heat transfer by free convection from heated horizontal bodies of finite height to an otherwise motionless fluid is selected for the following reasons: (1) If unusual flow conditions exist, bearing resemblance to any form of boiling, the presence of these flow conditions might be expected in free as well as in forced convection. (2) If the effects of strong free convection are responsible for a change in the quantitative heat transfer results for forced convection, then there must be a more thorough understanding of the free convection of heat to a supercritical fluid. The free convection heat transfer in a supercritical fluid is an interesting problem in itself, and a comparison of the results of this investigation with those of Griffith and Sabersky is desired. (3) The

resulting simplifications in the design of the test apparatus make it possible to optimize the clarity of the flow visualization and of the resulting photographs while simultaneously obtaining quantitative data on the heat transfer process.

Additional investigations are planned in the future for the forced convection of heat in a supercritical fluid past a heated wall, with visual observation of the thermal boundary layer. It is hoped that the experience gained from this free convection experiment with flow visualization techniques and in handling fluids at high pressures can be used to advantage in future forced convection experiments.

Carbon dioxide has been selected as the fluid medium for this investigation. The critical state of carbon dioxide occurs at an absolute pressure of 1071 psi and a temperature of 87.8^oF. Thermodynamic and transport properties of carbon dioxide in the supercritical region are among the best known of all fluids. In addition, carbon dioxide has a relatively stable molecular structure and is both nontoxic and noncorrosive.

II FREE CONVECTION IN SUPERCRITICAL FLUIDS

A. Influence of Property Changes

The unusually pronounced property value variations with temperature changes exhibited by a supercritical fluid in the region of its critical temperature may certainly be expected to have an influence on the free convection of heat in the critical region. One question which has arisen is whether or not the property variations will cause a fundamental change in the nature of the resulting flow patterns. In other words, will free convection heat transfer in a supercritical fluid from, for example, a heated vertical surface result in the same boundary layer type flow that we would expect in a fluid of nearly constant properties?

As first pointed out by Schmidt (1) the properties of a fluid in the region of its critical point are such that the effects of free convection may be expected to be especially strong. The primary factor leading to this conclusion is as follows: In the region of the critical temperature, the density of the fluid decreases rapidly with increasing temperature; this must result in large buoyancy forces, developed from relatively small temperature differences.

There is a correspondingly steep increase in the enthalpy of the fluid with increases in temperature; this should also increase the effectiveness of the free convection heat transfer. Less obvious are the effects of the variation of dynamic viscosity and thermal conductivity with temperature on the free convection heat transfer process.

In the case of a heated surface immersed in a supercritical fluid which has a below-critical bulk temperature, the magnitude of fluid properties some distance from the surface will be similar to the magnitude of properties of the liquid at subcritical pressures. The density, thermal conductivity, and dynamic viscosity are large compared with the vapor values. The state of the fluid in immediate contact with the heated surface will depend upon the surface temperature. If the surface temperature exceeds the critical temperature, then the density, conductivity, and viscosity of the fluid adjacent to the wall will be much smaller than that of the bulk fluid. The properties must vary continuously from the wall to the bulk conditions, depending upon the temperature profile within the fluid. In the absence of two separate phases and surface tension, ordinary boiling with a distinct interface between the liquid and vapor is not possible.

It may reasonably be expected that, in a large number of heat transfer situations involving a supercritical fluid, the flow will be similar to that expected for a constant property fluid. There is no general solution to the momentum and energy equations, even for laminar flow, which takes into account property variations of the complexity encountered in the critical region. Fritsch and Grosh (19) used a computer to integrate the steady two-dimensional boundary layer equations for the case of gravitational free convection from an isothermal, vertical wall to supercritical water, taking into account the variation of density and specific heat with temperature changes. Even to arrive at this solution required the selection of a reference temperature at which the viscosity and thermal conductivity were evaluated as constants. Fritsch and Grosh found that, if the results of the two extreme examples--wall temperature and bulk temperature--were compared, the selection of the reference temperature could cause differences of 10 to 75 percent in the quantitative heat transfer results. Fritsch and Grosh's final results, obtained using a mean film temperature to evaluate the viscosity and thermal conductivity, predict heat transfer coefficients which are 60 to 70 percent higher than those predicted by an analysis where all properties were selected at the reference temperature. Their analytical results

were in much closer agreement with experimental data than were the analytical results of the analysis with constant properties. It should be expected that a numerical integration of this type would give more accurate results than the constant property analysis whenever laminar free convection takes place in a supercritical fluid, although it would be desirable to eliminate the necessity of selecting a reference temperature altogether.

It has been suggested that the strong property variations which can occur in a supercritical fluid may lead to unusual flow conditions in place of those which would normally occur with a constant property fluid. The combination of unusually strong buoyant forces, together with pronounced changes in the density, viscosity, and conductivity within the boundary layer, presents the possibility of instabilities in the steady flow; this may result in unsteady flows other than the usual turbulent flows. There is the additional possibility that the property variations might cause a significant change in the structure of a turbulent flow. Goldmann (20) has suggested the possibility of unusual flows accompanying heat transfer to a supercritical fluid, placing particular emphasis on the concept of a "bubble-like" phenomenon.

Goldmann hypothesizes an "explosive" reduction in the density of the fluid as part of an unsteady flow phenomenon; this flow is one in which part of the denser bulk liquid touches a hot surface and suddenly acquires a large amount of energy. Goldmann compares this phenomenon to the formation of bubbles at subcritical pressures. Although his physical description may resemble that of an unsteady flow resulting from the transfer of heat to a supercritical fluid, the comparison with nucleate boiling must have limited validity as far as the heat transfer process is concerned. The surface tension is an extremely important factor in the high heat transfer coefficients observed under nucleate boiling conditions because a certain amount of superheating of the liquid adjacent to the heat transfer surface is required before nucleation can begin. Thus, in nucleate boiling there is a positive temperature difference between the superheated liquid near the heating surface and the vapor of the bubble at the saturation temperature. Conduction resulting from this temperature difference continues to supply the bubble with heat in excess of that conducted from the wall to the bubble. An increase in the surface tension increases the amount of superheating in the liquid which, in turn, increases the rate of bubble growth and the ultimate size of the bubble. In the case of supercritical pressures, the opposite is true.

Once part of the fluid near the wall becomes less dense, its temperature is greater than that of the surrounding fluid. Presumably, then, the conduction of heat in the fluid would tend to eliminate the low-density pocket. It is unlikely that the transfer of heat in this case would compare to that resulting from nucleate bubble agitation.

In examining the free convection flow resulting from heat transfer to a supercritical fluid it may also be fruitful to consider possible analogies with film boiling. In film boiling, at subcritical pressures, the heating surface is separated from the liquid by a distinct vapor film. A corresponding situation, without a distinct interface and surface tension, may occur with heat transfer to a supercritical fluid since the wire must be surrounded by a low-density layer of fluid. Waviness may occur in the region between this layer and the bulk fluid where the density increases similar to the waviness observed in certain instances at the edge of the vapor layer in film boiling.

Since there seems to be no a priori basis for predicting the nature of free convection flows in a supercritical fluid, experimental evidence is needed.

B. Free Convection Experiments in Supercritical Fluids

A very limited amount of literature has been published on experimental work with free convection in supercritical fluids. Schmidt (1) made some early measurements with supercritical ammonia in a closed circulation loop. Boggs and Holman (21) completed an experiment using Freon 12 in the same type of closed system. In both of these investigations, large fluctuations in temperature and pressure were observed during and after heat transfer through the loop when the bulk state conditions were very near the critical state. However, there is considerable uncertainty regarding the reason for these unsteady phenomena. In some cases, the fluid may have been at subcritical pressures in part of the loop, and in general these phenomena seem to have been associated with the closed loop configuration.

Schmidt (2) has also completed experiments on the equivalent conductivity of cylindrical cavities filled with various fluids near their critical states. The flow conditions and heat transfers in experiments of this type presumably depend very heavily on the exact geometry of the interior of the vessel as well as upon the nature of the properties. Schmidt's investigation included study of the effects of orientation in the gravitational field and of the effects of

subdividing the vessels on the heat transfer process.

Bonilla and Sigel (22) investigated free convection from a heated horizontal surface located at the bottom of a pool of n-pentane at pressures above and below the critical pressure. Their experiments were done at bulk temperatures 200° to 300° F below the critical temperature of n-pentane. For wall temperatures below the critical temperature they found the data satisfactorily correlated by expressing the Nusselt number in terms of the Raleigh number to the one-third power. When the wall temperature of the heated horizontal plate was near or above the critical temperature, so that large property differences existed between the wall and the bulk conditions, a limiting value on the Nusselt number of about 1300 was observed. This value was based on the pool diameter and on an average film temperature used to evaluate all of the property values except the change in density, which was calculated directly from the wall and bulk temperatures. Although no attempt was made to measure or visualize the flow, the investigators felt that the limiting value of the Nusselt number must correspond to a new flow regime which limited any further increase in the heat transfer coefficient.

Technical papers have been published describing two experiments on free convection from heated small, round, horizontal cylinders to supercritical fluids. Doughty and Drake (23) investigated the heat transfer from a 0.010-inch platinum wire to supercritical Freon 12 at bulk fluid temperatures near and above the critical temperature. Their results, which did not include any visualization or measurements of the flow, showed high heat transfer coefficients for bulk state conditions near the critical point. They did not publish any heat transfer data for supercritical fluid state conditions where the bulk temperature was below the critical temperature. Therefore, from their published data it is not possible to determine whether or not the high heat transfer coefficients would have occurred with heat transfer to the supercritical fluid at temperatures below the critical temperature. In general, the rates of heat transfer to the supercritical fluid were always at least twice those to the subcritical vapor for any given temperature difference. For temperature differences of about 8°F , the heat transfer rate to the fluid near the critical state was as much as 10 times higher than that to the subcritical vapor.

Griffith and Sabersky (18) investigated the heat transfer from a 0.010-inch Nichrome wire to Freon 114A over a somewhat wider range of bulk fluid pressures and temperatures. They used a Schlieren optical apparatus to visualize the flow conditions resulting from the heat transfer and discovered the existence of "bubble-like" activity on the surface of the wire. This particular flow condition occurred at moderately high heat fluxes and at supercritical pressures when the bulk fluid temperature was below the critical temperature. Their quantitative data did not demonstrate any abrupt increase in the heat transfer rate associated with this phenomenon. The heat flux and temperature differences were considerably larger than those used in the experiments of Doughty and Drake.

Recently Simon and Eckert (24) have published the results of some experiments with laminar free convection from a heated vertical plate to carbon dioxide at the critical state. They used a Zehnder-Mach interferometer to study the heat transfer process in detail for very small temperature differences and very small heat fluxes. The small temperature differences kept their experimental fluid at essentially constant property values. This optimized the use of interferometry and the comparison of experimental results with analytic

solutions but eliminated the feature of heat transfer to a supercritical fluid which is of interest here: the pronounced property changes associated with finite temperature differences.

Fritsch and Grosh (25) have published experimental results for the free convection from a vertical flat plate to supercritical water under conditions similar to those used in the previously mentioned computer analysis. In the laminar region investigated they found there was a systematic difference of approximately 20 percent between the results of their experiments and the results of their analyses. Provisions were made for some visual observations of the flow. The flow remained laminar in this investigation, which included temperature differences up to 24^oF.

III PROPERTIES OF SUPERCRITICAL CARBON DIOXIDE

A. Temperature-Dependent Properties

Fluids at supercritical pressures exhibit very pronounced property changes which occur with variations in temperature when the fluids are near their critical temperatures. At lower temperatures, a supercritical fluid has property values which are similar in magnitude to those of a liquid at subcritical pressures. At temperatures above its critical temperature, a supercritical fluid has properties much like those exhibited by vapor at subcritical pressures. If the pressure remains constant as the temperature of a supercritical fluid is increased past its critical temperature, then the properties of the fluid undergo pronounced changes; these changes do not include a change of phase in the thermodynamic sense. Surface tension and two separate phases are not present in fluids at supercritical pressures.

The property values for the density, dynamic viscosity, thermal conductivity, and enthalpy of carbon dioxide are shown in Figures 1 through 4 in Appendix A. These property values have been plotted against temperature for each of the five pressures used in this

investigation: 1000, 1100, 1200, 1300, and 1500 psia. The critical pressure of carbon dioxide is 1071 psia; the critical temperature is 87.8^oF.

Property variations in carbon dioxide at supercritical pressures exhibit considerable resemblance to those which accompany a change of phase at the subcritical pressure of 1000 psia. The subcritical phase change occurs at a particular temperature value-- the saturation temperature corresponding to the prevailing fluid pressure. At supercritical pressures, on the other hand, similar changes in the fluid properties are brought about by a finite temperature change occurring in the region of the critical temperature. A plot of density versus temperature, for example, shows that, if the carbon dioxide is at its critical pressure, the steepest part of the property value curve occurs when the fluid temperature is at the critical temperature. At a higher fluid pressure the steepest part of the property value curve occurs when the fluid temperature is at a slightly higher temperature, called the transposed critical temperature.

The property variations which accompany finite changes in temperature can be quite large. For instance, the density of carbon dioxide at the supercritical pressure of 1100 psia changes from 48 lb/ft³ at 76^oF to 16 lb/ft³ at 98^oF, dropping to one-third its initial value with a temperature increase of 22^oF. At similar pressure and temperatures, the values of dynamic viscosity and thermal conductivity also decrease sharply with increases in temperature. The viscosity and conductivity reach minimum values at a temperature slightly above the critical temperature; with further increases in temperature, viscosity and conductivity then slowly increase in value, as do the viscosity and conductivity of a vapor. The enthalpy of supercritical carbon dioxide increases sharply in the vicinity of the critical temperature; this increase corresponds to a peak in the specific heat of the fluid. At subcritical pressures there is a step increase in the enthalpy of the fluid as it changes from a liquid to a vapor which is equal to the latent heat of vaporization. The supercritical fluid exhibits an equivalent change in enthalpy over a small range of temperature.

Density values of carbon dioxide, presented in Figure 1, were obtained from the measurements of Michels and Michels (26) and from

the measurements of Michels, Blaisse, and Michels (27). The values for the thermal conductivity, presented in Figure 2, have been taken from the recent measurements of Michels, Sengers, and Van Der Gulick (28). The dynamic viscosity values presented in Figure 3 are taken from the measurements of Michels, Botzen, and Schuurman (29). The values for the enthalpy of carbon dioxide, presented in Figure 4, were obtained from the measurements made by Koppel and Smith (30). Supplementary values for each of these fluid properties at temperatures and pressures far above or below the critical point were obtained from the tabulations of the National Bureau of Standards (31).

B. Property Variations with Heat Transfer

Heat transfer by free or forced convection is accompanied by differences between the heat transfer surface temperature and the bulk fluid temperature. Thus, there is a temperature gradient, as well as a velocity gradient, in the vicinity of the heating surface. Such temperature gradients in a supercritical fluid can lead to large gradients in the fluid property values in the same region next to the heating surface.

Consider, for example, a heated solid body immersed in a fluid maintained at a supercritical pressure and a subcritical temperature. If the heat transfer surface is heated until it exceeds the fluid's critical temperature, then the density, for example, of the fluid near the heat transfer surface must be very low. A density gradient would then exist between the fluid at the heat transfer surface and the denser fluid some distance away from the heat transfer surface. Similarly, the other property values would vary according to the temperature profile. If the temperatures of the heat transfer surface and the bulk fluid are both below the critical temperature, the property gradients will be less pronounced. A similar condition occurs when the bulk fluid temperature is above the critical

temperature. In any case, the most pronounced effects of property variations should be expected when the temperature difference spans the transposed critical temperature.

The purpose of this investigation is to discover if this complicated situation, involving gradients of velocity, temperature, and fluid properties, has unusual effects on the flow and heat transfer which results with free convection from heated horizontal bodies in supercritical carbon dioxide.

IV DESCRIPTION OF APPARATUS

A. General Description

The apparatus used in conducting heat transfer experiments is designed to implement the following main objectives: (1) Visual observation of the free convection flow resulting from the transfer of heat to supercritical carbon dioxide from small, electrically heated, horizontal cylinders and strips. (2) Determination of the temperature differences between the heated wires and the bulk fluids. (3) Determination of the rate of heat transfer in order to compare quantitative data on the heat transfer process with corresponding photographic records made of the free convection flow.

The test chamber is so designed that the wires used as test sections can be secured in a horizontal position in the center of a cylindrical chamber. The test sections are parallel to glass windows at each end of the chamber. The optical flow visualization apparatus reproduces an enlarged Schlieren or shadowgraph image of the flow at the test section. Light for the flow visualization is supplied by a high-intensity Osram mercury vapor lamp. The flow visualization optics have been designed to enhance visual observation of the flow: patterns can be either photographed or projected directly onto a screen.

Through use of a free-piston hydraulic accumulator and pressurized cylinders of nitrogen gas, provisions are made for establishing and maintaining supercritical, as well as subcritical, carbon dioxide pressures in the test chamber. A precision Bourdon tube gauge measures the fluid bulk pressure. Also included as part of the test apparatus is a simple heat exchanger system, constructed to establish bulk fluid temperatures above or below room temperature. The test chamber design also includes a thermocouple probe immersed near the test section to measure the bulk fluid temperature. As the heat transfer surface is heated, a direct-current Wheatstone bridge measures change of resistance of the surface. Nichrome and Chromax wires and strips are used for the heat transfer surface.

Photographs of the apparatus appear as Figure 38; detailed illustrations appear as Figures 39 through 42 in Appendix D.

B. Test Section

Several requirements influence the selection of the material and the size of material needed for use as the heat transfer test section. Uniform dimensions and smooth surface conditions across the length of the test section are desired. The material must also have a high melting temperature and it must be chemically stable in the experimental environment. Limits on the amount of direct electrical current available in the laboratory indicated that, in order to obtain moderate heat fluxes, a material is required which has a high ratio of resistance to surface area. The method used to determine the surface temperature of the heated test section dictates that the test section material selected have a relatively large temperature coefficient of electrical resistivity. Nichrome and Chromax, nichel-chrome alloys produced by the Driver-Harris Company, have been selected as exhibiting those properties suited for use in this experimental application.

Round Nichrome wire, with a diameter of 0.010 inch, has been selected for use in the major portion of this investigation. A Chromax strip 0.001 inch thick and 0.125 inch wide is employed in a portion of the investigation and is used in two positions--as a horizontal

flat plate and as a short vertical wall. Nichrome and Chromel wires with diameters of 0.006 inch and 0.016 inch were also used in supplementary tests. In all tests, the total test section length is approximately 2.1 inches.

Initial investigations have revealed that use of randomly selected wire samples results in considerable variations in the experimental results. Close examination of the wires under a microscope indicates there exist significant variations in both smoothness and cleanliness of the wire surfaces. A careful procedure has subsequently been developed for the selection and preparation of the test sections. Initial investigations have also shown that annealing the test section helps to stabilize the resistance-measuring bridge circuit.

The first step in the preparation of the test sections is to select lengths of the wire or strip from a spool of the material. With the aid of a three-dimensional metallurgical microscope, visual examinations are made of the surface conditions of the samples. Wire samples with obvious surface imperfections are discarded. The samples are then degreased in a potassium hydroxide solution and rinsed with distilled water. Next the wire samples are annealed for 4 hours in a vacuum furnace at a temperature of 500^oF and cooled overnight at

furnace rates. During the heating process, the absolute pressure in the vacuum furnace is kept below 0.5μ of mercury and the resulting surface is bright and clean. As an additional precaution, the wires are immersed in a methyl-alcohol-bath ultrasonic cleaning apparatus.

After the sample preparation process is completed, the wire samples are again examined under a microscope. Samples exhibiting the most uniform surface conditions are selected for use as test sections in the experiments.

C. Test Chamber

The test chamber, specifically designed and constructed for conducting experiments involving free convection of heat to supercritical carbon dioxide, is built to safely contain noncorrosive fluids at pressures up to 1500 psia and temperatures up to 200^oF. The chamber itself is machined from mild steel and plated with cadmium. A photograph of the finished chamber appears in the Appendix as Figure 38; a drawing of the chamber construction appears as Figure 39.

The interior of the chamber forms a cylindrical volume 4.5 inches in diameter and 3.0 inches in length. At each end of the cylindrical cavity are windows of crown borosilicate glass which provide a circular field of vision 1.2 inches in diameter through the center of the chamber. These windows, each 1.5 inches thick, protrude into the cylindrical interior so that the total distance between the two inside walls of the windows is 2.0 inches.

Test sections are held in position in the center of the chamber, perpendicular to the optical path, between two electrodes extending through the walls to provide external electrical connections. These electrodes, machined from copper rod, provide pinch clamps for the

electrical and mechanical connection at each end of the test section. Micarta insulators and "o-ring" seals isolate the electrodes from the steel chamber.

By dismantling a single external clamp, one end of the chamber can be removed to facilitate the replacement of the test section. Provisions have been made for hydraulic connections and for use of a single thermocouple probe used to measure the bulk fluid temperature. Windows, electrodes, and the removable chamber end are all sealed with "o-ring" seals.

D. Pressure and Temperature Control

A free-piston hydraulic accumulator is included as part of the apparatus to allow pressurization without contamination of the carbon dioxide. The test chamber and one side of the hydraulic accumulator are first purged and filled with saturated carbon dioxide from a cylinder of carbon dioxide. After the valve on the cylinder of carbon dioxide is closed, the other side of the accumulator can be filled with nitrogen gas at the pressure desired for the test. The nitrogen side of the accumulator is connected to a cylinder of nitrogen gas, maintained at the desired test pressure. In this way, small changes in the total volume of the carbon dioxide during a test have negligible effect on the pressure in the test chamber.

A 12-inch Bourdon tube gauge with a 1500-psia full-scale deflection is used to measure carbon dioxide pressure in the test chamber. This gauge, manufactured by the Heise Bourdon Tube Company, has a calibrated accuracy of with 0.1% of full-scale deflection.

Stainless steel tubing connects the hydraulic accumulator with both the test chamber and the carbon dioxide cylinder. Teflon packing is used in the single valve between the accumulator and the test chamber. Prior to filling the apparatus with carbon dioxide, the

entire apparatus is cleaned with Cineclene, a commercial degreasing solvent. To remove all air before filling with carbon dioxide for the experiments, the apparatus is thoroughly purged with carbon dioxide.

Before conducting the heat transfer experiments, the desired temperature of the test chamber and of the carbon dioxide inside the chamber is attained by forcing water through several turns of copper tubing wound around the chamber exterior. Water temperature can be controlled by adjusting the flow rate through a heat exchanger immersed either in ice water or in heated water. The test chamber is wrapped with fiber glass insulation in order to reduce the heat transfer between the test chamber and the room.

The temperature control system is used to balance the rate of heat transfer to the test chamber during the experiments so that variations in the bulk temperature of the carbon dioxide are minimized. Tests are temporarily stopped whenever the bulk temperature, measured by a probe $\frac{1}{4}$ inch below the test section, varies more than 0.1°F from the desired temperature. Measurements are resumed when the bulk temperature has been restored to the desired test temperature.

Two copper-constantin thermocouples in series are used in the bulk temperature measurement mentioned above. One thermocouple junction is positioned at the end of a slender probe protruding from a sealed opening in the chamber bottom into the test chamber up to a point just below the test section. A second thermocouple junction is immersed in a distilled ice water bath maintained at 32.0°F . A Leeds and Northrup thermocouple potentiometer, Model 8686, is used to measure the thermocouple emf. Before installation, the thermocouple probe and the above-mentioned potentiometer have been calibrated with ASTM precision thermometers in different constant-temperature baths.

E. Resistance-Measuring Bridge

The most difficult measurement in this investigation is the determination of the heat transfer surface temperature. In view of the small dimensions of the electrically heated test section, a thermocouple is not suitable for direct measurement of the surface temperature. It was therefore decided to use a test section material that changed resistance in relation to temperature and to measure this change of resistance simultaneous with heating of the test section.

In order to measure the change of resistance of the test section, a Wheatstone bridge has been constructed, as shown in Figure 42, using the test section as one resistance leg. Three other legs each of equal resistance, made of manganin wire, are immersed in 20 liters of nonconducting transformer oil. These three manganin resistance legs are constructed in such a way that their changes of temperature and, particularly, their changes in resistance, are negligible compared to changes of resistance and temperature of the test section. In the case of the 0.010-inch-diameter Nichrome wire test section, the total surface area of each manganin resistance leg is 80 times the area of the Nichrome test section. The temperature coefficient of electrical resistivity for manganin at and slightly above room temperature is less than 1/100th that of Nichrome.

A variable resistor is connected across one of the external resistance legs so that resistance ratios of the legs of the Wheatstone bridge could be equalized when the test section and the carbon dioxide in the test chamber are at the same temperature. A direct electrical current source is connected to opposite ends of the Wheatstone bridge. As the heat flux (proportional to the square of the current) increases, the temperature of the test section increases, changing the resistance of the test section and unbalancing the Wheatstone bridge voltage. The voltage imbalance was measured across the center of the Wheatstone bridge with a Leeds and Northrup Speedomax self-balancing potentiometer and a precision potential divider, manufactured by the W.G. Pye Co. of Great Britain.

The direct-current electricity is supplied by a 120-volt source in the laboratory. Current is controlled with two large variable rheostats in series and measured with a Weston Model 931 ammeter. The heat flux at the test section is calculated taking into account the known dimensions of the test section, the test section resistance, and half of the total current through the Wheatstone bridge. The change of resistance of the test section is calculated using the

total current and voltage imbalance across the Wheatstone bridge, as shown in the circuit analysis presented in Appendix E.

The change of resistance of the test section material in relation to change in temperature has been measured in a separate calibration experiment using an E.S.I. Model 250-C1 impedance bridge connected to a length of test section material prepared in the same manner as are the wire samples used in this experiment. The wire sample, together with ASTM precision thermometers, is placed in a bath of nonconducting transformer oil. The temperature of the oil bath is slowly varied and the resistance versus temperature relationship for the material is recorded. The results of this calibration show that, for the Nichrome 0.010-inch-diameter wire, the change in resistance is linear in relation to temperature change for temperatures up to 400^oF. The equivalent coefficient of resistivity, as based on an initial resistance at 77.0^oF, is found to be 0.0000825 per ^oF.

F. Optical Flow Visualization

The test chamber is mounted on an optical bench, as shown in Figure 38. A schematic diagram of the optical system is presented as Figure 41. This system, designed to produce either a shadowgraph or a Schlieren image of the flow near the test section, is illuminated by an Osram Model HBO short-arc super-pressure mercury vapor lamp. Two achromatic objective lenses with 18-inch focal lengths, a single condensing lens, and two variable slits have also been included as part of the flow visualization apparatus.

It is possible to focus the image either directly on a screen or directly on the plane of film in a camera. The projected image of the test section is magnified by a factor of approximately 10. Photographic records have been made with a Speed Graphic camera, without lens, using the focal plane shutter at 1/1000 of a second and using Polaroid 3000 Speed film.

V EXPERIMENTAL PROCEDURES

A. Preparation

The wire or strip to be used in the test section is first selected, cleaned, and annealed as discussed in Section IV. After the interior of the test chamber has been degreased and the optical windows cleaned, the test section material is cut to length and clamped in position between the two electrodes within the chamber. Two copper blocks used as clamps in each electrode have been polished previously, and care is taken to see that their edges are parallel after the test section has been secured. After the test section is installed, one of the electrodes is withdrawn slightly by tightening an external nut so that the test section is pulled straight, but not stretched.

The end of the test chamber is then installed and the chamber is thoroughly purged with carbon dioxide. The hydraulic accumulator and the test chamber are filled with carbon dioxide from a siphon cylinder holding the fluid in a saturated state (approximately 900 psi at room temperature). After the cylinder valve has been closed, the opposite side of the hydraulic accumulator is filled with nitrogen gas until the pressure of the entire system reaches the value desired for the test. The nitrogen side of the accumulator is connected to an extra cylinder of nitrogen maintained at the pressure desired for the test. Measurable

changes in the pressure of the system are eliminated by adding or removing nitrogen gas.

The desired bulk temperatures are established before a test by flowing water from the temperature control system through the external copper coils wound around the test chamber. For experiments to be conducted at temperatures above room temperature, the water in the heat exchanger is heated with a thermostated electrical immersion heater; for experiments to be conducted at lower temperatures, the heat exchanger is filled with crushed ice. Fine adjustments in the water temperature are made with a mixing valve that combines the water flowing through the heat exchanger with water at room temperature. Because of the small size of the stainless steel tubing connecting the test chamber to the hydraulic accumulator (1/8-inch internal diameter and 3-foot length), it is not necessary to control the temperature of the fluid in the accumulator. When the experiments involve temperatures below the prevailing room temperatures, dry nitrogen gas can be released near the exterior of the optical windows to prevent the condensation of water from the air in the laboratory.

In the preparation of photographic records of the flow patterns, the Osram mercury vapor lamp is started and the optics adjusted so that a clear image is focused on the plane of the film. Preliminary investigations with both Schlieren and shadowgraph techniques have indicated that the shadowgraph optics result in the clearest image for the flow patterns encountered in the supercritical region and also for nucleate boiling at subcritical pressures. For this reason, in the investigations with carbon dioxide, shadowgraph techniques have been used exclusively.

B. Test Procedure

The test procedure is separated into two parts. Since the necessity of continually re-establishing the desired bulk temperature makes it impractical to record both types of data at once, the quantitative data and the flow pattern photographs are taken on separate occasions.

Once the desired test pressure and bulk temperature are established inside the test chamber, a small electrical current (see Appendix E) is passed through the Wheatstone bridge circuit. The external balancing resistor is then adjusted until the deflection of a micro-voltmeter across the center of the bridge is null. In this way, the ratios of the two resistance legs on each side of the Wheatstone bridge are equalized when the test section temperature equals that of the carbon dioxide. After checking to confirm that the temperature and pressure remain at the desired values, the electrical current is switched on and the rheostats adjusted until a predetermined current through the test section is established. The voltage imbalance across the Wheatstone bridge is shown on the self-balancing millivolt potentiometer and is recorded along with the electrical current reading. The rheostats are then readjusted to the next electrical current setting.

Two to four electrical current settings can be established and the data recorded before the bulk temperature moves $\pm 0.1^{\circ}\text{F}$ from the desired test temperature. The tests are then temporarily interrupted until the test temperature in the chamber can be re-established. At this time, the balance of the Wheatstone bridge is rechecked before additional data are recorded.

Photographs of the shadowgraph images are taken according to a similar procedure, except that the current through the test section is switched off between each photograph so that secondary motions in the test chamber are minimized. The focal plane shutter is set to produce a 1/1000 of a second exposure time. During the film exposure, all lights in the laboratory, with the exception of the mercury vapor lamp, are switched off.

C. Test Conditions

The test section selected for the major part of the investigation is a 0.010-inch-diameter Nichrome wire. Quantitative and qualitative data for this test section, when secured in a horizontal position, have been recorded at 15 different carbon dioxide state conditions in the supercritical region of the carbon dioxide. Data also have been taken with the same test section geometry in two subcritical carbon dioxide state conditions. At bulk carbon dioxide pressures of 1200, 1300, and 1500 psia, tests have been conducted at bulk temperatures of 49.0^o, 77.0^o, 107.0^o, and 137.0^oF. At a pressure of 1100 psia, tests have been conducted at temperatures of 49.0^o, 77.0^o, and 107.0^oF. At a subcritical pressure of 1000 psia, tests have been conducted at temperatures of 49.0^o and 77.0^oF. Quantitative data have been recorded for experiments conducted with electrical currents in the test section measuring 0.51, 1.00, 1.50, and 1.75 amperes and at electrical currents from 2.00 to 5.00 amperes at 0.10-ampere intervals. The maximum electrical current of 5.0 amperes corresponds to a test section heat flux of approximately 0.44 btu/in²/sec. Whenever the data indicate that the temperature of the wire has exceeded 500^oF, the test is stopped at a current less than 5 amperes. This precaution is taken to eliminate any possibility of

overheating the test section. Two complete tests have been made on different occasions for each bulk state condition.

Photographs of the flow conditions near the 0.010-inch-diameter Nichrome wire have been taken for each bulk state condition with currents which correspond approximately to heat fluxes of 0.05, 0.10, 0.15, 0.20, 0.30, and 0.40 btu/in²/sec. In particularly interesting cases, additional photographs have been taken.

In two tests conducted at a pressure of 1200 psia and a temperature of 77.0^oF, the test chamber has been rotated 90^o so that the length of wire assumes a vertical position. Quantitative data and photographs of the flow have been recorded for this situation.

Two other horizontal cylindrical wires with diameters of 0.016 inch and 0.006 inch, respectively, have been also used as test sections in the chamber. Although no attempt has been made to measure the temperature of these wires, the flow conditions for both wires were investigated and recorded photographically at bulk carbon dioxide pressures of 1100, 1200, and 1300 psia and at a single bulk temperature of 77.0^oF.

Additional quantitative measurements of the heat transfer to supercritical carbon dioxide have been made with a 0.001- by 0.125-inch Chromax strip held between the test chamber electrodes. Tests were conducted with the Chromax strip at one bulk carbon dioxide state condition of 1200 psia and 77.0^o F with two different orientations of the strip: Two tests were conducted with the strip positioned parallel to the horizontal plane; two additional tests were conducted with the electrodes rotated 90^o so that the test strip formed a 0.125-inch-high vertical wall.

VI EXPERIMENTAL RESULTS

A. Horizontal Wire in Supercritical Carbon Dioxide

Included in Appendix H are the data for experiments conducted with a 0.010-inch-diameter Nichrome wire test section mounted in a horizontal position. The quantitative results of these experiments are presented, as plots of heat flux versus the temperature difference between the wire and the bulk carbon dioxide, in Figures 5 through 20 in Appendix B. Photographs of shadowgraph images of typical flow patterns accompanying the heat transfer are shown as Figures 25 through 30 in Appendix C.

In the range of bulk state conditions used in this investigation, the results of experiments conducted in supercritical carbon dioxide are similar whenever the bulk temperature of the carbon dioxide is below the level at which strong property changes occur. As shown in the quantitative results and photographs (see Figure 25) taken at wire surface temperatures up to a maximum of between 180°F and 200°F , laminar flow is present at the wire and for some distance above the wire. In this laminar flow region, the slope of the heat flux versus temperature difference curve decreases with increasing

heat flux. It should be noted that the maximum temperature differences observed coincident with laminar flow correspond to wire surface temperatures which are approximately 100°F above the critical temperature. Maximum heat fluxes occurring with laminar flow depend upon the bulk state conditions, and range from 0.060 to 0.120 Btu/in.²-sec.

At slightly higher heat fluxes and corresponding temperature differences, laminar flow is replaced by an unusual flow condition in which the flow oscillates with an irregular periodicity between two distinct flow patterns. The average frequency of this fluctuation varies between 20 to 250 cycles per minute, depending on the bulk state conditions and the average heat flux through the wire surface. As shown in Figure 26, one of these two flow patterns appears to be the same as the laminar flow pattern occurring at lower heat fluxes. The other of these two flow patterns, also shown in Figure 26, appears to be identical to the "bubble-like" flow pattern observed at higher heat fluxes. Variation of the wire temperature accompanies the oscillating flow patterns, as indicated by the instruments used to measure the wire temperature. For this oscillating flow condition, data corresponding to the average wire temperature have been recorded and the quantitative results show a rapid increase in the heat flux for

very small variations in the temperature difference. This oscillating flow is observed for heat flux values ranging from 0.040 to 0.080 Btu/in.²-sec above the maximum heat fluxes where laminar flow occurs alone.

To confirm that the existence of these unusual flow conditions is associated with the heat transfer process rather than with the Wheatstone bridge circuitry employed in measuring the wire temperature, the entire circuitry and associated measuring instruments have been removed and direct current supplied to the test section alone. The oscillating flow conditions are again observed.

With an additional increase in the heat flux, the oscillating flow condition is replaced by a single flow pattern (see Figure 27), visually identified by characteristic "bubble-like" forms along the underside of the wire and by a turbulent flow rising above the wire. This latter flow obscures further observation of flow conditions at the top of the wire. Although less distinct than the bubbles of nucleate boiling at subcritical pressures, the pockets of low-density fluid along the underside of the wire appear to fluctuate in size and position. High-speed motion pictures (approximately 2500 frames per minute) taken of this unsteady flow condition show that the lack

of distinct interfaces at the edges of these "bubble-like" forms makes it difficult to identify single "bubbles" and to study their behavior with time. The dimensions of these "bubble-like" forms are two to three times larger than those of the nucleate bubbles observed at subcritical pressures.

The quantitative results obtained from experiments conducted with "bubble-like" flow are usually distinguished by three characteristics. First, at the heat flux level where the oscillating flow condition ends and the "bubble-like" flow begins, there is often a range of heat fluxes where, on different occasions, either flow condition can be observed, depending primarily upon whether the heat flux is being increased or decreased at the time of the test. In such cases the "bubble-like" flow is accompanied by wire temperatures which are lower than the average wire temperature measured coincident with occurrence of oscillating flow. For this reason, it is not unusual to observe a decrease in the average wire temperature concurrent with an increase in heat flux as the flow conditions change from oscillating to "bubble-like." Second, for a low heat flux range at the beginning of the "bubble-like" flow condition, the wire temperature increases very slowly, resulting in a steep curve of the heat flux versus

temperature difference. This steep initial slope of the heat transfer curve occurs mainly in the results of tests with carbon dioxide pressures of 1300 and 1500 psia. Third, for higher heat fluxes and temperature differences, the slope of the heat transfer curve decreases until there is a nearly direct proportionality between the heat flux and the temperature difference. These conditions have been measured for heat fluxes up to $0.44 \text{ Btu/in.}^2\text{-sec}$ and for temperature differences up to 450°F . Spot calculations show that the temperature difference continues to be approximately proportional to the heat flux at higher heat flux rates. Preliminary investigations have shown no changes in the basic flow patterns up to the point of mechanical failure resulting from melting of the wire.

Several of the experiments conducted with the Nichrome wire mounted in a horizontal position have been carried out at bulk temperatures above the transposed critical temperature where the strong property changes occur. See, for example, Figures 19 and 30. In each of these cases, laminar flow exists only at heat fluxes below $0.040 \text{ Btu/in.}^2\text{-sec}$ and the relationship between heat flux and temperature difference for laminar flow is approximately linear. These heat transfer conditions correspond to free convection of heat

to a gas, with fluid property changes between the wall and bulk state conditions which are much less pronounced than those changes occurring in the previously discussed experiments at lower bulk temperatures. These present experimental results differ somewhat from results obtained in tests conducted at bulk temperatures below the transposed critical temperatures. The primary difference appears in the magnitude of the quantitative results: the heat transfer rates associated with any particular temperature difference are only about half those recorded for the denser bulk state conditions. In addition, the oscillating flow does not appear. The laminar flow region is limited to a smaller range of heat flux and, above this range, it is replaced by flow conditions described as "bubble-like" except that the forms on the wire are less distinct than the "bubble-like" shapes discussed previously. These "bubble-like" forms develop gradually after transition to turbulent flow has already occurred in the boundary layer flow on the wire, and they are not accompanied by an immediate increase in the heat transfer rate. Although there was much less evidence of "bubble-like" motion, occasional short steep segments occur in the heat transfer curves (see Figure 14) corresponding to data on "bubble-like" flow taken when these flows were accompanied by whistling noises from the test section.

B. The Effect of Wire Diameter

In addition to the 0.010-inch-diameter Nichrome wire employed in the main portion of the investigation, two other cylindrical wires have been prepared in an identical manner. One is a 0.006-inch-diameter wire of Chromel A material; the other is a 0.016-inch-diameter wire of Nichrome material. No attempt has been made to measure the surface temperature of these samples when they are used as test sections. Experiments have been conducted with each of the wires mounted in a horizontal position in carbon dioxide at a bulk temperature of 77.0°F and pressures of 1300, 1200, and 1100 psia. Flow pattern variations in relation to heat flux have been recorded and photographs taken of the shadowgraph images. Some of these photographs appear in Appendix C as Figure 31. Flow patterns observed are substantially the same as those observed with the 0.010-inch-diameter Nichrome wire: laminar, oscillating, and "bubble-like" flow conditions occur in each test.

The average frequency of the oscillating flow condition has been measured for each of the three wire diameters at several heat flux rates. These measurements are presented in Figure 24 of Appendix B. Although the oscillating flow does not occur at identical heat flux

ranges for the different wire diameters, two conclusions regarding the average frequency of these flow oscillations can be drawn from the above experimental results. First, frequency of the oscillations decreases with an increase in wire diameter; second, frequency generally increases with an increase in heat flux.

C. Horizontal Wire in Subcritical Carbon Dioxide

Several experiments have been conducted with the 0.010-inch-diameter Nichrome wire mounted in a horizontal position with the carbon dioxide pressure at 1000 psia--just below the critical pressure. Data on film boiling have been recorded for bulk temperatures of 49.0° and 77.0°F. These data are obtained in the following manner: Each experiment is started with an initial heat flux of 0.280 Btu/in.²-sec and data recorded at successively decreasing heat fluxes until the film boiling is replaced by nucleate boiling. The results of these experiments are shown in Figure 20 of Appendix B. The quantitative results obtained for film boiling closely resemble a major part of the quantitative results obtained for "bubble-like" flow conditions at supercritical pressures.

Photographs of the film boiling flow patterns appear as Figure 32 in Appendix C. These flow patterns are dissimilar to the "bubble-like" flow patterns and appear to show vapor detaching from the wire with very few flow disturbances occurring on the underside of the wire.

Several photographs--and an approximate indication of the maximum heat flux for the nucleate boiling region--have also been

obtained. The nucleate boiling process in carbon dioxide is accompanied by the condensation of some impurity on the heat transfer surface, which subsequently interferes with measurements being made of the wire temperature. Increasing the purity of the carbon dioxide reduces the rate of impurity collection but does not eliminate the problem. Since this phenomenon was not present in the supercritical region, no attempt has been made to isolate or eliminate the offending substance, except to complete all the experiments conducted in the supercritical region before starting the tests at 1000 psia. In addition, the apparatus is disassembled so the chamber and test section can be cleaned between each of the boiling experiments.

The two "burn-out" heat fluxes in the nucleate boiling region have been measured at approximately 0.25 and 0.14 Btu/in.²-sec for bulk temperatures of 49.0° and 77.0°F, respectively. The saturation temperature for carbon dioxide at 1000 psia is 82°F. Photographs of typical nucleate boiling under these bulk state conditions appear as Figure 33 of Appendix C. The nucleate boiling bubbles on the underside of the wire are smaller and more distinct than the "bubble-like" forms observed with heat transfer to supercritical carbon dioxide.

To observe free convection flow patterns near a horizontal wire in a nonboiling liquid with nearly constant properties, an additional experiment has been conducted using distilled, degassed water at room temperature and with a pressure of 1500 psia inside the apparatus. There is no indication of "bubble-like" flow at surface temperatures up to the saturation temperature of 596^oF on the horizontal 0.010-inch-diameter Nichrome wire.

D. Vertical Wire in Supercritical Carbon Dioxide

Two tests have been conducted using the 0.010-inch-diameter Nichrome wire held in a vertical position in carbon dioxide maintained at 1200 psia and 77.0^oF. The results of these two tests are shown graphically in Figure 21 of Appendix B. Photographs of the flow patterns under these experimental conditions have been taken at three different elevations along the center half of the wire--the only part of the wire within the view of the shadowgraph apparatus. Some of these photographs appear as Figures 34 and 35 of Appendix C.

It has been observed that the transition from laminar to turbulent flow occurs at some position on the wire, even at the lowest heat fluxes employed (0.005 Btu/in.²-sec), and that, when the heat flux is 0.020 Btu/in.²-sec, flow transition starts near the center of the wire. Photographs of the flow transition, which was followed by large growth in the boundary layer thickness, show that the point of transition is not stationary but oscillates back and forth along the wire. At higher heat fluxes turbulent flow, which obscures the wire itself, occurs along the entire visible section of the wire.

The quantitative data in Figure 21 are based on average wire temperature, as measured by the Wheatstone bridge. These results must be considered as an average relationship between heat flux and temperature along the vertical wire, since the actual temperature of the wire along its 2-inch height undoubtedly varies considerably. Also, the size and shape of the test chamber are not best suited for experiments using a vertical test section, and it is very likely that considerable variations in temperature existed through the height of the test chamber even though the bulk temperature, as measured by the thermocouple probe at the center of the chamber, is kept at $77.0^{\circ} \pm 0.1^{\circ} \text{F}$. The average quantitative results for experiments conducted using the vertical wire are similar to the quantitative results for experiments using the horizontal wire. The possibility exists that the "bubble-like" flow is present but unobserved beneath the fluid flowing upward past the wire. However, the fact that the point of transition to turbulent flow continually moves lower as the heat transfer rate is increased must also be considered when interpreting the results from this experiment.

In summary, although the quantitative data for the two different cases are similar, the flow conditions resulting from experiments

using the vertical wire exhibit no apparent resemblance to the flow conditions resulting from experiments conducted at the same bulk state conditions using the horizontal wire.

E. Horizontal Strip in Supercritical Carbon Dioxide

To further investigate the effects of geometry on the free convection flow patterns and heat transfer in the supercritical region, a Chromax strip with a width of 0.125 inch and a thickness of 0.001 inch has been prepared and installed in the test section. Another Wheatstone bridge, constructed with resistance legs equal to the nominal 0.828-ohm resistance of the 2.08-inch test section, was used to determine the temperature of the strip. Tests were conducted at 1200 psia and 77.0^oF, with the strip mounted in two different horizontal positions. In one test, the strip was placed with its broad side horizontal; in the other two tests, the strip was placed with its broad side vertical, thus forming a short 0.125-inch-high wall.

As might be expected, the visual patterns in both of these strip orientations do not give a clear picture of the actual flow conditions at the surface of the strip. In the horizontal configuration (see Figure 36) considerable unsteady motion occurs on the top side of the strip and, except at high heat fluxes, steady flow occurs on the underside of the strip. At high heat fluxes, the flow appears to be similar to that observed on the underside of the round wire at

supercritical pressures when the bulk temperature exceeds critical temperature. With the strip mounted in the vertical position (see Figure 37), the shadowgraph images show only that, in the wake above the strip, the distance between the point at which the flow becomes turbulent and the top of the strip diminishes as the heat flux is increased until the flow in the entire visible wake appears to be turbulent.

The quantitative results of experiments conducted with both positions of the strip are almost identical, with the horizontal-position experimental results showing a slightly lower temperature difference at any given heat flux. The experimental results for both configurations indicate a steady increase in the temperature difference between the surface temperature of the strip and the bulk fluid temperature with increasing heat flux rates without any sharp changes in the slope of the heat transfer curve.

The quantitative heat transfer results obtained with laminar flow conditions occurring on the strips up to temperatures of 150°F are similar to the results obtained with the horizontal wire. However, laminar flow on the strips persists to much higher temperature differences and, after a temperature difference of 150°F , the

relationship between heat flux and temperature difference is nearly linear. Quantitative results of these tests are shown in Figures 22 and 23 of Appendix B.

VII DISCUSSION OF EXPERIMENTAL RESULTS

A. Laminar Free Convection in Supercritical Carbon Dioxide

The experimental results from this investigation discussed in Section VI indicate that, whenever laminar flow exists and the temperatures span the region of strong property changes, the plot of heat flux versus temperature difference shows negative curvature. For each of the test sections employed, the experimental heat transfer curve exhibits this negative curvature.

Similar experimental results were obtained by Fritsch and Grosh (25) in experiments conducted on laminar free convection of heat from a 0.50-inch vertical wall to supercritical water. Fritsch and Grosh (19) used a numerical integration technique to solve the steady free convection boundary layer equations for these flow conditions. Their solution, which takes into account density and specific heat variation in relation to temperature and employs a reference temperature in order to evaluate viscosity and thermal conductivity, yields analytical results which agree closely with their experimental results.

Therefore, in laminar flow it appears that free convection heat transfer can be adequately explained in terms of the usual boundary layer equations for steady flow in a gravitational field. The difficulty in analytically predicting heat transfer results for free convection laminar flow in a supercritical fluid then depends entirely on complications encountered in solving these differential equations for temperature-dependent fluid properties. The possibility remains, however, that stability limits of the laminar flow are affected by the fluid property variations and that these limits may differ, therefore, from the usual ones.

B. "Bubble-Like" Flow in Free Convection to Supercritical Carbon Dioxide

As described in Section VI, "bubble-like" flow patterns have been observed on the undersides of horizontal wires of three different diameters. These flow patterns appear to be the same as those patterns observed by Griffith and Sabersky (18) which occur on a horizontal wire heated in supercritical Freon 114A. In each case, unsteady pockets of low-density fluid are observed on the undersides of the wires. The shape of these pockets resembles the characteristic round shape of nucleate bubbles, thus these pockets are described as "bubble-like." Flow near the top surfaces of the wires is obscured by the turbulence of flow rising from the wire.

"Bubble-like" flow is preceded by an oscillating flow condition in each of the horizontal-wire tests conducted with carbon dioxide at bulk fluid temperatures below the transposed critical temperature so that the temperature profile spans the region of strong property changes. In these cases, "bubble-like" flow is accompanied by an improvement in heat transfer compared with that occurring with laminar flow. Plots made of several tests show that the first portion of the heat transfer curve for the "bubble-like" flow is

sometimes very steep (see Figure 5) and resembles a nucleate boiling curve. The remainder of the heat flux curve for this flow condition exhibits less slope and indicates that a nearly linear relationship exists between heat flux rate and temperature difference. This latter curve resembles curves plotted from data on film boiling at subcritical pressures, although the flow patterns in the "bubble-like" case are dissimilar to those observed in the film boiling region.

"Bubble-like" flow patterns which occur when the bulk temperature of the carbon dioxide is above the transposed critical temperature are not preceded by the oscillating flow condition. The effects of the "bubble-like" flow on the heat transfer process are not as pronounced as at bulk temperatures below the transposed critical temperature.

"Bubble-like" flow is not observed in experiments using the vertical wire or the Chromax strip mounted as a short vertical wall. Quantitative results of experiments using the vertical wire resemble results of experiments where "bubble-like" flow occurred on the horizontal wire; however, the similarities may well be a result of turbulent flow along the comparatively great vertical height of the

vertical wire's heat transfer surface. In these experiments, with increasing heat flux the region of transition to turbulent flow is observed to descend the length of the wire. Presumably, the increase in slope of the heat transfer curve corresponds to the change from a predominantly laminar heat transfer process to a predominantly turbulent heat transfer process, as turbulent flow exists finally along almost the entire length of the wire.

The occurrence of the "bubble-like" flow patterns observed in this investigation depends upon the fluid property changes, the heat flux rate, the geometry of the heat transfer surface, and the orientation of the surface in the gravitational field. Once the "bubble-like" flow is established, its effect upon heat transfer seems to depend on the magnitude of the changes in the fluid property values between those properties at the heat transfer surface and those at the bulk state conditions of the fluid.

It appears that the unusual "bubble-like" flow condition results from a hydrodynamic instability occurring in the laminar flow field under the combined effects of gravity and large property changes due to the temperature gradients of the heat transfer. The occurrence of "bubble-like" forms might be expected to result in

an agitation of the fluid next to the wire surface, such as is caused in subcritical boiling by the growth and collapse of nucleate bubbles. The heat transfer rates which accompany the "bubble-like" flow cannot be explained by the usual boundary layer equations, and one may conclude that sufficient agitation is caused by the "bubble-like" flow to account for the improvement in heat transfer.

A similar type of hydrodynamic instability occurs in the Benard problem (32), where an initially motionless fluid, heated at a bottom plane surface, develops a cellular convection pattern after the heat transfer rate reaches a certain minimum value. The instability in the Benard problem results from a density stratification in the gravitational field, with the less dense material at the bottom of the volume of fluid. Rayleigh and others have shown that the minimum heat flux effecting the Benard flow pattern is determined by the other boundary conditions and by the fluid properties.

Several investigators¹ have studied the effects of property .

¹Reference 32 cites the stability studies mentioned here and includes a bibliography of the work published in the field.

variations on hydrodynamic instability. Rayleigh analyzed the stability of a stratified, inviscid fluid with continually varying density. Harrison investigated the stability of two superimposed homogeneous fluids with different densities and viscosities. The effects of density variations in inviscid fluids on the stability of steady shear flow have been treated by Prandtl, Taylor, Case, and others. In each of these investigations, property changes and flow conditions were considered which are relatively simple compared to those occurring in this investigation; in fact, those conditions considered in previous studies do not correspond very closely to the conditions existing in the present investigation. Nevertheless, these investigations do indicate that property variations, particularly variations of the magnitude of those occurring with heat transfer in the supercritical region, can be expected to have significant influences on the occurrence of hydrodynamic instabilities; they corroborate the interpretation of the observed "bubble-like" flow as resulting from a hydrodynamic instability.

The "bubble-like" flow observed in this investigation, with its particular dependence on geometry and gravity, does not appear to be as general a phenomenon as nucleate boiling, which depends primarily

on the state conditions and occurs with any geometry and flow condition and without gravity. The same statement applies to a comparison of "bubble-like" flow with the usual type of turbulent flow. For this reason, if "bubble-like" flow of some kind does occur with forced convection for one certain set of conditions, it should not necessarily be expected to occur in all cases of forced convection heat transfer to supercritical fluids. The dependence of "bubble-like" flow on geometry and gravity might explain the differences between the experimental results obtained for forced convection, discussed in Section I. This dependence may also explain why these results and interpretations of these results have been susceptible of differing opinions on whether or not heat transfer to supercritical fluids could be adequately explained without postulating flow patterns different from those usually observed in constant-property fluids.

The experimental results of this investigation indicate that there are both similarities and significant differences between heat transfer with "bubble-like" flow in supercritical fluids and heat transfer with nucleate boiling in liquids at subcritical pressures. The results also indicate that the boundaries of the pockets

observed in the "bubble-like" flow are less distinct than those of nucleate bubbles, which exhibit a sharp physical division between the vapor and liquid phases. On the other hand, the distinguishability of the "bubble-like" forms indicates that there are steep density gradients associated with the boundaries of the low-density regions.

In Section II it was noted that there are some essential differences between the temperature distribution in the immediate vicinity of a nucleate boiling bubble and the temperature distribution in the vicinity of any "bubble-like" form in a supercritical fluid. The lack of surface tension, and hence the absence of superheating, indicates that the heat transfer conditions existing in the supercritical "bubble-like" flow should be fundamentally different from those associated with nucleate boiling. High-speed motion pictures of the "bubble-like" flow confirm such a hypothesis and there appears to be less agitation of the fluid near the heat transfer surface with the "bubble-like" flow than with nucleate boiling. "Agitation" is here assumed to be related to bubble motion and, when these motion pictures are projected at normal speeds, the frequencies and velocities of the "bubble-like" flow appear to be lower than those expected for nucleate

bubbles. This lesser agitation is believed to explain why the "bubble-like" flow observed at supercritical pressures is generally less effective as a heat transfer process than nucleate boiling at subcritical pressures.

In addition to a visual similarity to nucleate boiling, the first part of the "bubble-like" flow also behaves like nucleate boiling in another respect: both exhibit a considerable increase in the heat transfer rate compared with laminar flow at the same temperature difference; in some cases the beginning portion of the heat transfer curve for "bubble-like" flow is very steep. However, whereas in free convection nucleate boiling this increase would be expected to start at a surface temperature within a few degrees of the saturation temperature, the surface temperature associated with the onset of "bubble-like" flow is approximately 100^oF above the critical temperature.

As mentioned earlier in this section, the heat transfer results for the "bubble-like" flow corresponding to higher temperature differentials are very similar to the experimental results obtained with film boiling at subcritical pressures. In both cases, the relation between heat flux and temperature is approximately linear, although

the slope of the curve for "bubble-like" flow is steeper than that for film boiling, as shown in Figures 8 and 20. However, although the film boiling process is not accompanied by "bubble-like" forms on the underside of the wire, there must be considerable similarity in the heat transfer processes of these two phenomena. Both types of flow have a layer of low-density fluid near the wire surface; both are influenced by the geometry of the heat transfer surface and by its orientation in the gravitational field. In both cases, disturbances at the interface of the low-density film and the higher density bulk fluid occur and appear to have some effect on the heat transfer.

C. Oscillating Flow Conditions in Free Convection to Supercritical Carbon Dioxide

One unusual result of this investigation is the observation of distinct oscillations between two different flow patterns. These oscillations occur in a definite range of heat flux values for free convection from a horizontal wire in a supercritical fluid under conditions of strong property changes. Through visual observation of shadowgraph images, high-speed motion pictures, and photographs of this phenomenon, it can be seen that the flow oscillates between steady laminar flow and unsteady "bubble-like" flow. This oscillation is accompanied by corresponding variations in the test section temperature.

Temperature data recorded for this flow condition indicate the average wire temperature for the oscillating flow cycle. It appears that, at a particular condition in the laminar region, the increase of heat flux and surface temperature results in an instability of the steady flow which subsequently develops into the "bubble-like" flow. Presumably, at this point, the heat transfer mechanism of "bubble-like" flow is so much more effective than that of laminar flow that the test section temperature quickly drops to a level at which the "bubble-like"

density pockets collapse and the flow again becomes laminar until the temperature increases to the level where the oscillating flow cycle repeats itself.

In Appendix G this hypothetical oscillation cycle is discussed. This cycle is presented in terms of a heat capacitor limit cycle with constant heat input and heat transfer from the test section surface at two different rates which are associated with the two differing flow conditions. If this hypothetical cycle represents a correct interpretation of the nature of the oscillation, then it may be concluded that, among other factors, the ratio of heat capacity to surface area of the wire should tend to lower the frequency of oscillation with increasing wire diameter. This was found to be true, as shown in Figure 24. It would also be expected that, as the heat input and, hence, the average heat flux is increased, "bubble-like" flow would persist for an increasing fraction of the time period of the total oscillation. This second expectation has been confirmed through visual observations and studies of the high-speed motion pictures taken of the oscillations at different heat fluxes.

A most interesting observation regarding oscillating flow is the implied absence of a single flow condition capable of steadily

transferring heat from the wire over a finite range of heat flux rates. Presumably this absence is the result of a laminar flow instability developing directly into the "bubble-like" flow which, in turn, requires a higher heat flux to be maintained continuously. The required heat flux value apparently is not obtained until the heat flux is near the higher levels of heat flux associated with oscillating flow.

VIII SUMMARY AND CONCLUSIONS

Heat transfer rates in free convection from a small horizontal cylinder in carbon dioxide have been measured as a function of the surface temperature of the cylinder for a large range of supercritical bulk state conditions. Shadowgraph images of the flow patterns accompanying the heat transfer have been recorded photographically. In each of the tests, laminar flow has been observed at low heat fluxes. At higher heat fluxes, unusual "bubble-like" flow patterns have been observed. The "bubble-like" flow patterns are accompanied by an improvement in the heat transfer when temperatures of the heat transfer surface and the bulk fluid span the transposed critical temperature. In this case, the laminar and "bubble-like" flow patterns are separated by a range of heat flux values in which the flow oscillates between these two different patterns.

Supplementary experiments have included the investigation of the flow conditions observed with heat transfer from two additional horizontal cylinders of different diameters. In these experiments, laminar, oscillating, and "bubble-like" flow patterns are also observed.

The heat transfer from a thin horizontal strip has been measured for two different strip orientations--mounted as a short vertical wall and mounted as a horizontal surface. Neither the quantitative heat transfer data nor the photographs of the flow reveal any unusual flow patterns occurring with use of these strips.

Another supplementary experiment using the original cylindrical test section mounted in a vertical position has given quantitative heat transfer results which are similar to those obtained for "bubble-like" flow on the horizontal cylinder. However, the vertical surface was covered by a thick turbulent boundary layer, and no "bubble-like" forms have been observed.

Measurements have been made of film boiling heat transfer from a horizontal cylinder to subcritical carbon dioxide. Quantitative data recorded on the supercritical "bubble-like" heat transfer condition resemble the data recorded for film boiling, except for a limited range of heat flux rates at the beginning of the "bubble-like" flow condition. In this case, the heat transfer curves are sometimes very steep, similar to nucleate boiling curves. Although somewhat larger, the shapes of the "bubble-like" forms observed in supercritical carbon dioxide resemble those of nucleate boiling bubbles.

On the basis of the experimental results, and on the basis of interpretations made in the course of this investigation, the following conclusions can be made: (1) A "bubble-like" flow condition, unlike the flow expected in a fluid with constant property values, does occur with free convection heat transfer to a supercritical fluid. (2) This flow condition results from a hydrodynamic instability in the preceding laminar flow structure. (3) The occurrence of the "bubble-like" flow depends on the changes in fluid properties and on the geometrical orientation of the heating surface. (4) The "bubble-like" flow condition can have a strong effect on the heat transfer process when large changes in the property values are present.

In future investigations it would be interesting to study the structure of forced convection flows with heat transfer to a supercritical fluid. If a phenomenon similar to the "bubble-like" flow occurs with a similar dependence on the geometry and orientation of the heat transfer surface, then this dependence may explain the divergent opinions about the occurrence of such an unusual flow condition.

REFERENCES

1. Schmidt, E., E. Eckert, and U. Grigull, "Heat Transfer by Liquids Near the Critical State," Army Air Force Translation, No. 527, Headquarters Air Materiel Command (Dayton, Ohio, April 1946).
2. Schmidt, E., Experiments and Investigations on Heat Transfer by Liquids At or Near Their Critical Points, Contract No. (U.S.) N 62558-1906, Final Report (1963).
3. Dean, L.E. and L.M. Thompson, "Study of Heat Transfer to Liquid Nitrogen," ASME Paper No. 56-SA-4 (1956).
4. Bringer, R.P. and J.M. Smith, "Heat Transfer in the Critical Region," J. AIChE, Vol. 3, No. 1 (1957), pp. 49-55.
5. Koppel, L.B. and J.M. Smith, "Turbulent Heat Transfer in the Critical Region," Proceedings of 1961 International Heat Transfer Conference (August 1961), Part III, Paper 69, pp. 585-590.
6. Powell, W.B., "Heat Transfer to Fluids in the Region of the Critical Temperature," Jet Propulsion, Vol. 27 (July 1957), pp. 776-783.
7. Dickinson, N.L. and C.P. Welch, "Heat Transfer to Supercritical Water," Trans. ASME, Vol. 80 (April 1958), pp. 746-752.

8. Randall, D.G., "Some Heat Transfer and Fluid Friction Experiments with Supercritical Water," Reactor Heat Transfer Conference (November 1956).
9. Del Bene, J.V. and J.P. Barger, Heat Transfer to Supercritical Freon-12, Massachusetts Institute of Technology, Contract Nonr 1891-(14), Technical Reports to Office of Naval Research (1959).
10. Hines, W.S. and H. Wolf, "Heat Transfer Vibrations with Hydrocarbon Fluids at Supercritical Pressures and Temperatures," ARS Propellants, Combustion and Liquid Rockets Conference (April 1961).
11. Szetela, E.J., "Preliminary Analysis of Heat Transfer to Hydrogen Including the Effects of Varying Fluid Properties," ARS Propellants, Combustion and Liquid Rockets Conference (April 1961).
12. Armand, A.A., N.V. Tarasova, and A.S. Conkov, "An Investigation of Heat Transfer from Wall to Steam Near Critical Region," (in Russian), Heat Transfer at High Heat Flux and Other Special Conditions, papers edited by A.A. Armand (Gosenergoizdat, Moscow-Leningrad, 1959), pp. 41-50.
13. Miropolsky, Z.L. and M.E. Shitsman, "Heat Transfer to Water and Steam with Varying Specific Heat (In the Near Critical Region)," (in Russian), Journal of Technical Physics, Vol. 27, No. 10 (1951), pp. 2359-2372.

14. Petukhov, B.S., E.A. Krasnoschekov, and V.S. Protopopov, "An Investigation of Heat Transfer to Fluids Flowing in Pipes under Supercritical Conditions," Proceedings of 1961 International Heat Transfer Conference (August 1961), Part III, Paper 67, pp. 569-578.
15. Goldman, K., "Heat Transfer to Supercritical Water at 5000 psi Flowing at High Mass Flow Rates through Round Tubes," Proceedings of 1961 International Heat Transfer Conference (August 1961), Part III, Paper 66, pp. 561-568.
16. Goldman, K., "Heat Transfer to Supercritical Water and Other Fluids with Temperature-Dependent Properties," AICHE Chem. Eng. Progress Symposium Series, Nuclear Engineering, Part 1, Vol. 50, No. 11 (1954), pp. 105-113.
17. Deissler, R.G., "Heat Transfer and Fluid Friction for Fully Developed Turbulent Flow of Air and Supercritical Water with Variable Fluid Properties," Trans. ASME, Vol. 76 (1954), pp. 73-85.
18. Griffith, J.D. and R.H. Sabersky, "Convection in a Fluid at Supercritical Pressures," ARS Jour., Vol. 30, No. 3 (March 1960), pp. 289-291.

19. Fritsch, C.A. and R.J. Grosh, "Free Convective Heat Transfer to a Supercritical Fluid," Proceedings of 1961 International Heat Transfer Conference (August 1961), Part V, Paper 121, pp. 1010-1016.
20. Goldman, K., "Special Heat Transfer Phenomena for Supercritical Fluids," Nuclear Development Associates, Inc., Report NDA-2-31 (November 1956).
21. Boggs, J.P. and J.H. Holman, "Heat Transfer to Freon 12 Near the Critical State in a Natural-Circulation Loop," ASME Journal of Heat Transfer (August 1960), pp. 221-226.
22. Bonilla, C.F. and L.A. Sigel, "High Intensity Natural Convection Heat Transfer Near the Critical Point," 4th National Heat Transfer Conference (August 1960), AIChE Paper No. 28.
23. Doughty, D.L. and R.M. Drake, "Free Convection Heat Transfer from a Horizontal Right Circular Cylinder to Freon 12 Near the Critical State," Trans. ASME, Vol. 78 (1956), pp. 1843-1850.
24. Simon, H.A. and E.R.G. Eckert, "Laminar Free Convection in Carbon Dioxide Near Its Critical Point," Int. J. Heat Mass Transfer, Vol. 6 (1963), pp. 681-690.
25. Fritsch, C.A. and R.J. Grosh, "Free Convective Heat Transfer to Supercritical Water Experimental Measurements," ASME Journal of Heat Transfer (November 1963), pp. 289-294.

26. Michels, A. and C. Michels, "Isotherms of CO₂ between 0° and 150° and Pressures from 16 to 250 atm," Proc. Roy. Soc. London, A 153 (1935), pp. 201-214.
27. Michels, A., B. Blaisse, and C. Michels, "The Isotherms of CO₂ in the Neighborhood of the Critical Point and Round the Coexistence Line," Proc. Roy. Soc. London, A 160 (1937), pp. 358-375.
28. Michels, A., J.V. Sengers, and P.S. Van Der Gulik, "The Thermal Conductivity of Carbon Dioxide in the Critical Region," Physica, Vol. 28 (1962), pp. 1216-1237.
29. Michels, A., A. Botzen, and W. Schuurman, "The Viscosity of Carbon Dioxide between 0°C and 75°C and at Pressures up to 2000 Atmospheres," Physica, Vol. 23 (1957), pp. 95-102.
30. Koppel, L.B. and J.M. Smith, "Thermal Properties of Carbon Dioxide in the Critical Region," Journal of Chemical and Engineering Data, Vol. 5, No. 4 (October 1960), pp. 437-440.
31. National Bureau of Standards, Circular #564, Chapter 4, "The Thermodynamic Properties of Carbon Dioxide" (1955), pp. 138-195.
32. Chandrasekhar, S., Hydrodynamic and Hydromagnetic Stability (London: Oxford University Press, 1961), Chapter II, pp. 9-75.

Appendix A

PROPERTIES OF CARBON DIOXIDE

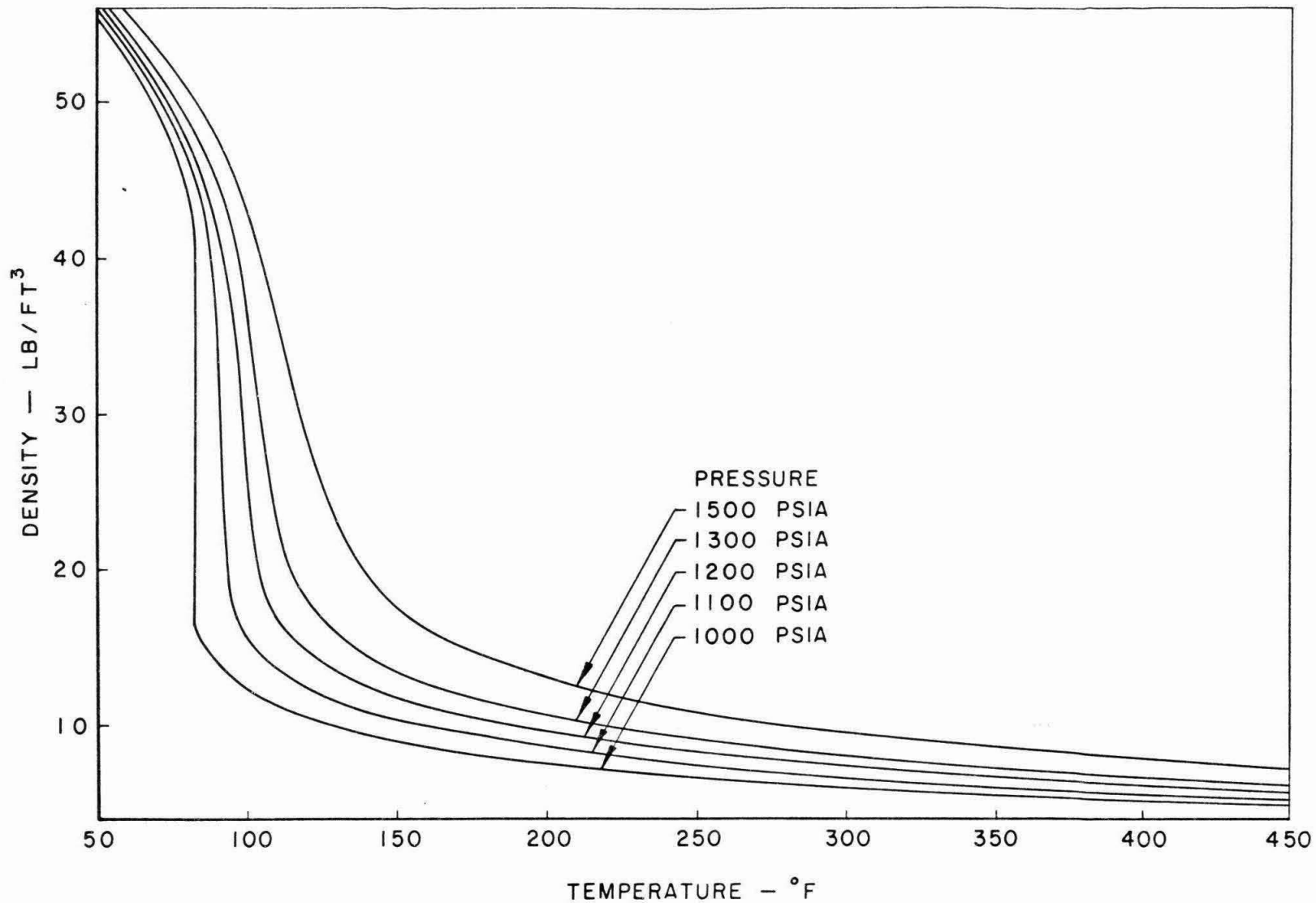


FIG. 1. DENSITY OF CARBON DIOXIDE

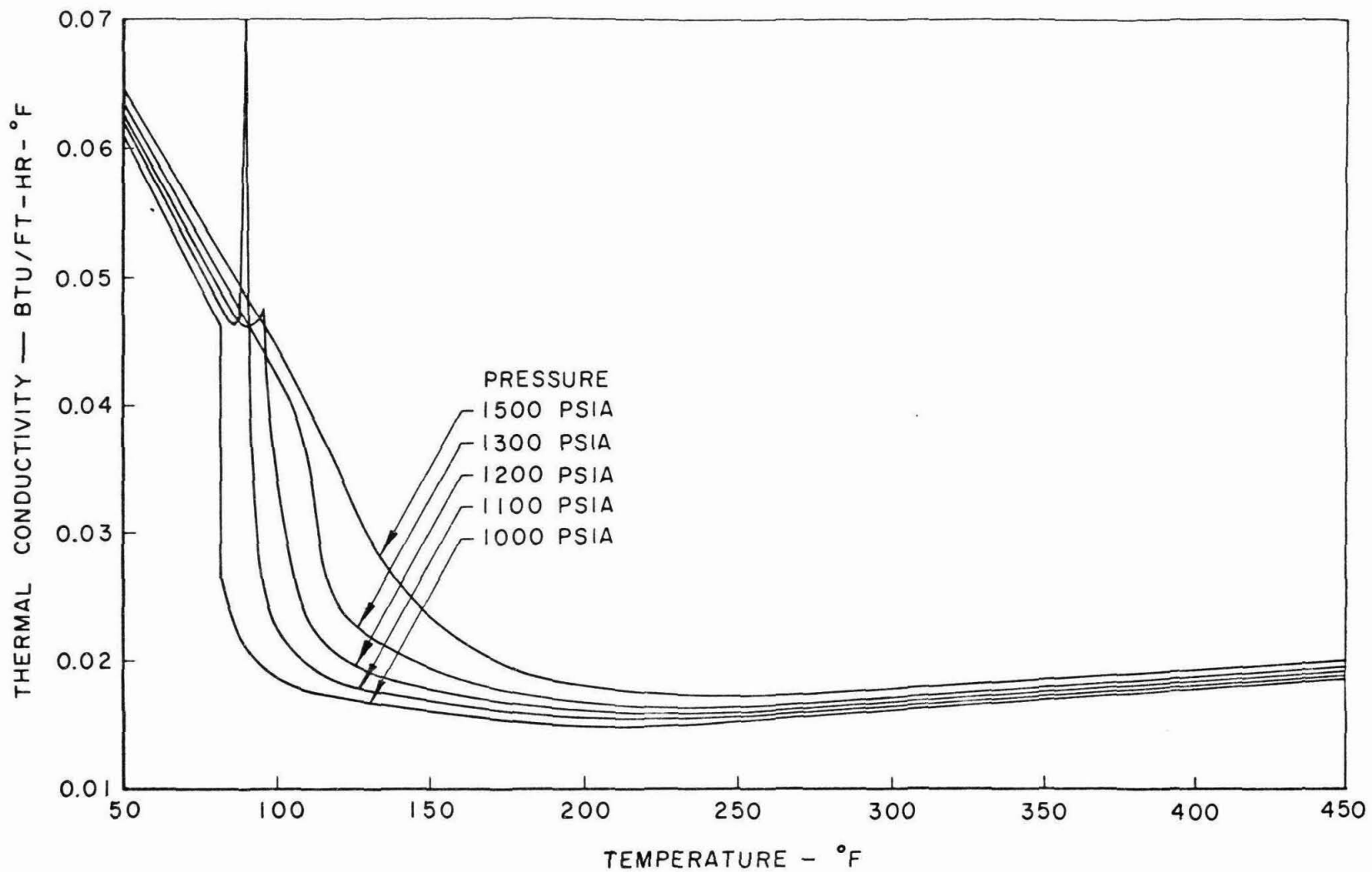


FIG. 2. THERMAL CONDUCTIVITY OF CARBON DIOXIDE

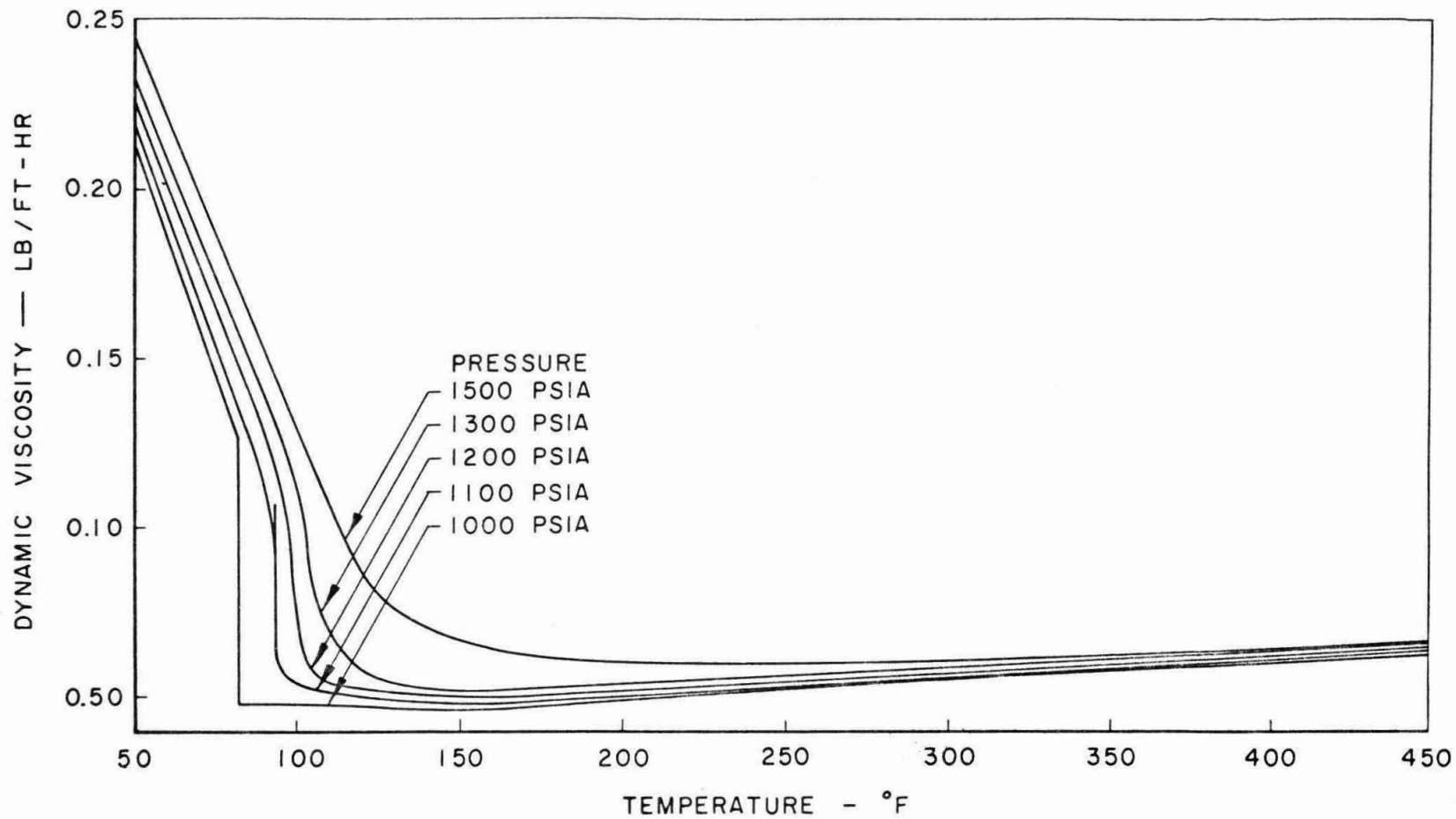


FIG.3. DYNAMIC VISCOSITY OF CARBON DIOXIDE

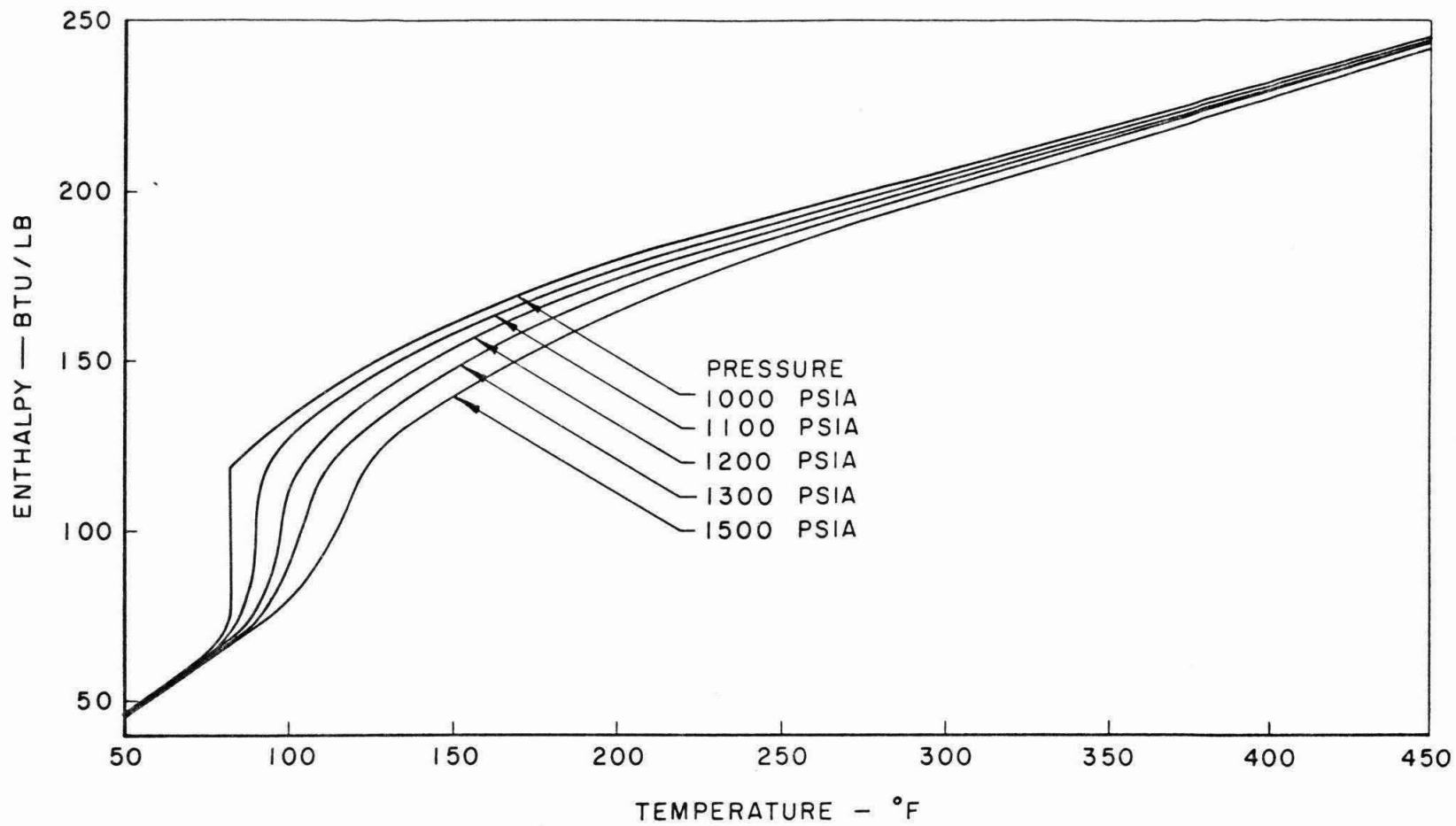


FIG. 4. ENTHALPY OF CARBON DIOXIDE

Appendix B

EXPERIMENTAL RESULTS

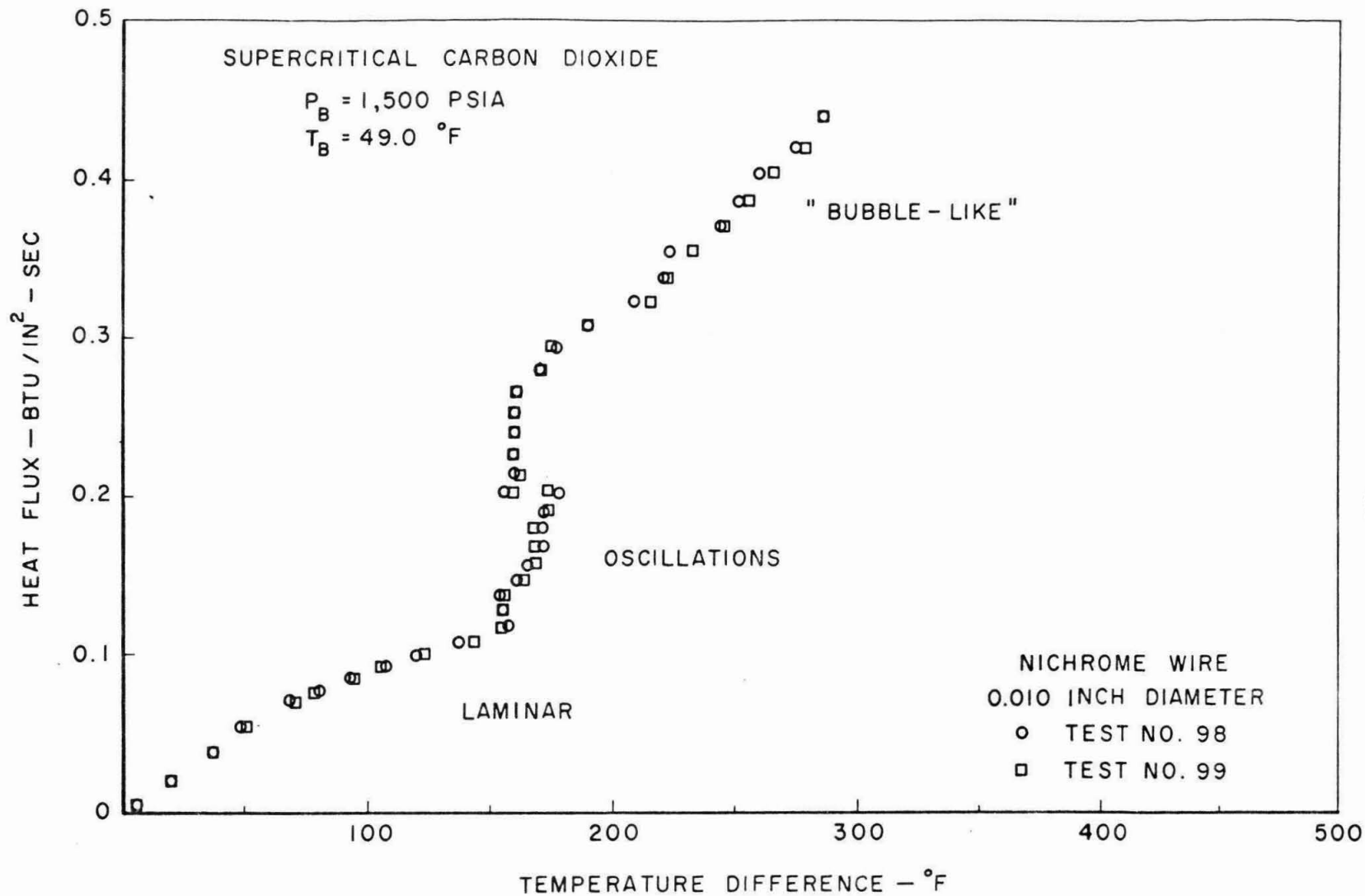


FIG. 5. FREE CONVECTION HEAT TRANSFER FROM A HORIZONTAL CYLINDER
TO SUPERCRITICAL CARBON DIOXIDE AT 1500 psia AND 49.0 °F

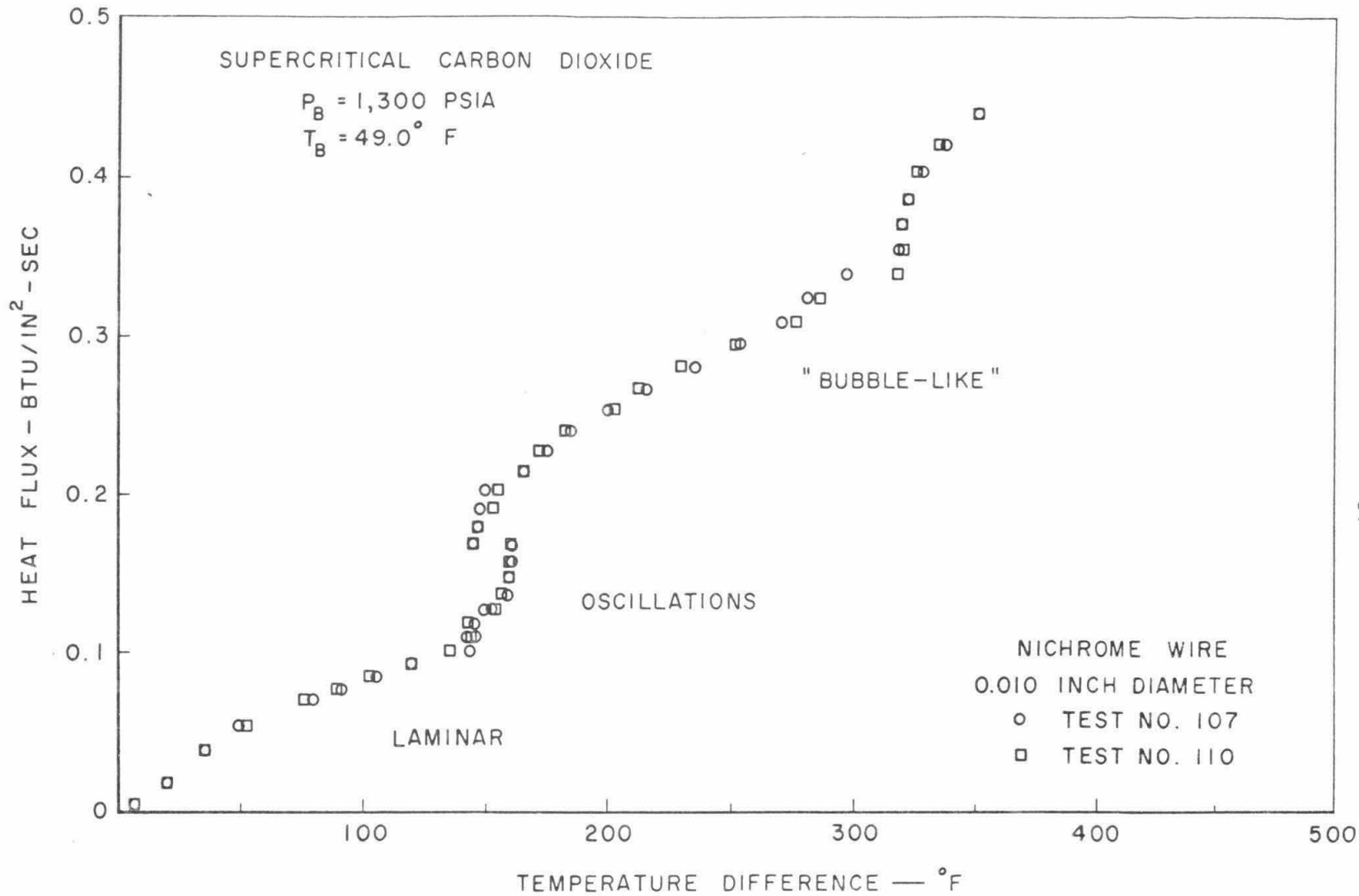


FIG. 6. FREE CONVECTION HEAT TRANSFER FROM A HORIZONTAL CYLINDER TO SUPERCRITICAL CARBON DIOXIDE AT 1300 psia AND 49.0°F

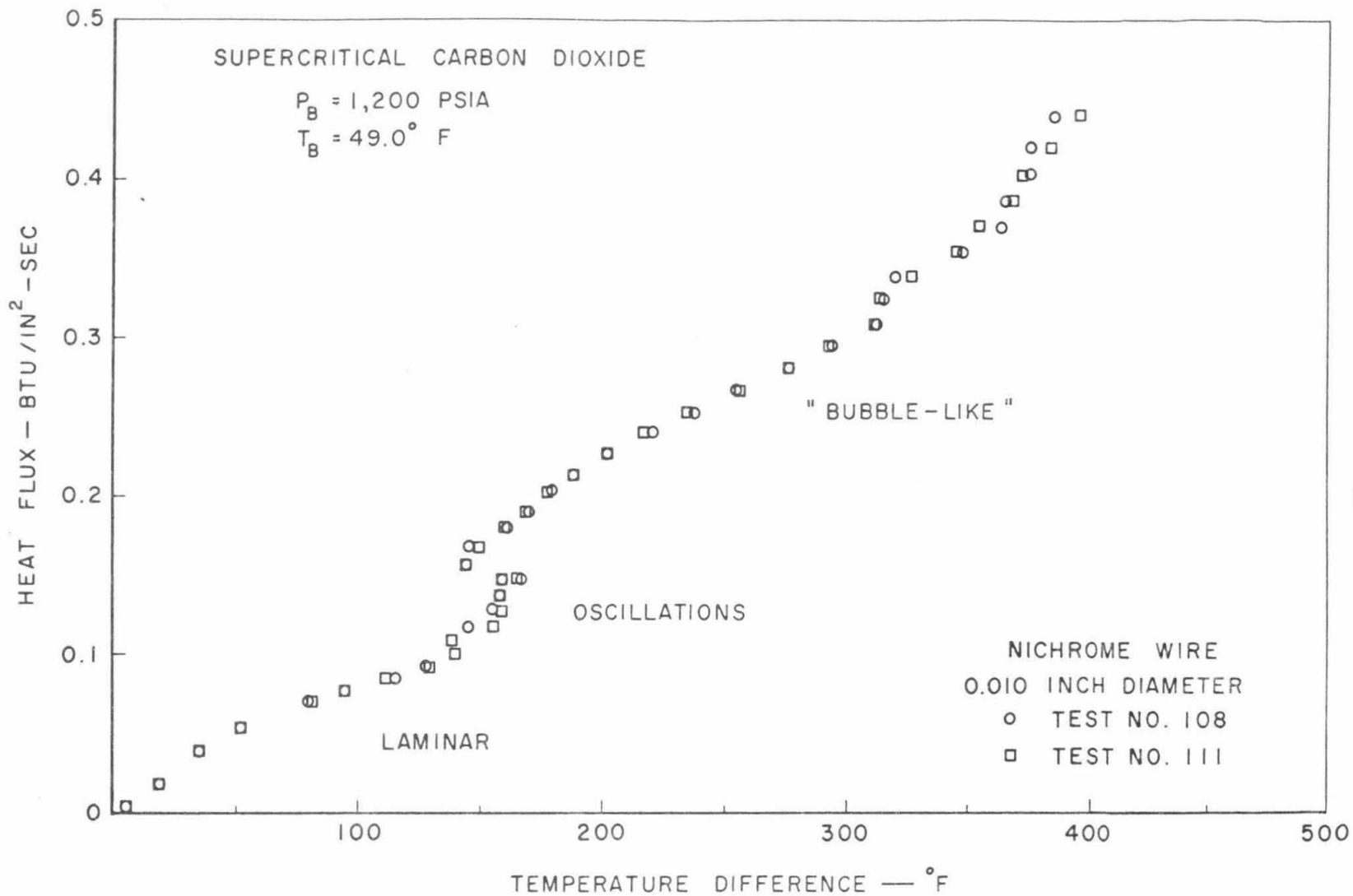


FIG. 7. FREE CONVECTION HEAT TRANSFER FROM A HORIZONTAL CYLINDER TO SUPERCRITICAL CARBON DIOXIDE AT 1200 psia AND 49.0°F

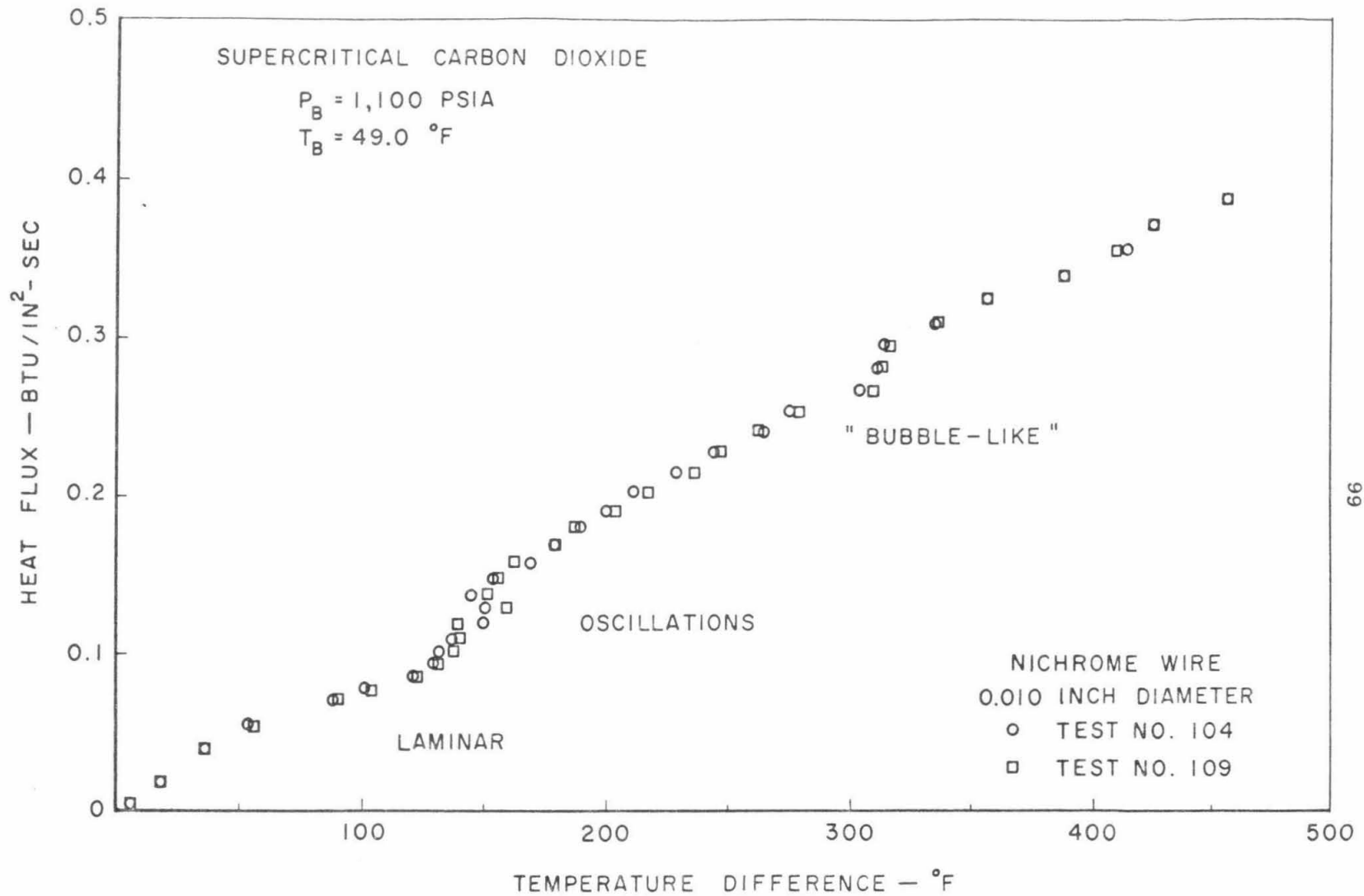


FIG. 8. FREE CONVECTION HEAT TRANSFER FROM A HORIZONTAL CYLINDER TO SUPERCRITICAL CARBON DIOXIDE AT 1100 psia AND 49.0 °F

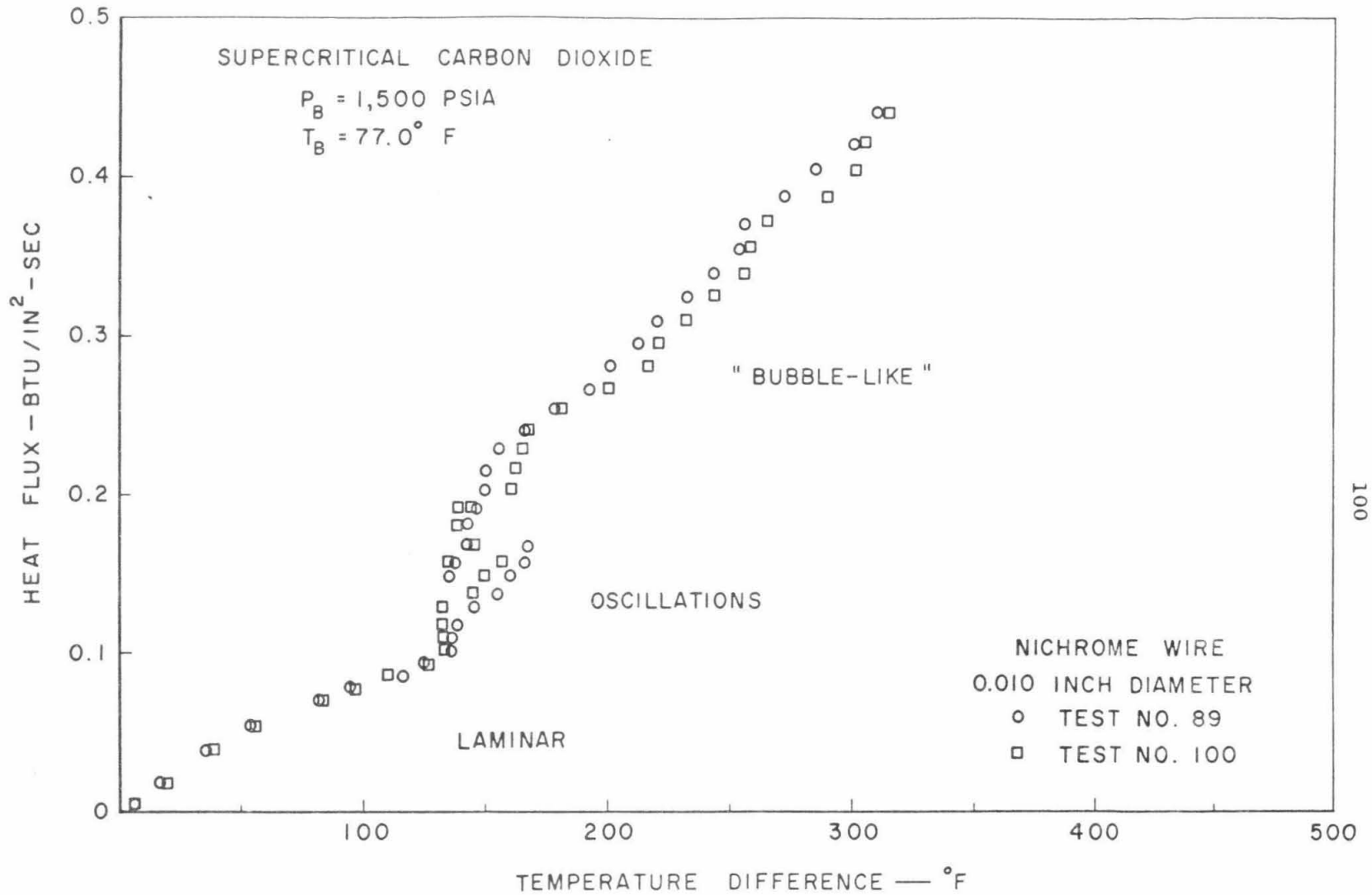


FIG. 9. FREE CONVECTION HEAT TRANSFER FROM A HORIZONTAL CYLINDER
 TO SUPERCRITICAL CARBON DIOXIDE AT 1500 psia AND 77.0°F

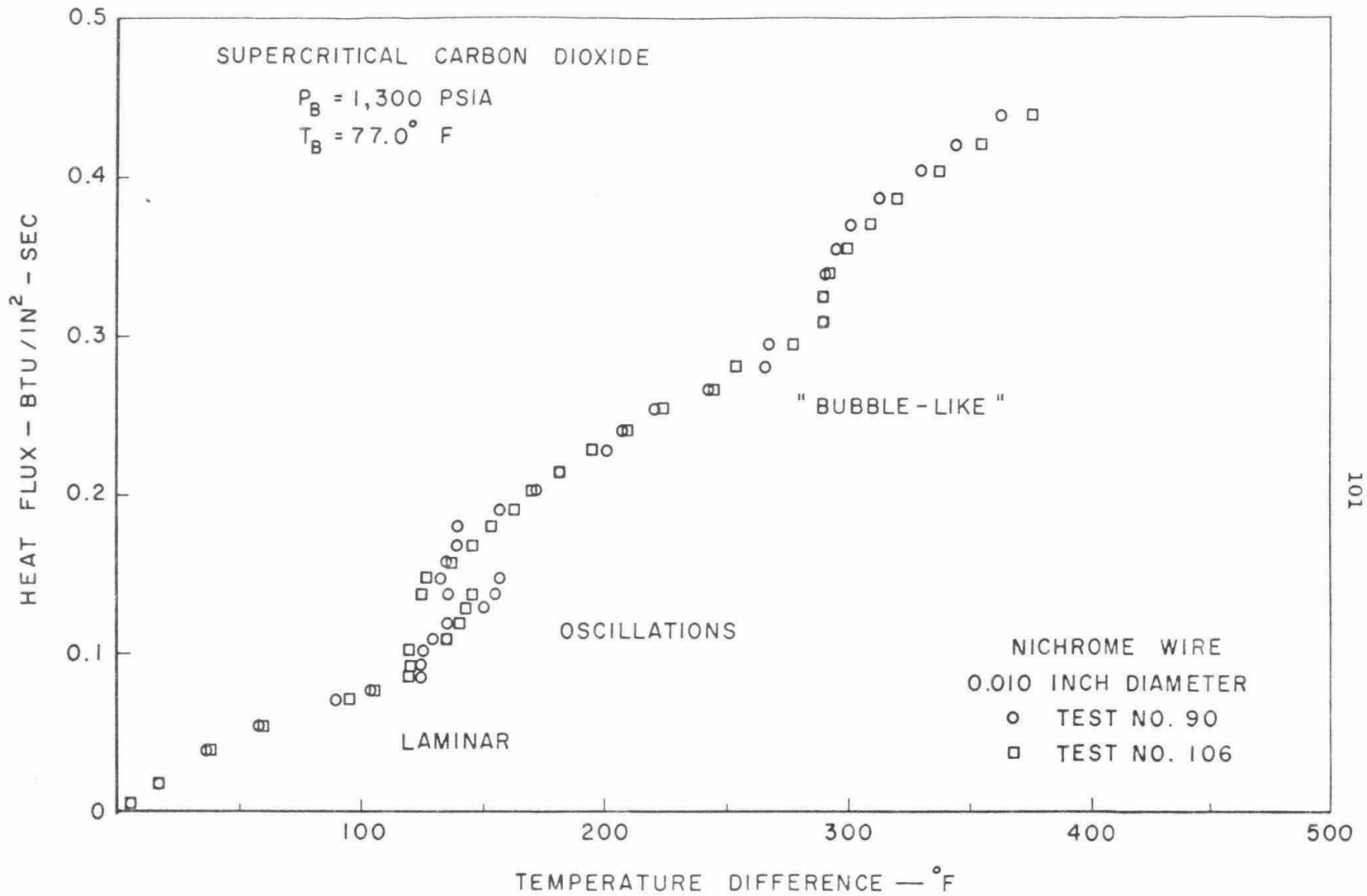


FIG. 10. FREE CONVECTION HEAT TRANSFER FROM A HORIZONTAL CYLINDER
 TO SUPERCritical CARBON DIOXIDE AT 1300 psia AND 77.0 °F

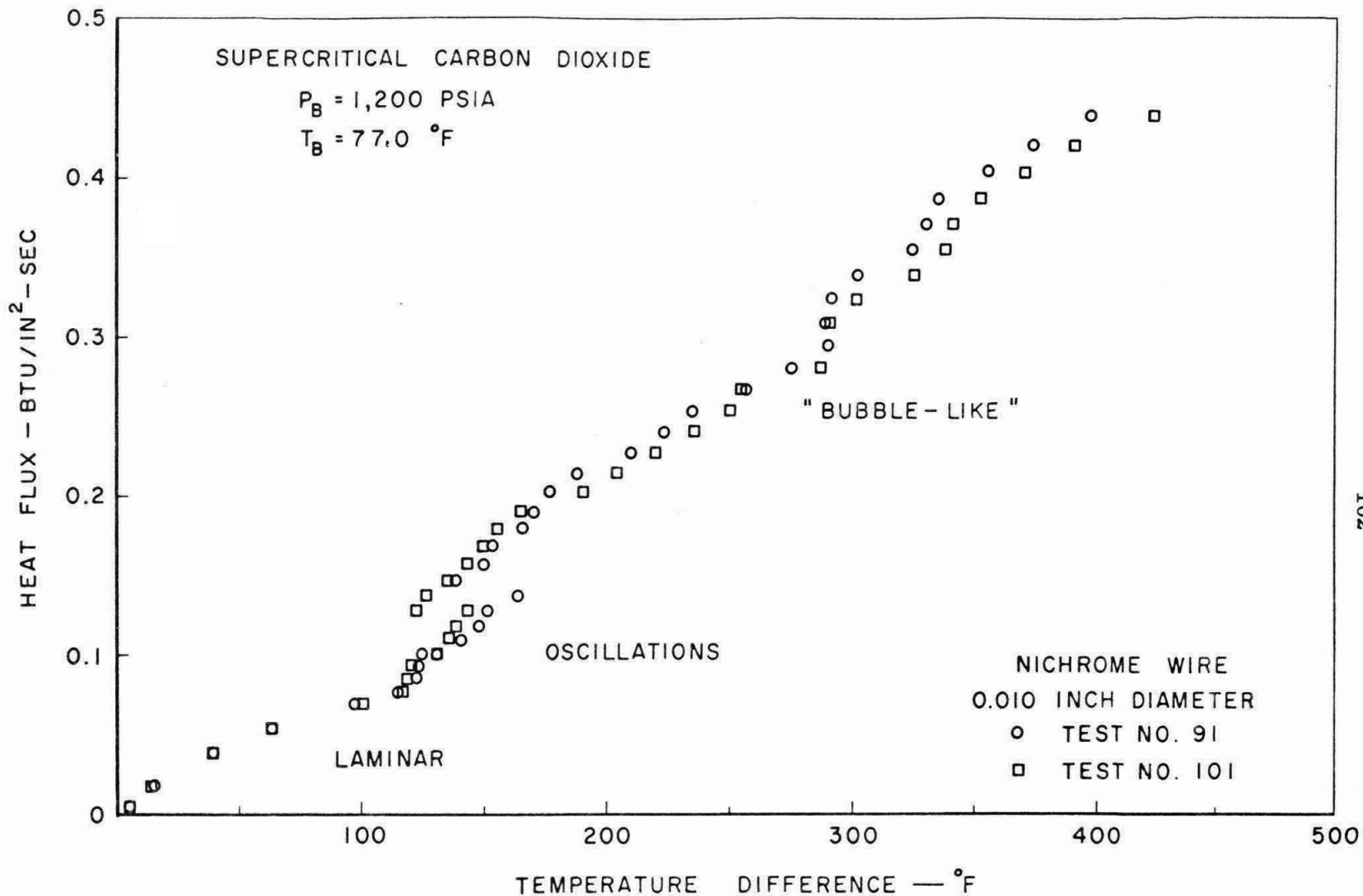


FIG. 11. FREE CONVECTION HEAT TRANSFER FROM A HORIZONTAL CYLINDER
 TO SUPERCritical CARBON DIOXIDE AT 1200 psia AND 77.0 °F

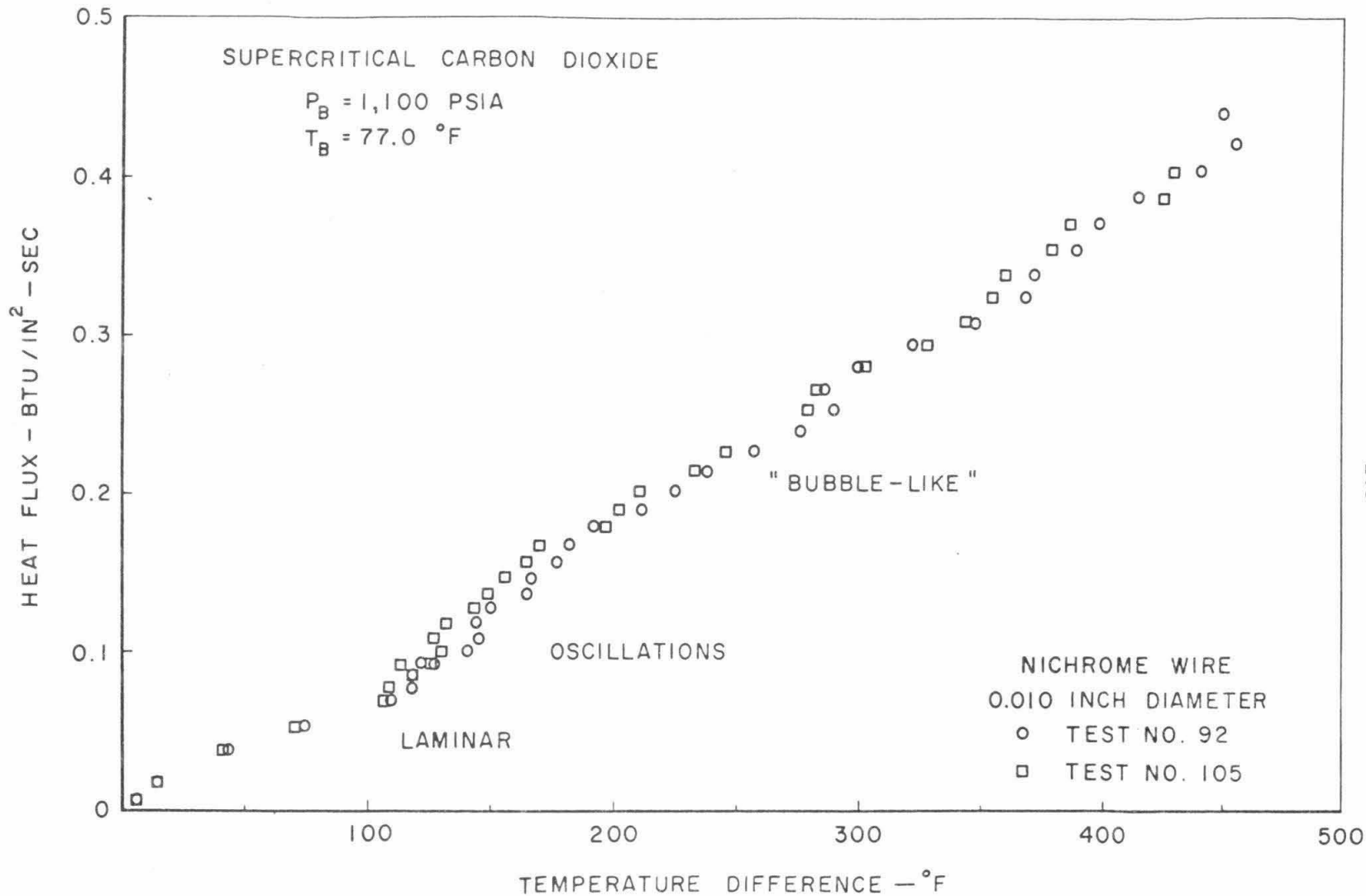


FIG. 12. FREE CONVECTION HEAT TRANSFER FROM A HORIZONTAL CYLINDER TO SUPERCRITICAL CARBON DIOXIDE AT 1100 psia AND 77.0 °F

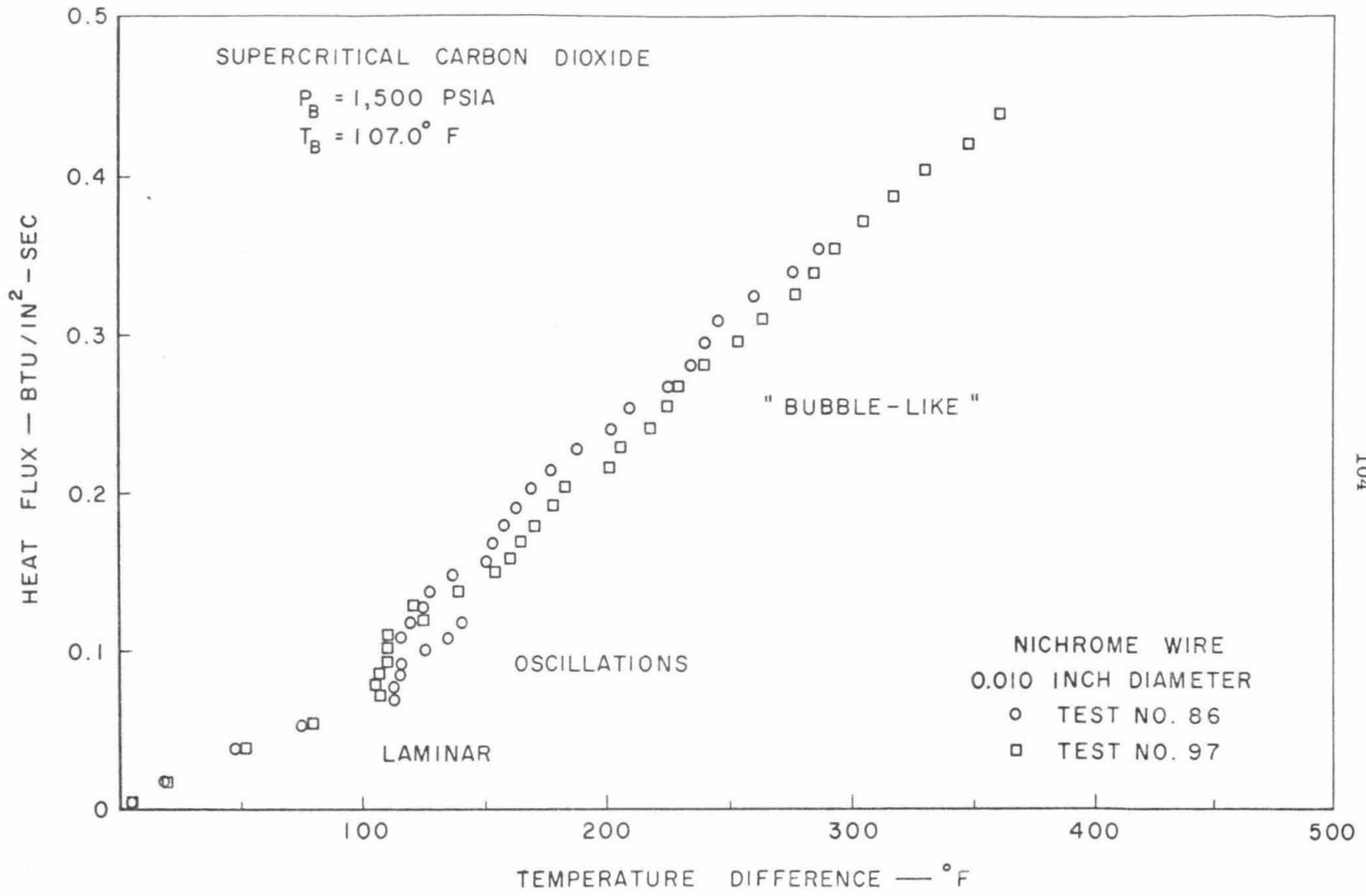


FIG. 13. FREE CONVECTION HEAT TRANSFER FROM A HORIZONTAL CYLINDER TO SUPERCRITICAL CARBON DIOXIDE AT 1500 psia AND 107.0 °F

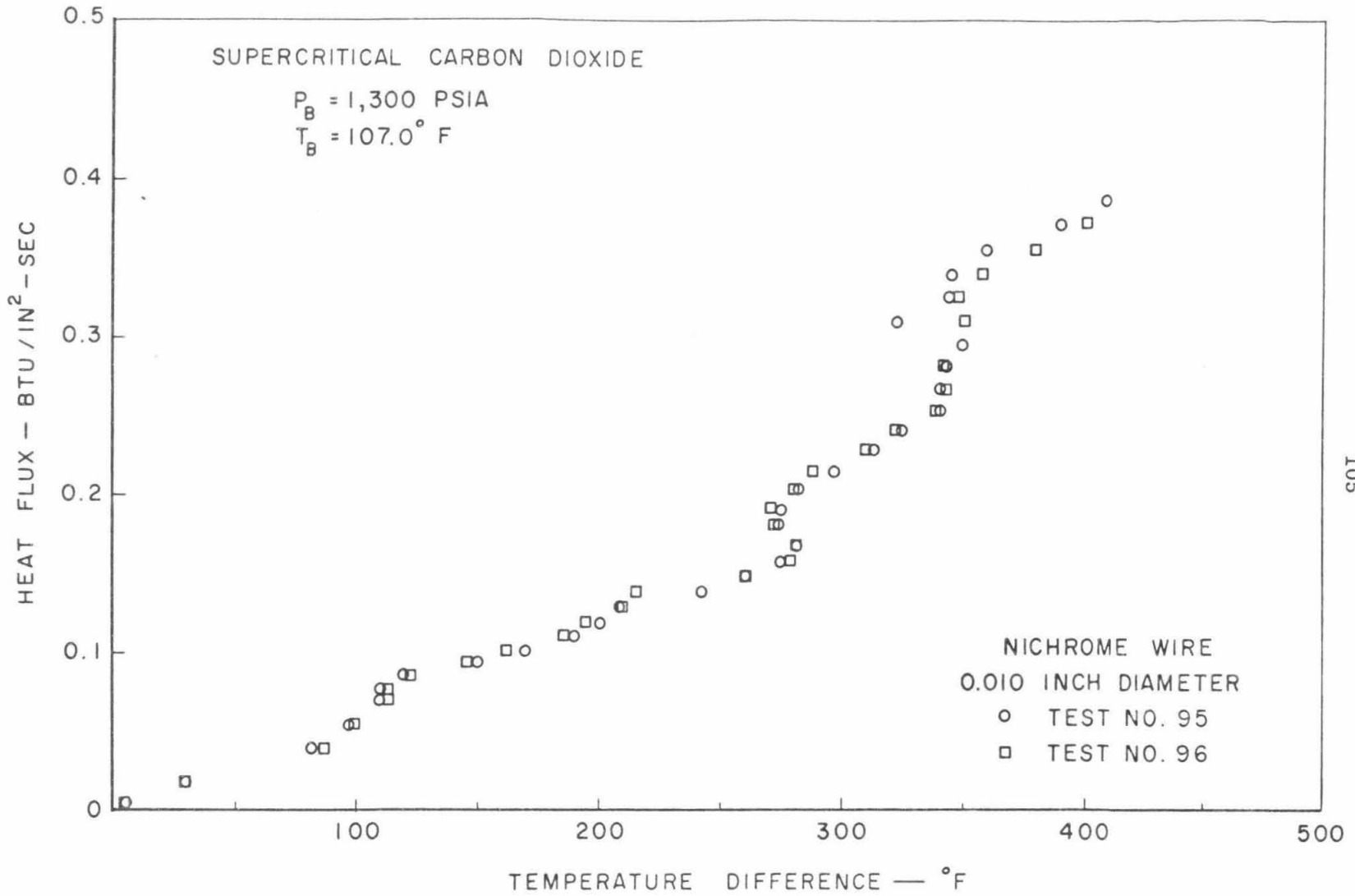


FIG. 14. FREE CONVECTION HEAT TRANSFER FROM A HORIZONTAL CYLINDER
TO SUPERCRITICAL CARBON DIOXIDE AT 1300 psia AND 107.0°F

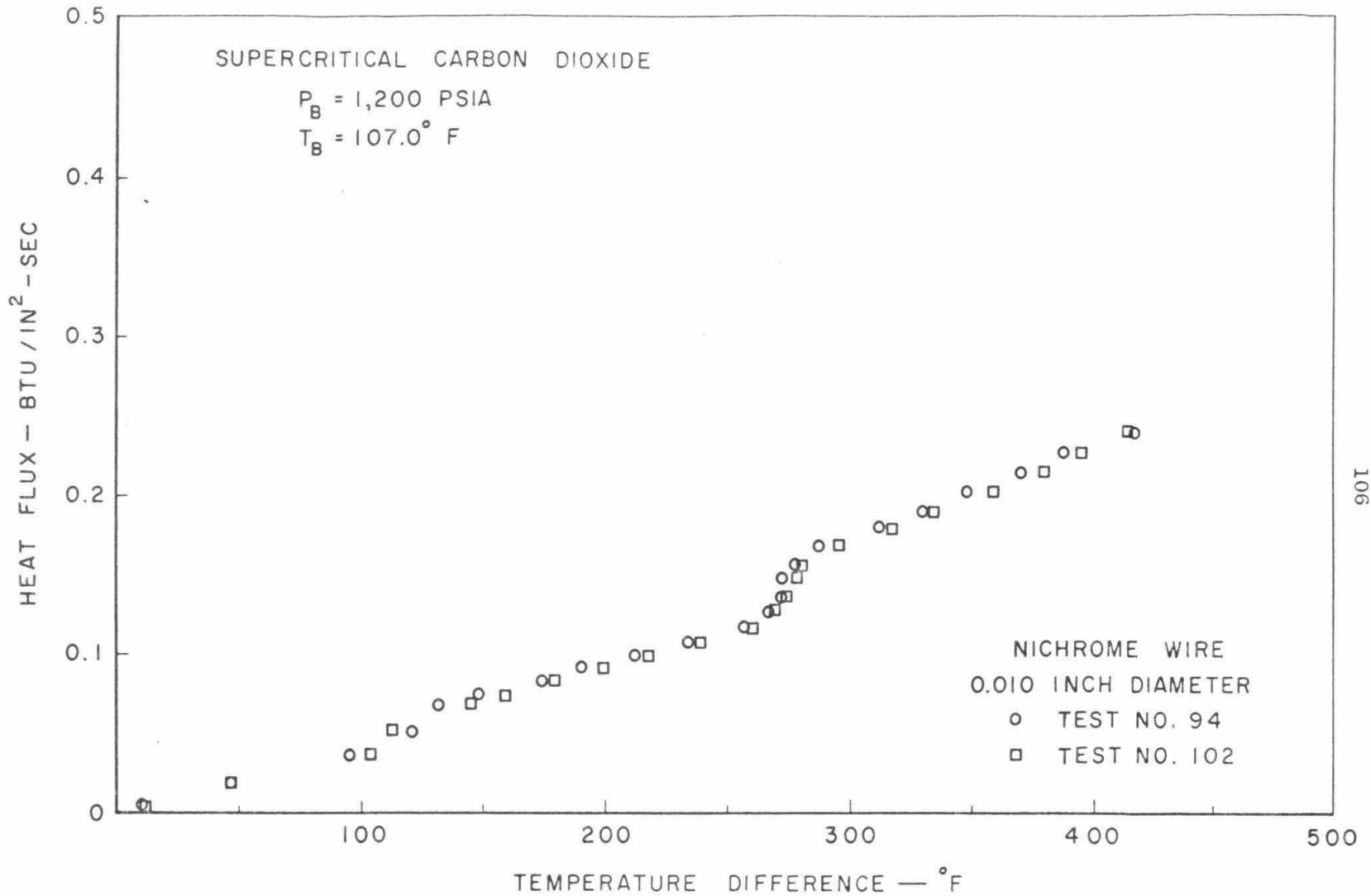


FIG. 15. FREE CONVECTION HEAT TRANSFER FROM A HORIZONTAL CYLINDER
TO SUPERCRITICAL CARBON DIOXIDE AT 1200 psia AND 107.0 °F

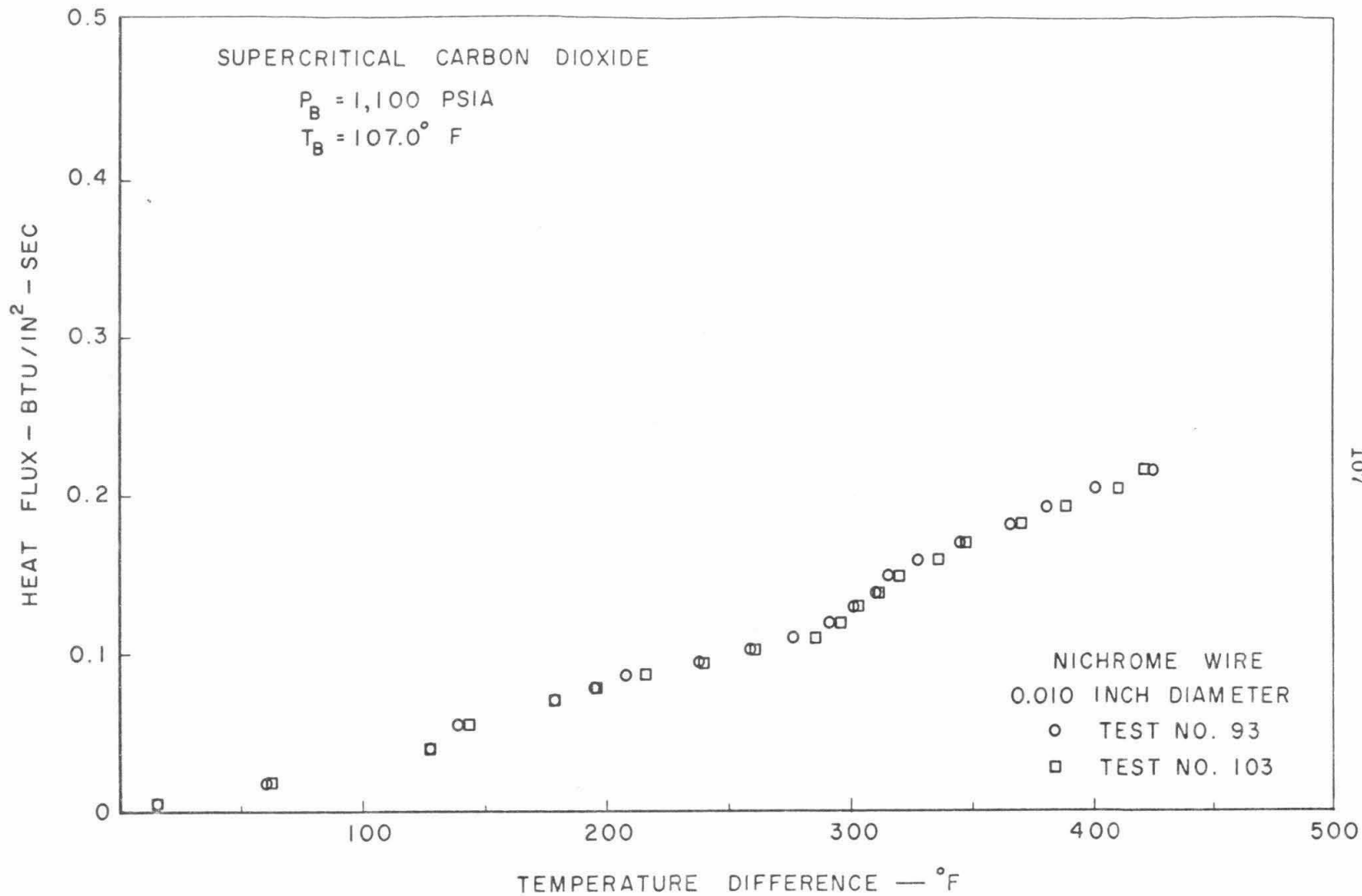


FIG. 16. FREE CONVECTION HEAT TRANSFER FROM A HORIZONTAL CYLINDER
TO SUPERCRITICAL CARBON DIOXIDE AT 1100 psia AND 107.0 °F

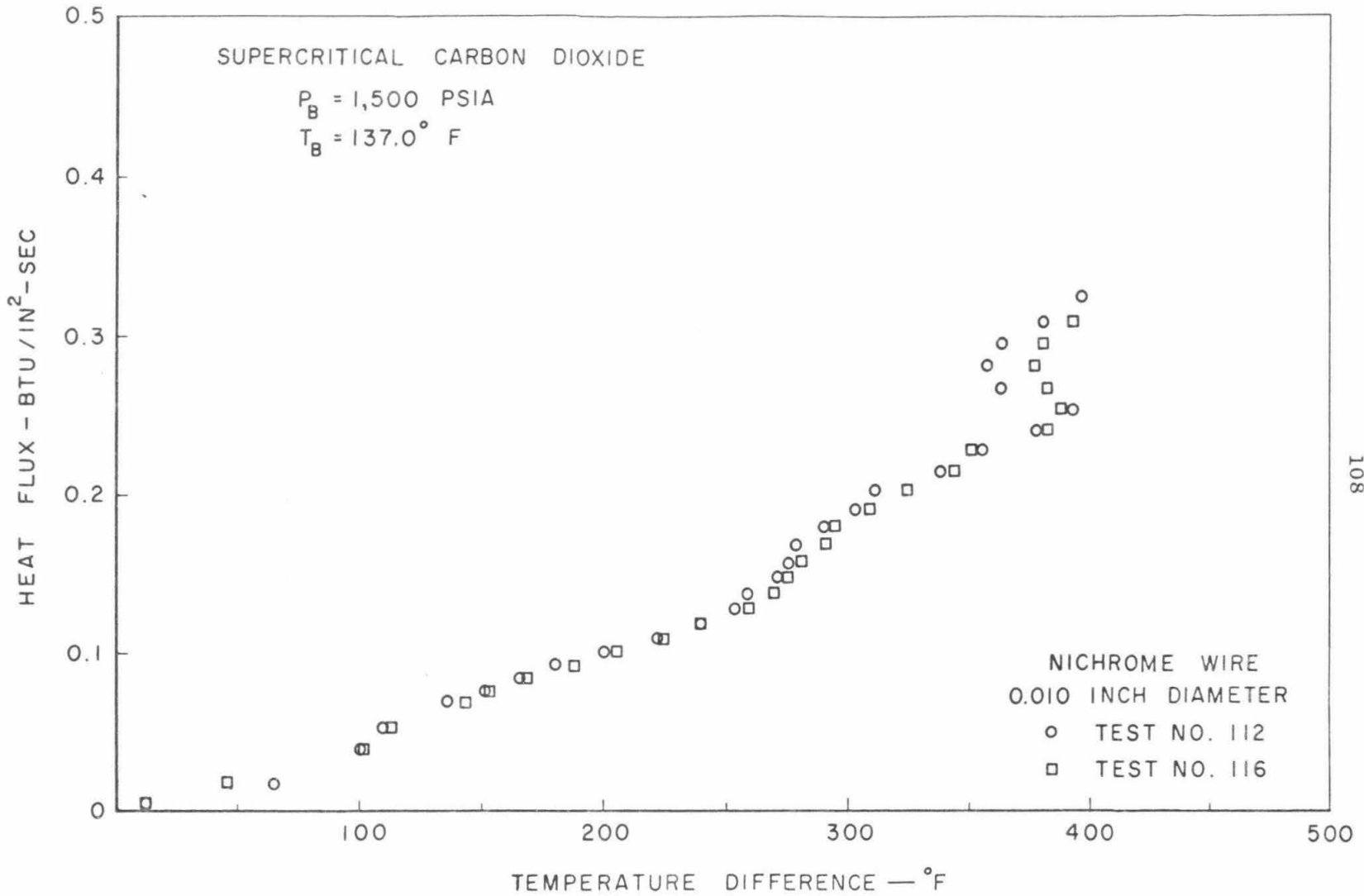


FIG. 17. FREE CONVECTION HEAT TRANSFER FROM A HORIZONTAL CYLINDER TO SUPERCRITICAL CARBON DIOXIDE AT 1500 psia AND 137.0°F

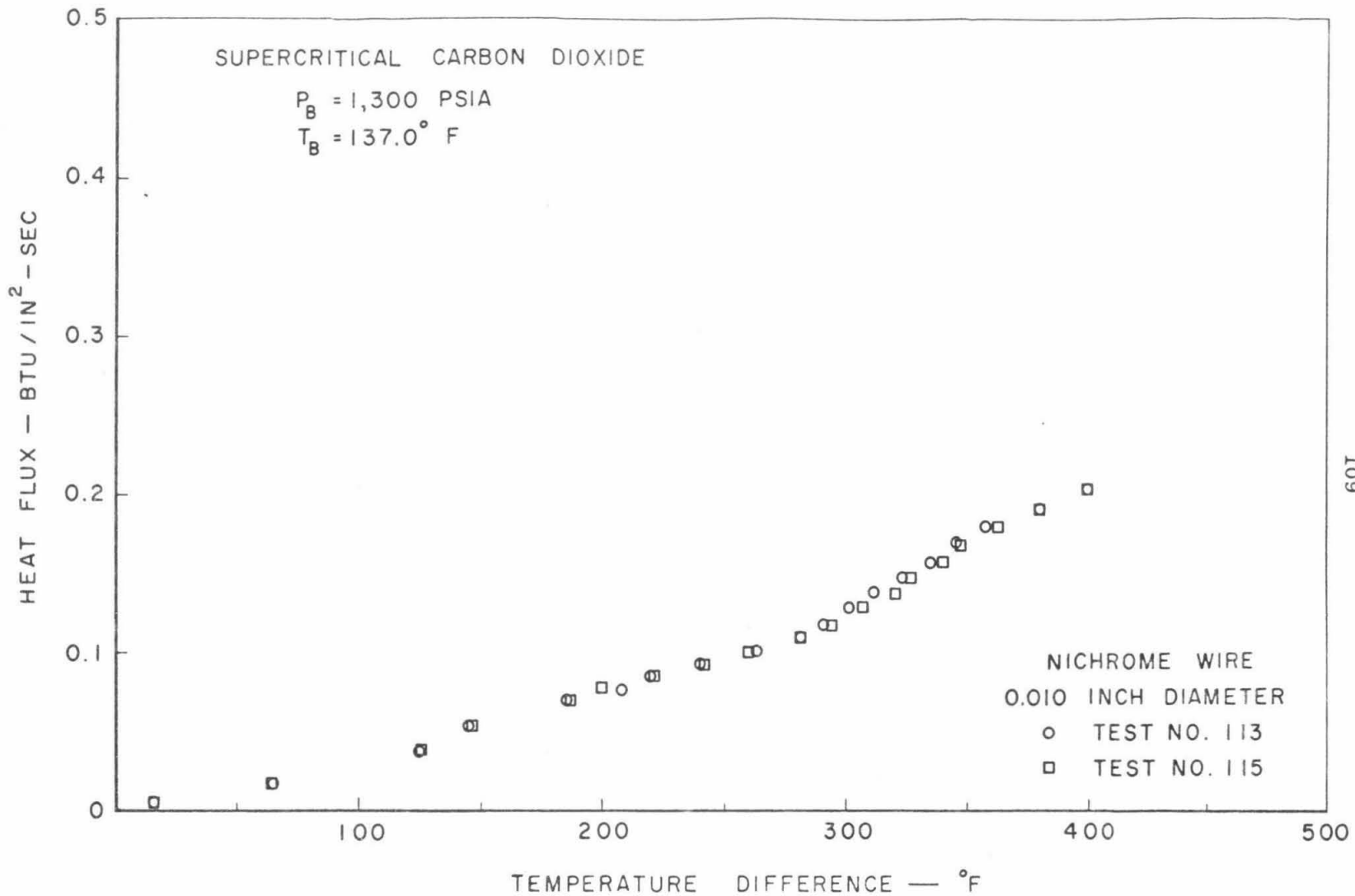


FIG. 18. FREE CONVECTION HEAT TRANSFER FROM A HORIZONTAL CYLINDER TO SUPERCRITICAL CARBON DIOXIDE AT 1300 psia AND 137.0°F

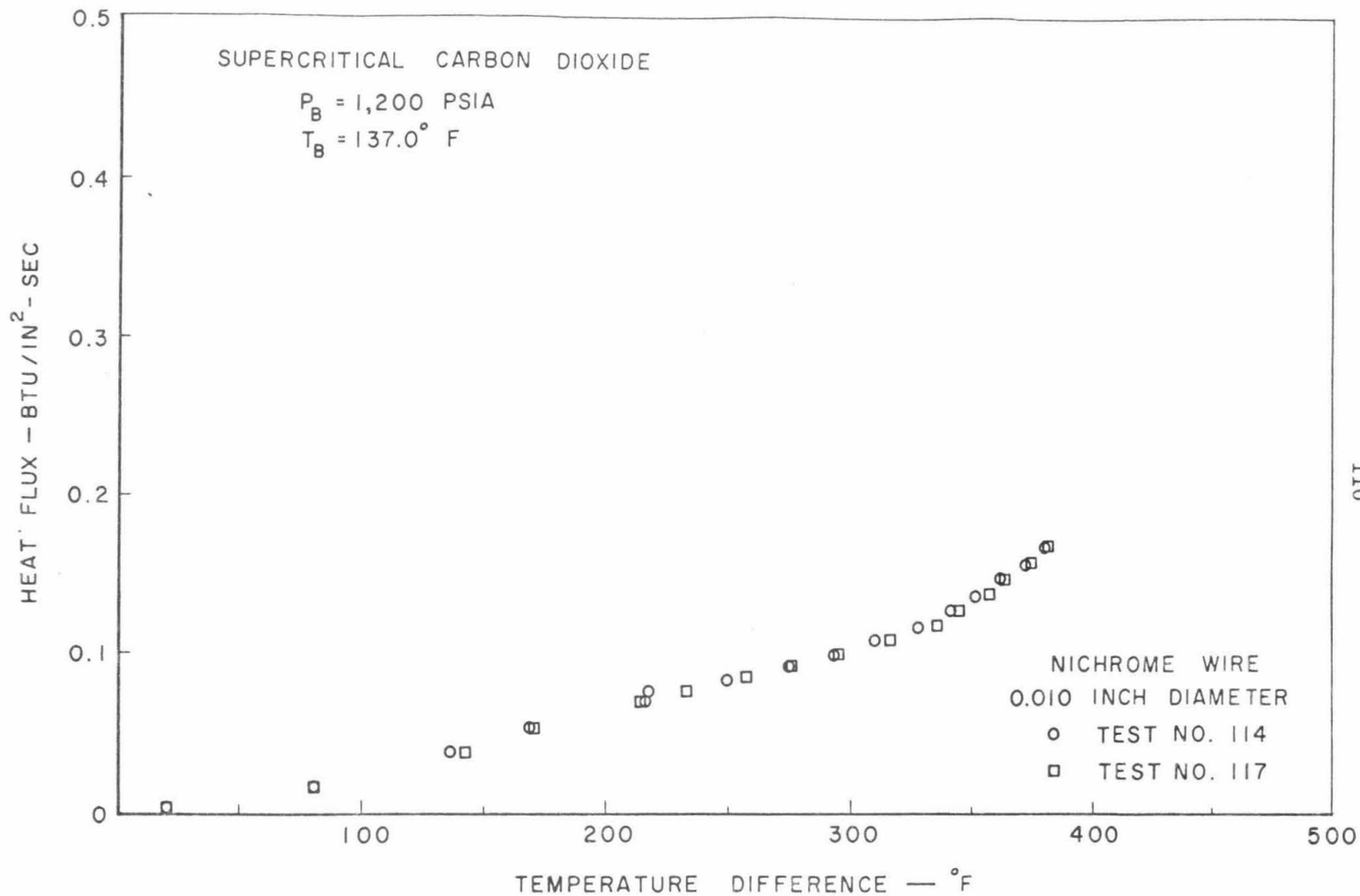
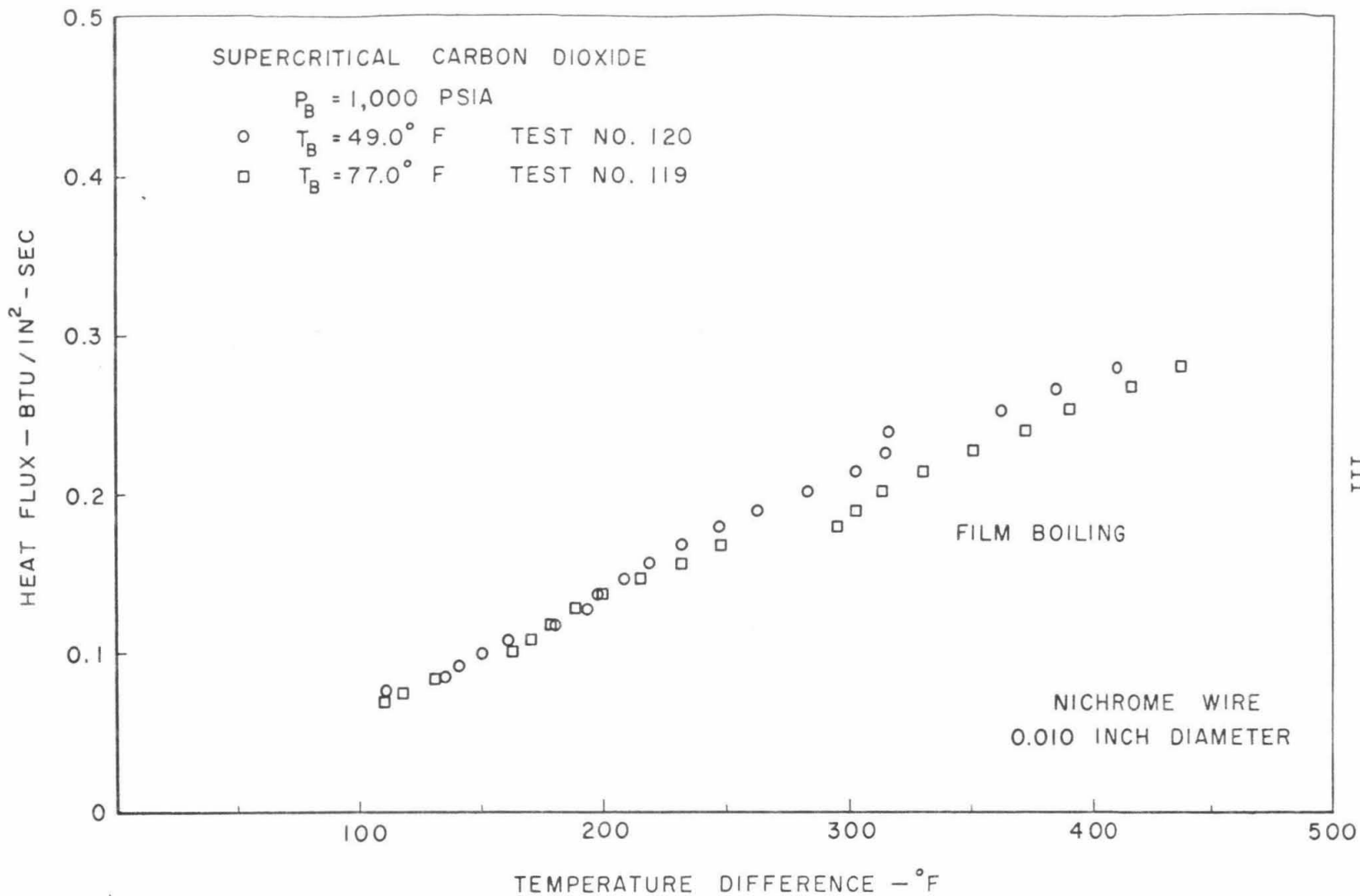


FIG. 19. FREE CONVECTION HEAT TRANSFER FROM A HORIZONTAL CYLINDER TO SUPERCRITICAL CARBON DIOXIDE AT 1200 psia AND 137.0°F



111

FIG. 20. FILM BOILING HEAT TRANSFER FROM A HORIZONTAL CYLINDER TO SUBCRITICAL CARBON DIOXIDE AT 1000 psia, 49.0° AND 77.0°F

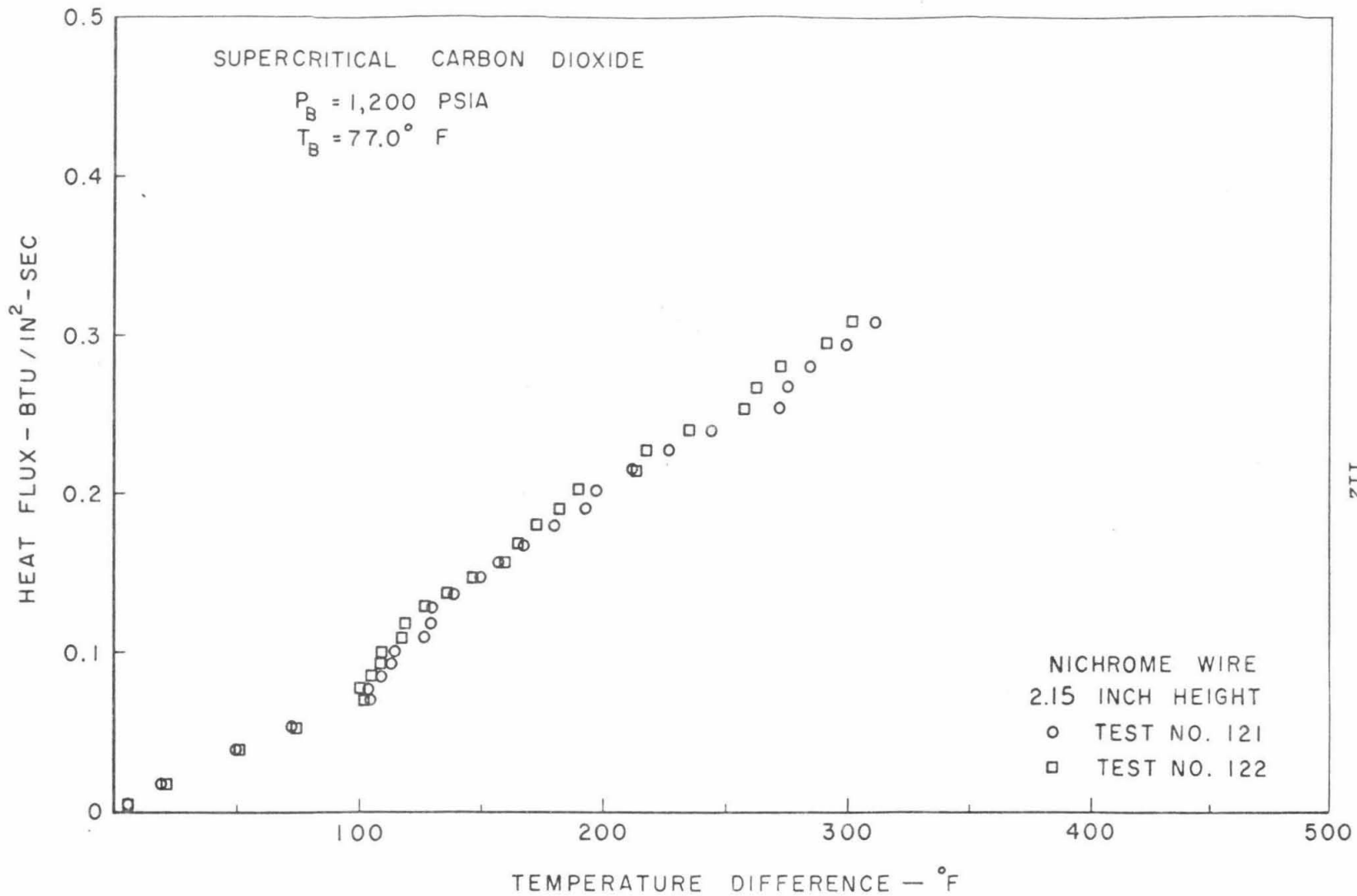


FIG. 21. FREE CONVECTION HEAT TRANSFER FROM A VERTICAL CYLINDER
TO SUPERCRITICAL CARBON DIOXIDE AT 1200 psia AND 77.0°F

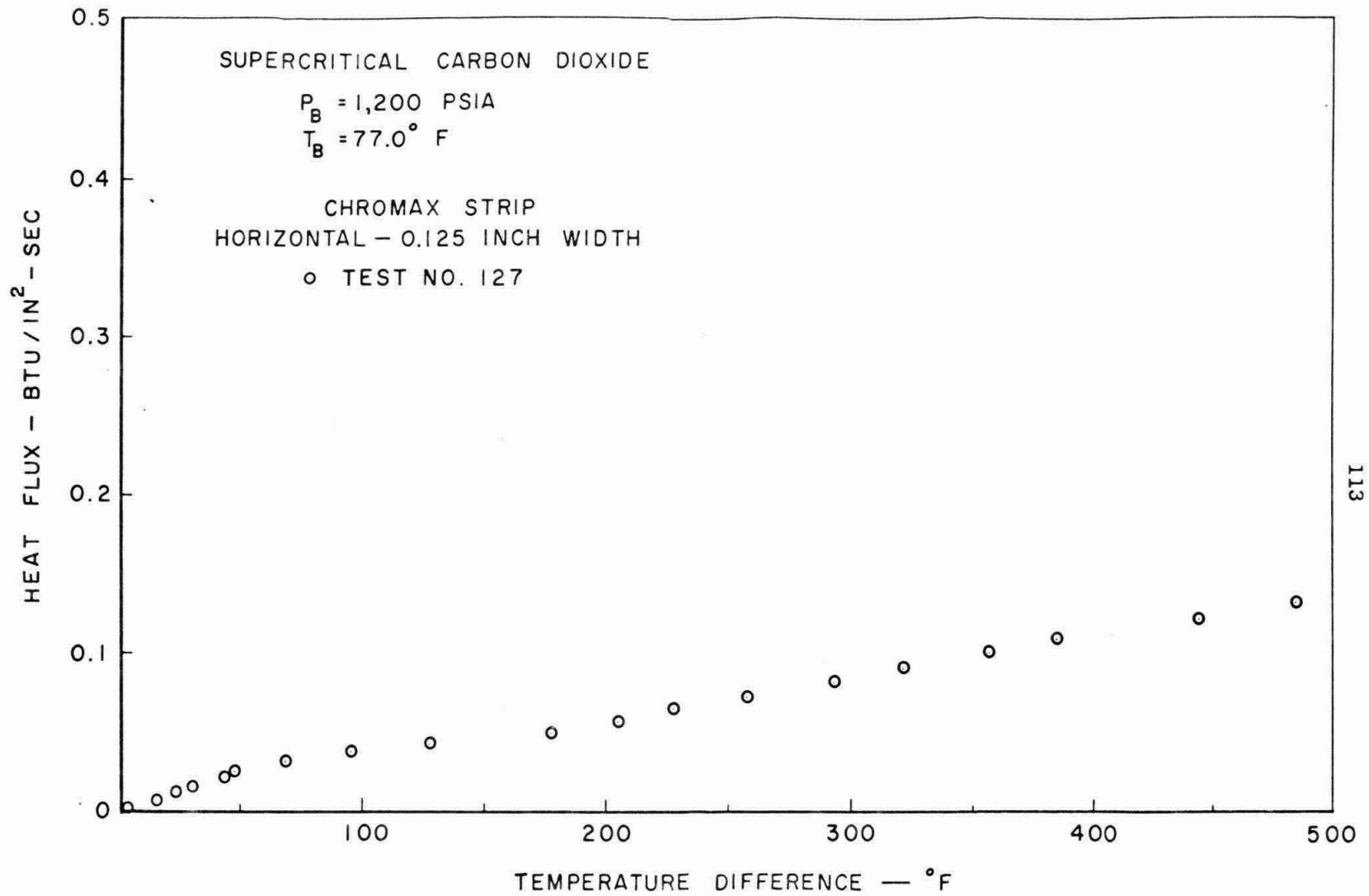


FIG. 22. FREE CONVECTION HEAT TRANSFER FROM A HORIZONTAL STRIP
 TO SUPERCRITICAL CARBON DIOXIDE AT 1200 psia AND 77.0° F

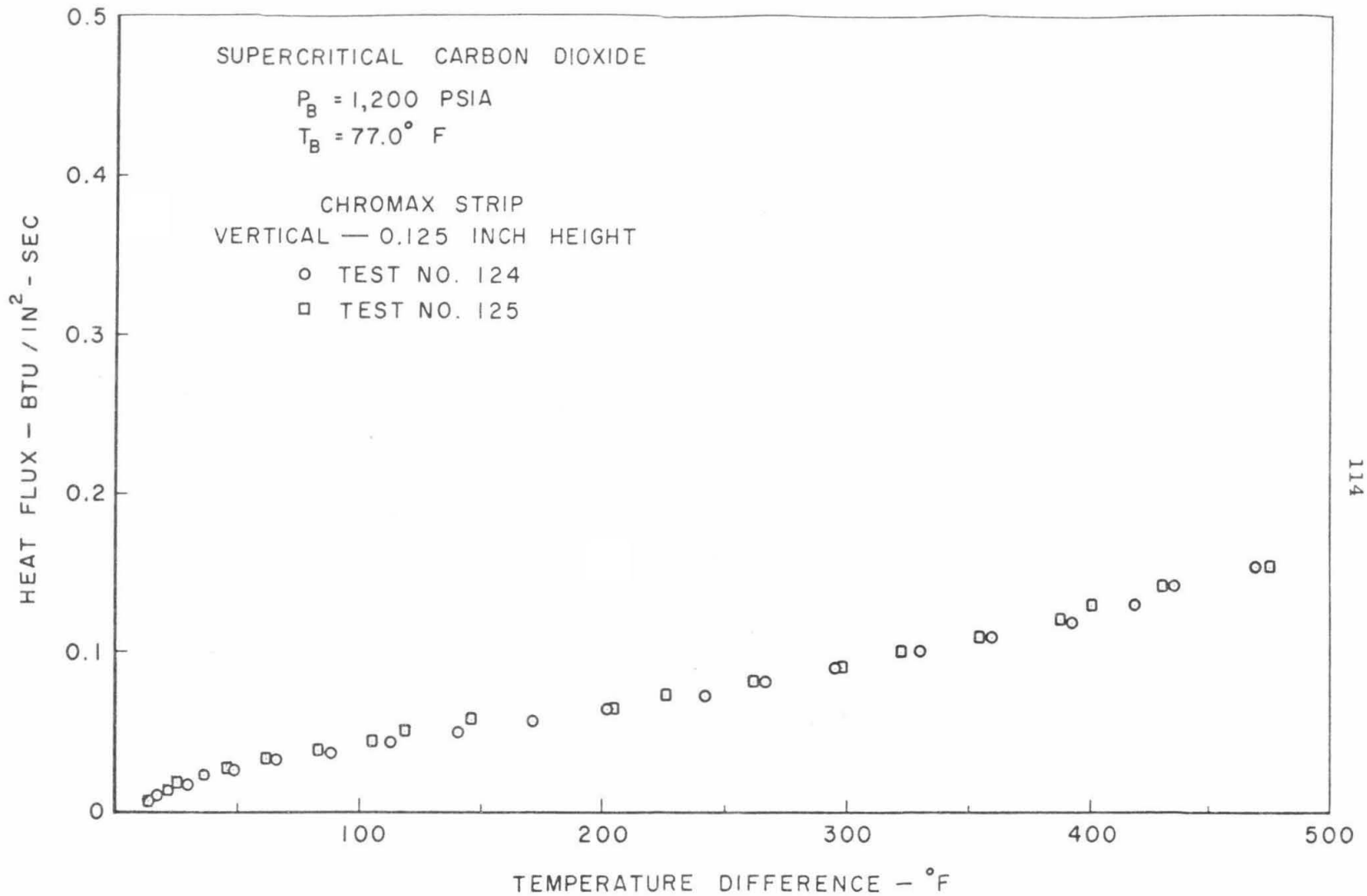


FIG. 23. FREE CONVECTION HEAT TRANSFER FROM A SHORT VERTICAL WALL TO SUPERCritical CARBON DIOXIDE AT 1200 psia AND 77.0° F

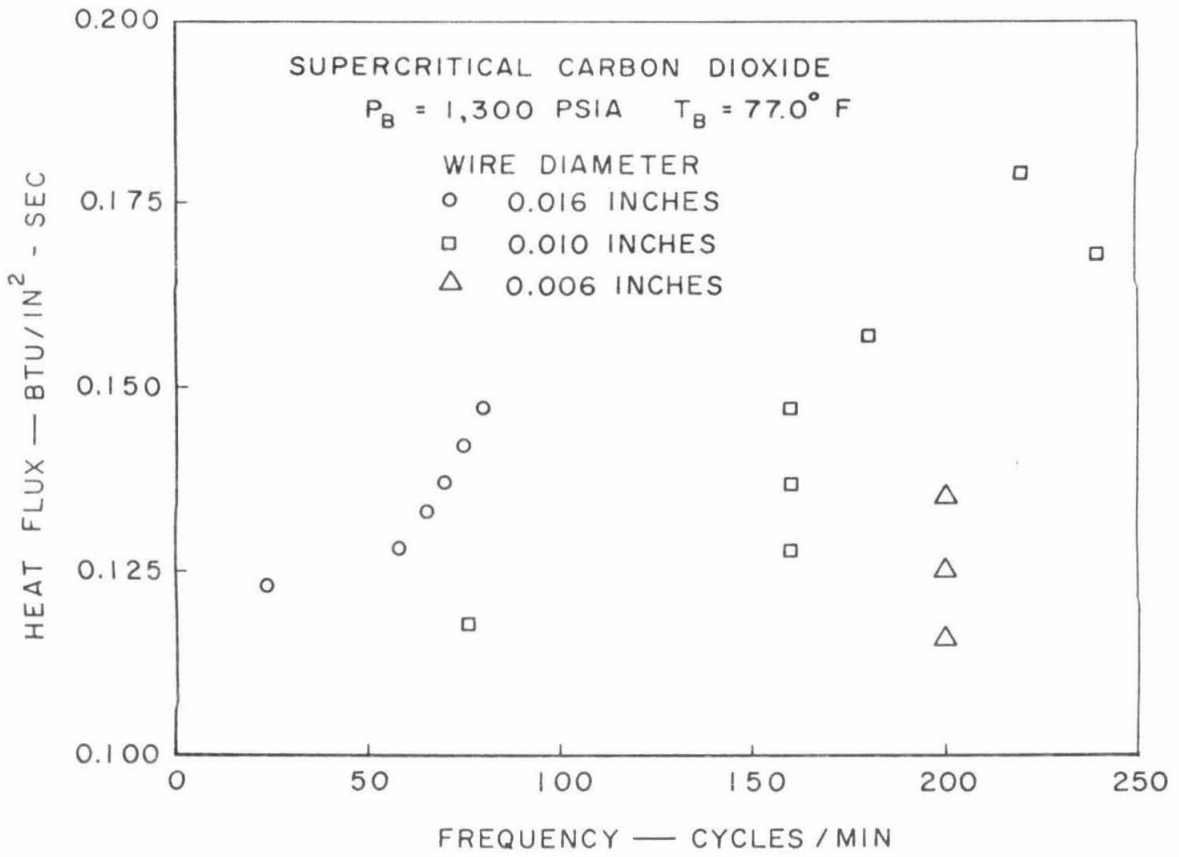
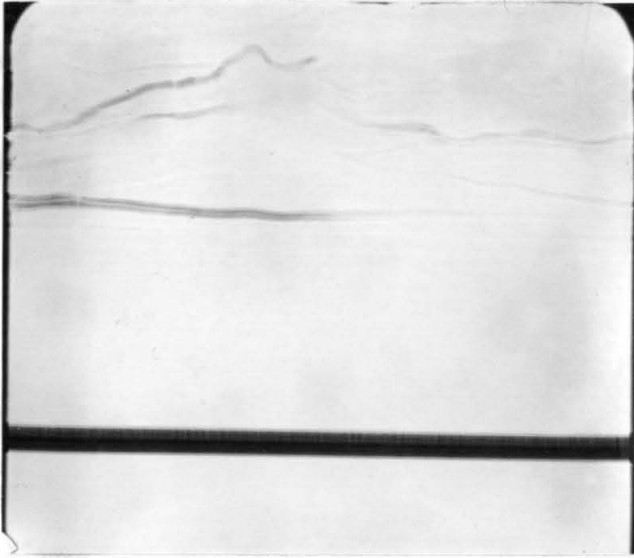


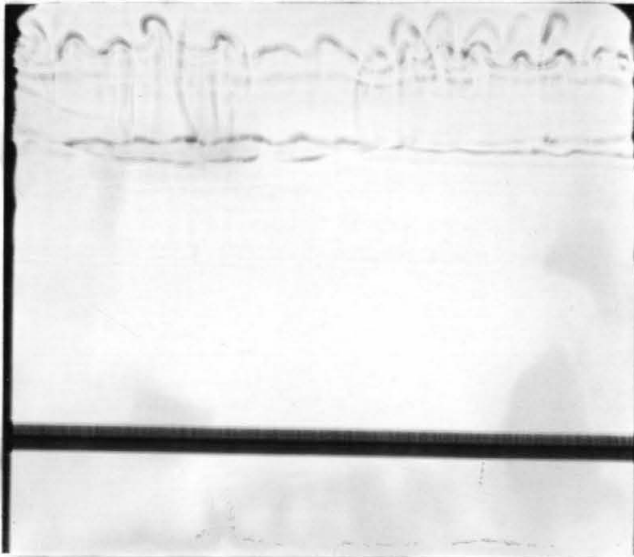
FIG. 24. THE INFLUENCE OF WIRE DIAMETER AND HEAT FLUX RATES ON THE FREQUENCY OF FLOW OSCILLATIONS WITH FREE CONVECTION HEAT TRANSFER TO SUPERCRITICAL CARBON DIOXIDE AT 1300 psia AND 77.0° F

Appendix C

FLOW PATTERN PHOTOGRAPHS



$$q = 0.05 \text{ BTU/IN.}^2\text{-SEC} \quad \Delta T = 56^\circ \text{ F}$$

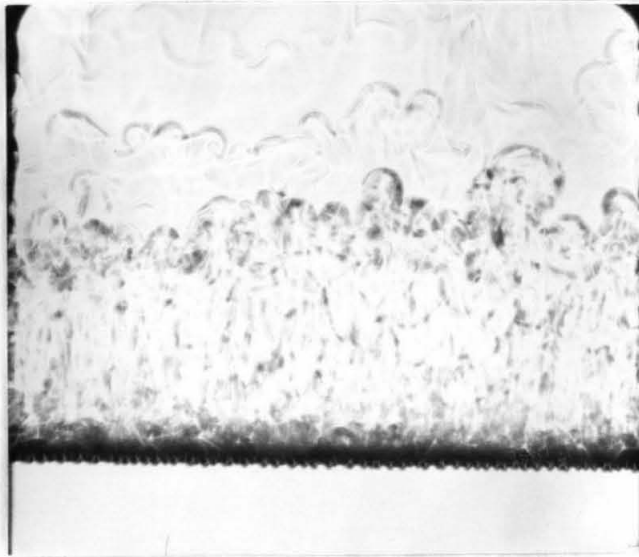


$$q = 0.075 \text{ BTU/IN.}^2\text{-SEC} \quad \Delta T = 110^\circ \text{ F}$$

FIG. 25. LAMINAR FREE CONVECTION FROM A HORIZONTAL CYLINDER
 IN SUPERCRITICAL CARBON DIOXIDE
 AT 1200 psia AND 77.0^o F
 (Wire Diameter 0.010 Inch; Image Magnified 9X)

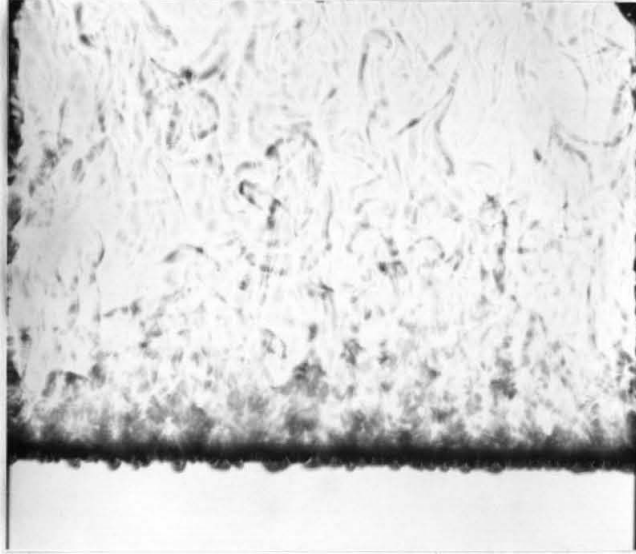


LAMINAR PHASE OF OSCILLATING FLOW CONDITION

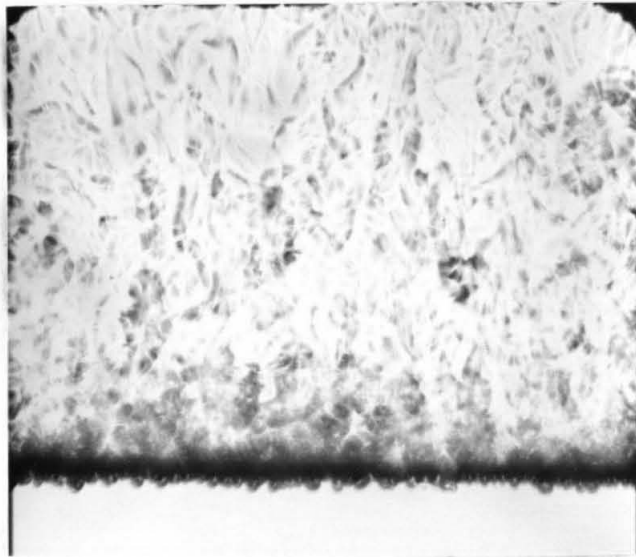


"BUBBLE-LIKE" PHASE OF OSCILLATING FLOW CONDITION

FIG. 26. OSCILLATING FLOW CONDITION WITH FREE CONVECTION FROM A
 HORIZONTAL CYLINDER IN SUPERCRITICAL CARBON DIOXIDE
 AT 1200 psia AND 77.0° F
 ($q = 0.10 \text{ Btu/in.}^2\text{-sec}$; Image Magnified 9X)

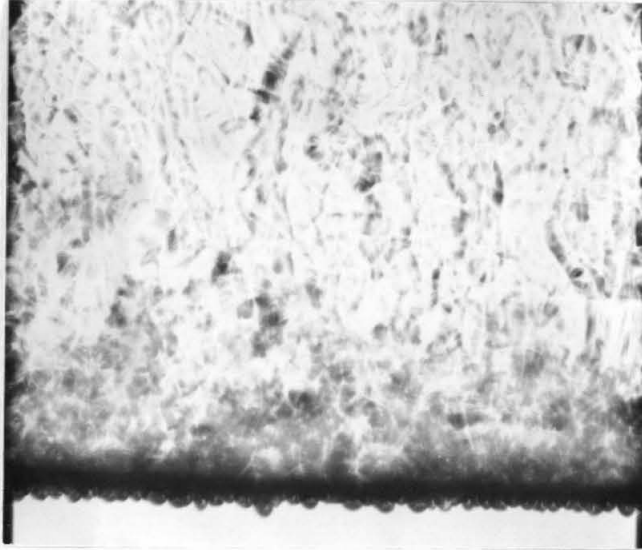


$$q = 0.15 \text{ BTU/IN.}^2\text{-SEC} \quad \Delta T = 144^\circ \text{F}$$

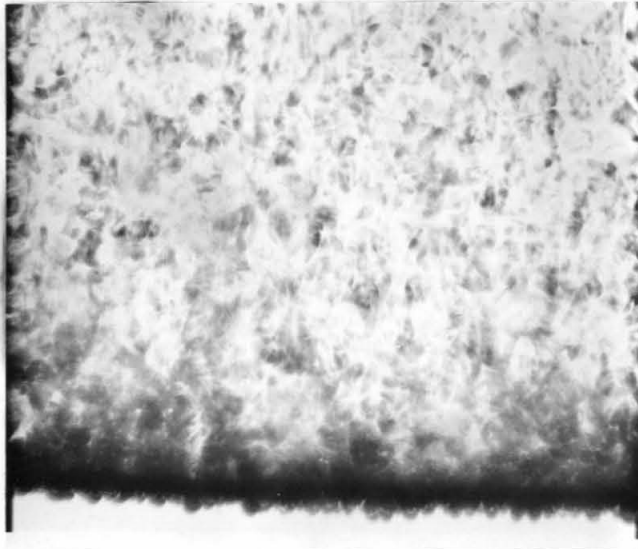


$$q = 0.20 \text{ BTU/IN.}^2\text{-SEC} \quad \Delta T = 185^\circ \text{F}$$

FIG. 27. "BUBBLE-LIKE" FLOW WITH FREE CONVECTION FROM A
 HORIZONTAL CYLINDER IN SUPERCRITICAL CARBON DIOXIDE
 AT 1200 psia AND 77.0°F
 (Wire Diameter 0.010 Inch; Image Magnified 9X)

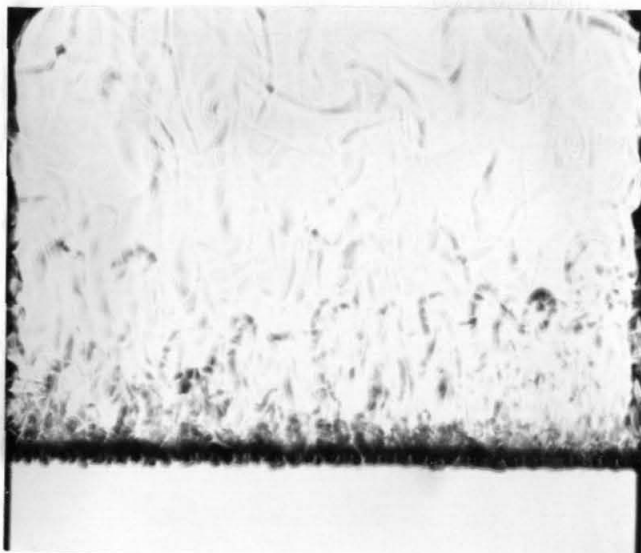


$$q = 0.30 \text{ BTU/IN.}^2\text{-SEC} \quad \Delta T = 290^\circ \text{ F}$$

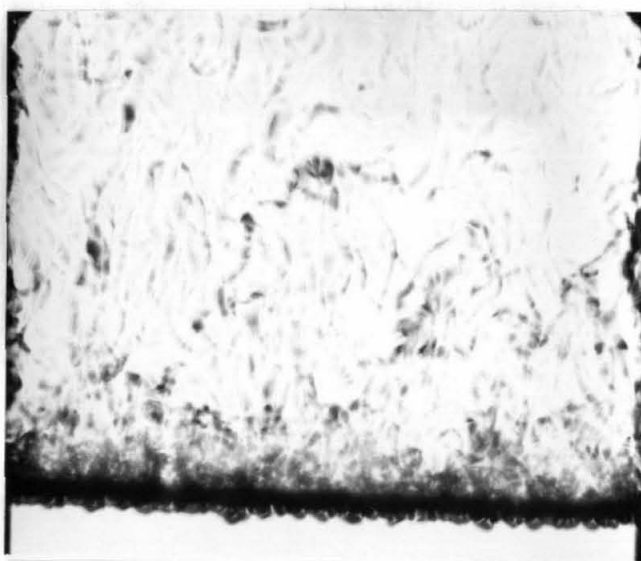


$$q = 0.40 \text{ BTU/IN.}^2\text{-SEC} \quad \Delta T = 368^\circ \text{ F}$$

FIG. 28. "BUBBLE-LIKE" FLOW WITH FREE CONVECTION FROM A
 HORIZONTAL CYLINDER IN SUPERCRITICAL CARBON DIOXIDE
 AT 1200 psia AND 77.0^o F
 (Wire Diameter 0.010 Inch; Image Magnified 9X)

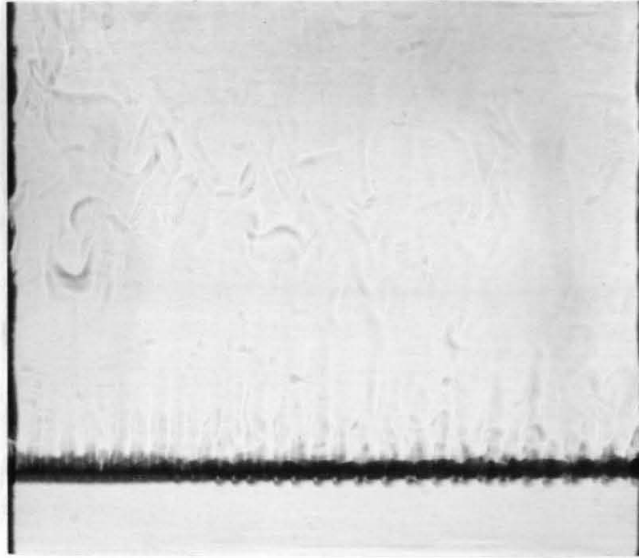


$$q = 0.20 \text{ BTU/IN.}^2\text{-SEC} \quad \Delta T = 158^\circ \text{F}$$

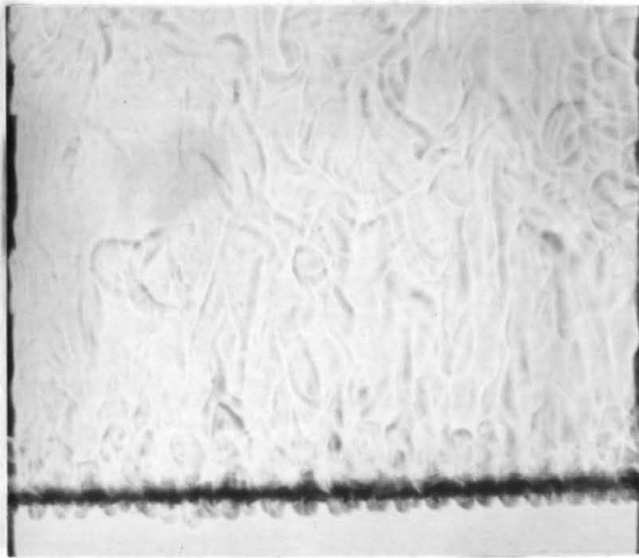


$$q = 0.40 \text{ BTU/IN.}^2\text{-SEC} \quad \Delta T = 264^\circ \text{F}$$

FIG. 29. "BUBBLE-LIKE" FLOW WITH FREE CONVECTION FROM A
 HORIZONTAL CYLINDER IN SUPERCRITICAL CARBON DIOXIDE
 AT 1500 psia AND 49.0°F
 (Wire Diameter 0.010 Inch; Image Magnified 9X)

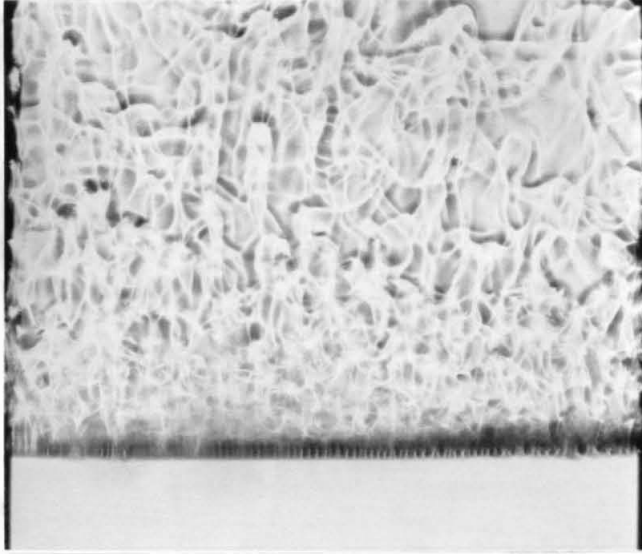


$$q = 0.05 \text{ BTU/IN.}^2\text{-SEC} \quad \Delta T = 160^\circ \text{ F}$$

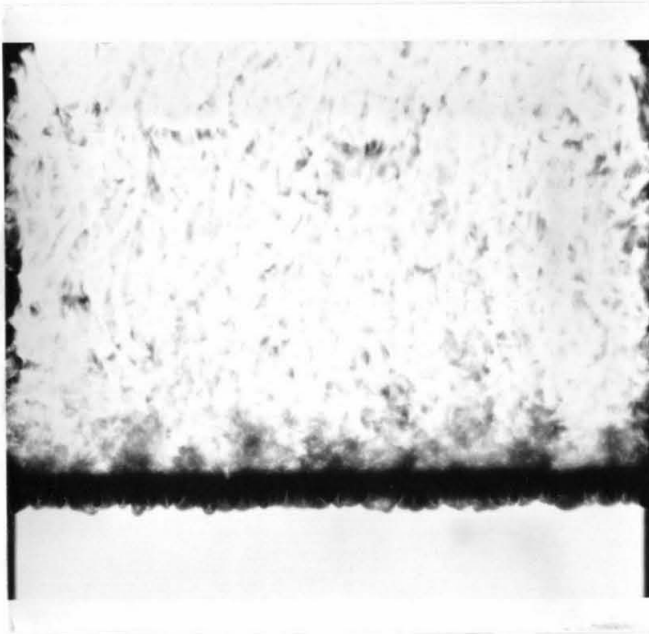


$$q = 0.15 \text{ BTU/IN.}^2\text{-SEC} \quad \Delta T = 365^\circ \text{ F}$$

FIG. 30. "BUBBLE-LIKE" FLOW WITH FREE CONVECTION FROM A
 HORIZONTAL CYLINDER IN SUPERCRITICAL CARBON DIOXIDE
 AT 1200 psia AND 137.0 °F
 (Wire Diameter 0.010 Inch; Image Magnified 9X)

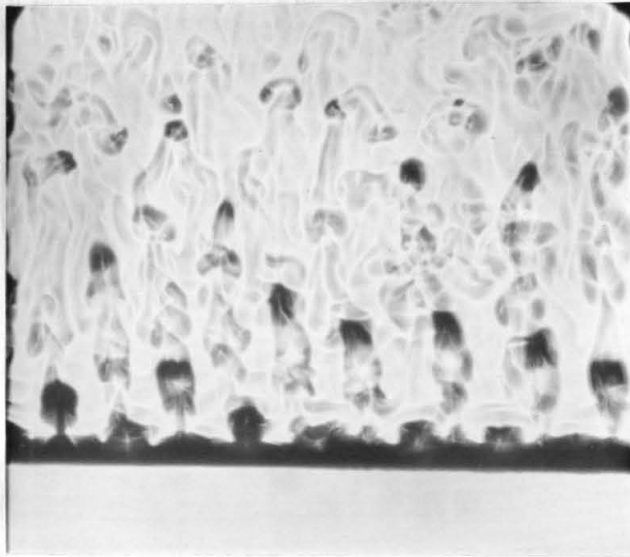


WIRE DIAMETER 0.006 INCH $q = 0.15 \text{ BTU/IN.}^2\text{-SEC}$

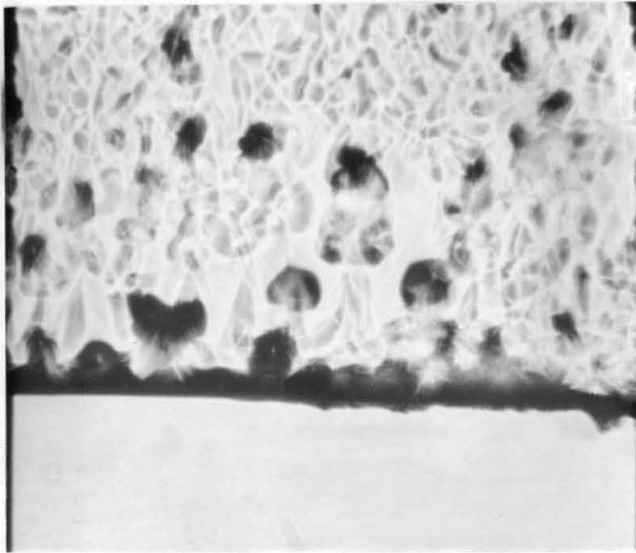


WIRE DIAMETER 0.016 INCH $q = 0.20 \text{ BTU/IN.}^2\text{-SEC}$

FIG. 31. "BUBBLE-LIKE" FLOW WITH FREE CONVECTION FROM A
 HORIZONTAL CYLINDER IN SUPERCRITICAL CARBON DIOXIDE
 AT 1200 psia AND 77.0^oF
 (Image Magnified 9X)

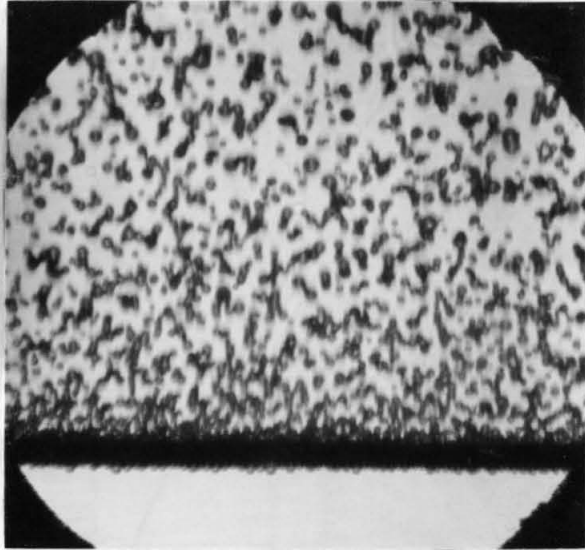


$$q = 0.10 \text{ BTU/IN.}^2\text{-SEC} \quad \Delta T = 150^\circ \text{F}$$

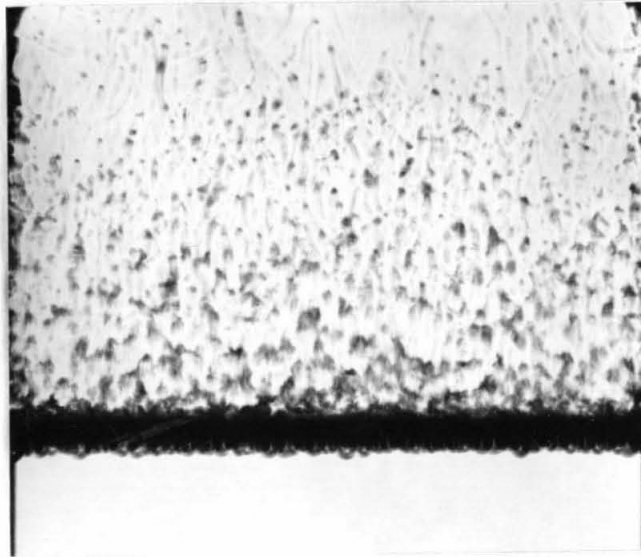


$$q = 0.20 \text{ BTU/IN.}^2\text{-SEC} \quad \Delta T = 280^\circ \text{F}$$

FIG. 32. FILM BOILING ON A HORIZONTAL CYLINDER
IN SUPERCRITICAL CARBON DIOXIDE
AT 1000 psia AND 49.0^oF
(Wire Diameter 0.010 Inch; Image Magnified 9X)

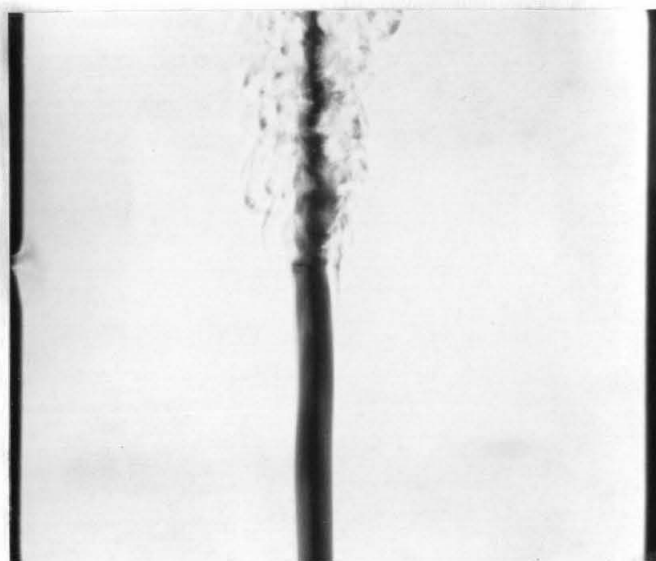


WIRE DIAMETER 0.010 INCH

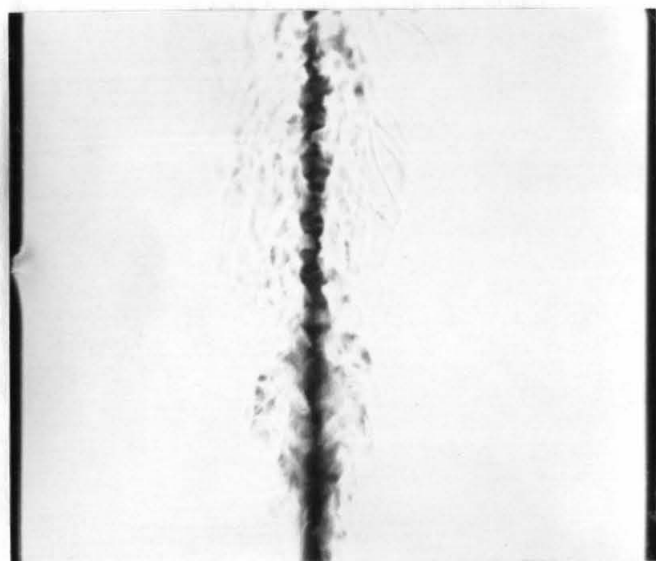


WIRE DIAMETER 0.016 INCH

FIG. 33. NUCLEATE BOILING ON A HORIZONTAL CYLINDER
IN SUBCRITICAL CARBON DIOXIDE
(Image Magnified 9X)

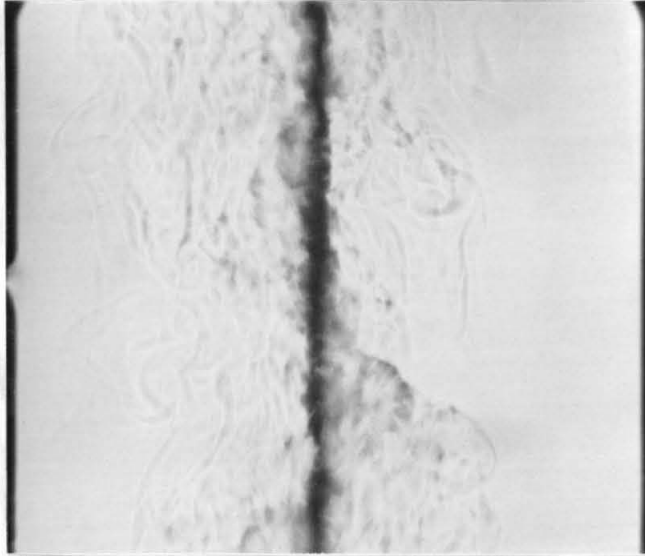


TWO PHOTOS OF THE TRANSITION TO TURBULENT
FLOW AT THE SAME HEAT FLUX

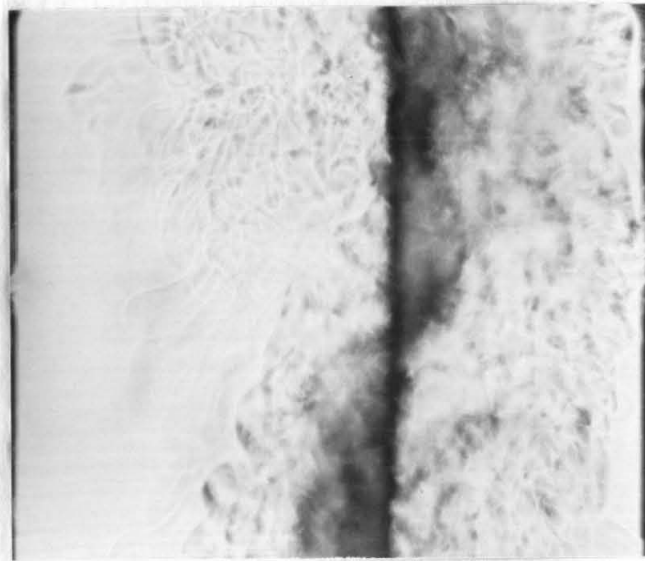


$$q = 0.02 \text{ BTU/IN.}^2\text{-SEC} \quad \Delta T = 21^{\circ} \text{ F}$$

FIG. 34. FREE CONVECTION ALONG A VERTICAL WIRE IN SUPERCRITICAL
CARBON DIOXIDE AT 1200 psia AND 77.0^o F
(Center of 2-Inch Height; Image Magnified 9X)

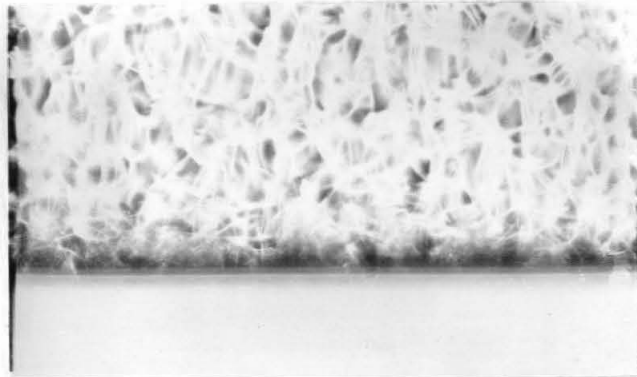


$$q = 0.10 \text{ BTU/IN.}^2\text{-SEC} \quad \Delta T = 115^{\circ}\text{F}$$

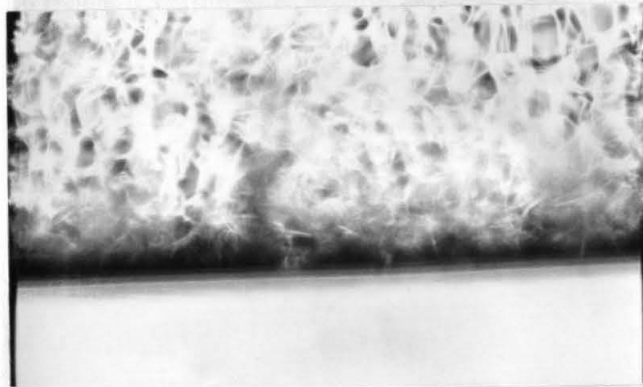


$$q = 0.30 \text{ BTU/IN.}^2\text{-SEC} \quad \Delta T = 312^{\circ}\text{F}$$

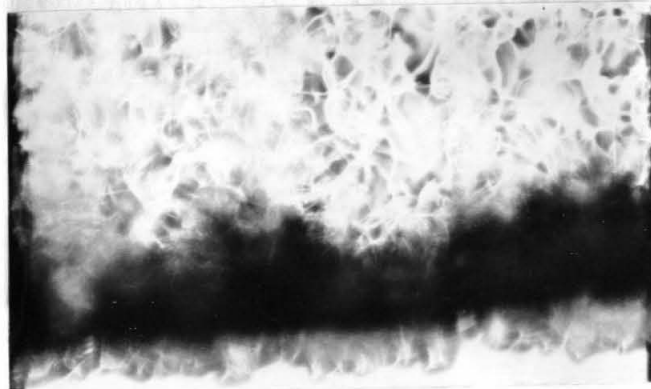
FIG. 35. FREE CONVECTION ALONG A VERTICAL WIRE IN SUPERCRITICAL CARBON DIOXIDE AT 1200 psia AND 77.0°F (Center of 2-Inch Height; Image Magnified 9X)



$$q = 0.025 \text{ BTU/IN.}^2\text{-SEC} \quad \Delta T = 58^{\circ} \text{ F}$$

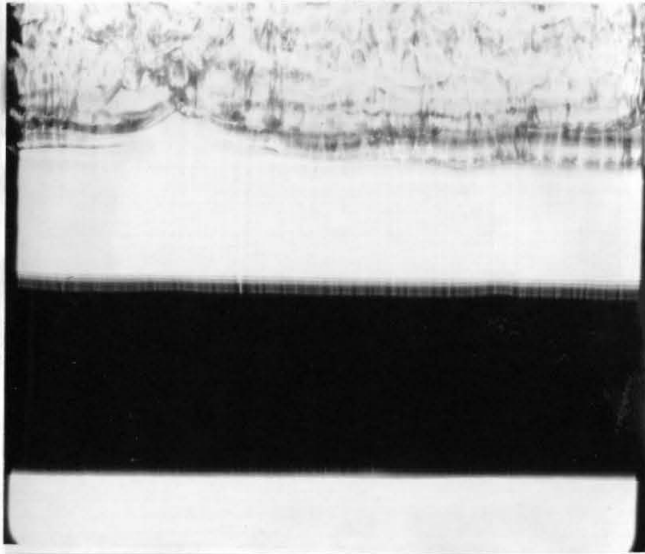


$$q = 0.05 \text{ BTU/IN.}^2\text{-SEC} \quad \Delta T = 168^{\circ} \text{ F}$$

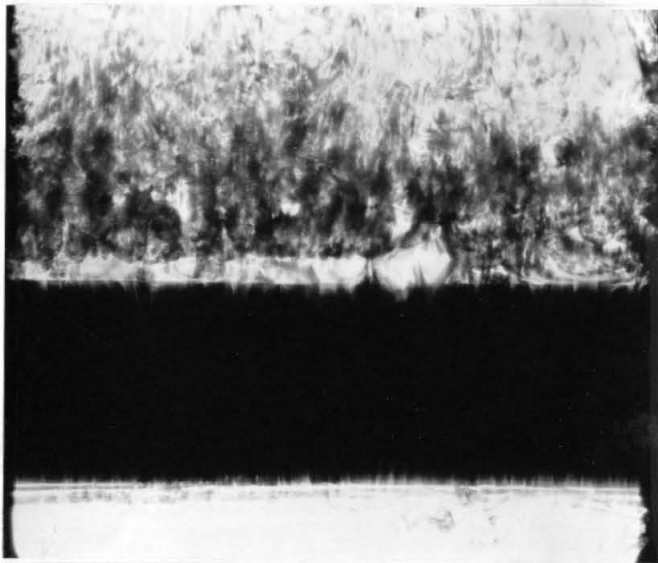


$$q = 0.10 \text{ BTU/IN.}^2\text{-SEC} \quad \Delta T = 405^{\circ} \text{ F}$$

FIG. 36. FREE CONVECTION FROM A HORIZONTAL STRIP
 IN SUPERCRITICAL CARBON DIOXIDE
 AT 1200 psia AND 77.0°F
 (Strip Width 0.125 Inch; Image Magnified 9X)



$$q = 0.05 \text{ BTU/IN.}^2\text{-SEC} \quad \Delta T = 173^\circ \text{F}$$

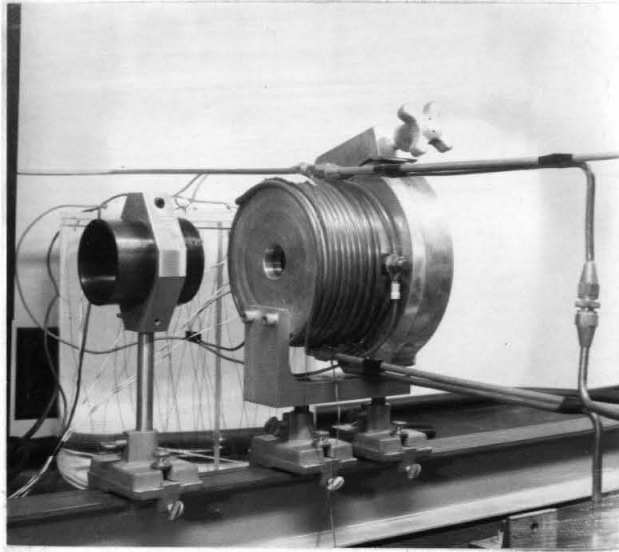


$$q = 0.10 \text{ BTU/IN.}^2\text{-SEC} \quad \Delta T = 415^\circ \text{F}$$

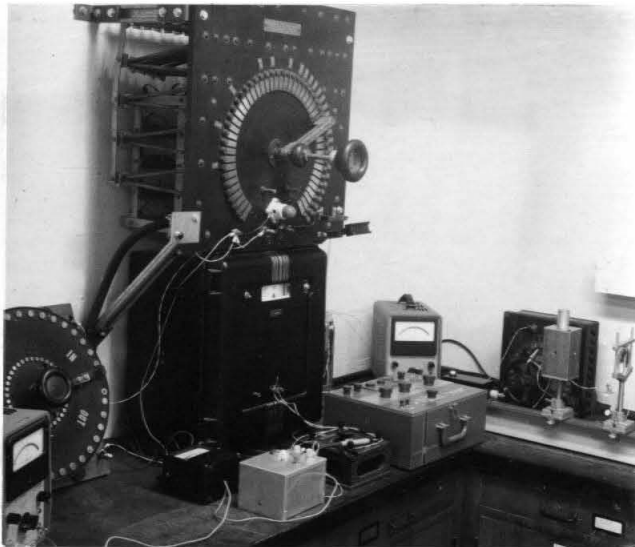
FIG. 37. FREE CONVECTION FROM A SHORT VERTICAL WALL
TO SUPERCRITICAL CARBON DIOXIDE
AT 1200 psia AND 77.0°F
(Height 0.125 Inch; Image Magnified 9X)

Appendix D

APPARATUS

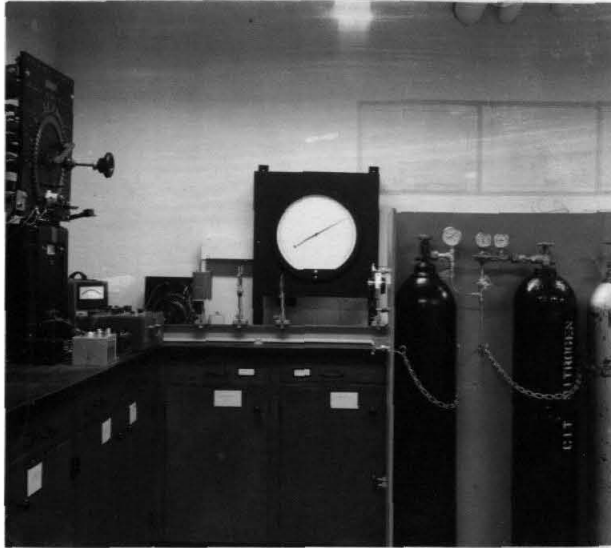


TEST CHAMBER

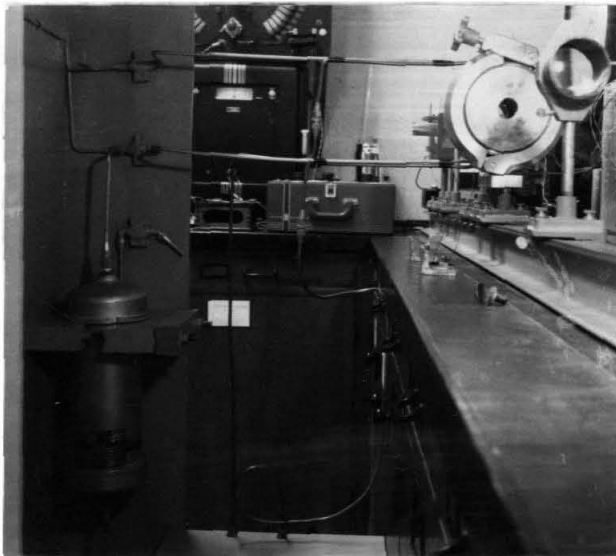


GENERAL VIEW OF INSTRUMENTATION

FIG. 38A. PHOTOGRAPHS OF THE APPARATUS



PRESSURE GAUGE AND GAS CYLINDERS



TEST CHAMBER ON OPTICAL BENCH
HYDRAULIC ACCUMULATOR

FIG. 38B. PHOTOGRAPHS OF THE APPARATUS

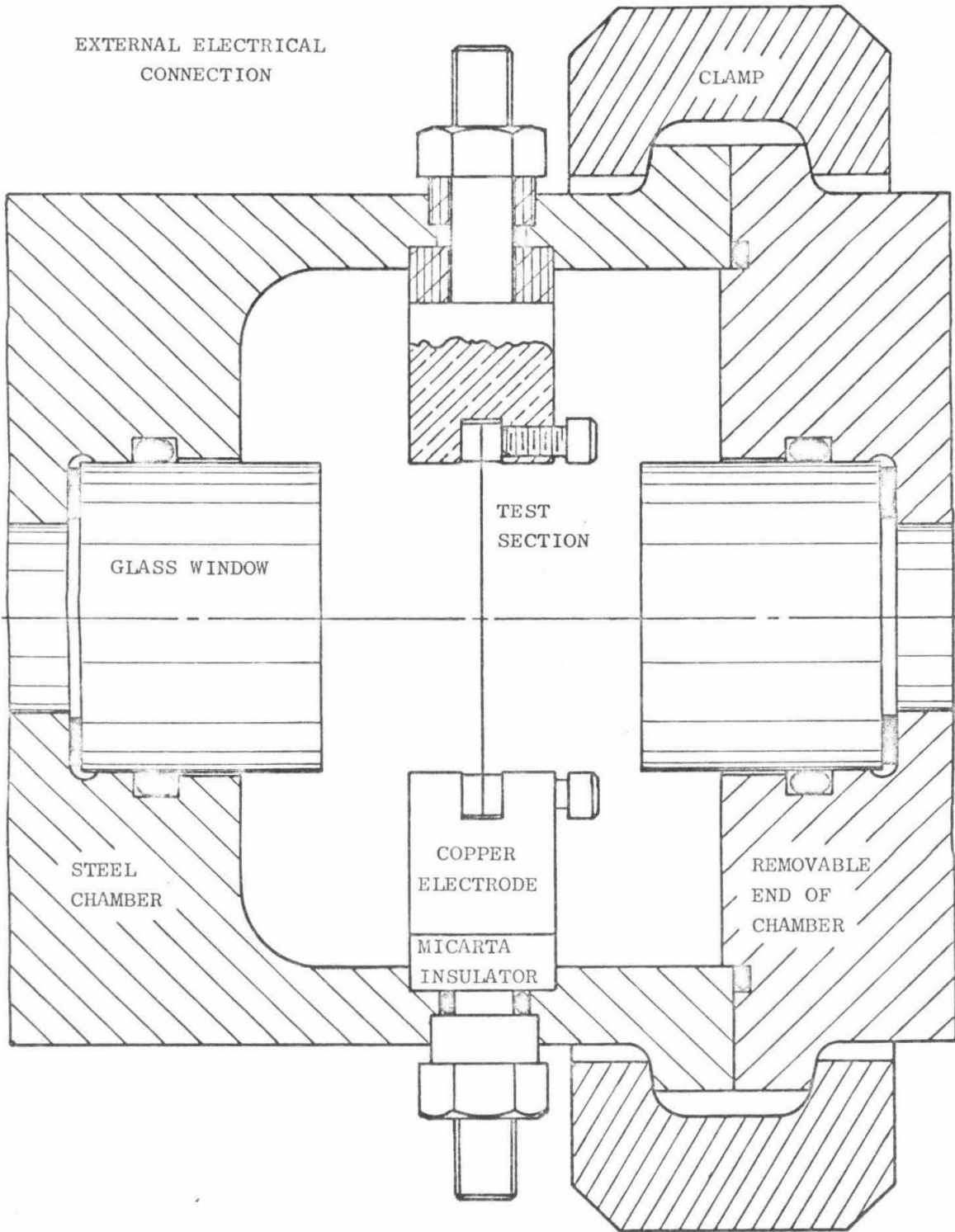
EXTERNAL ELECTRICAL
CONNECTION

FIG. 39. DRAWING OF THE TEST CHAMBER

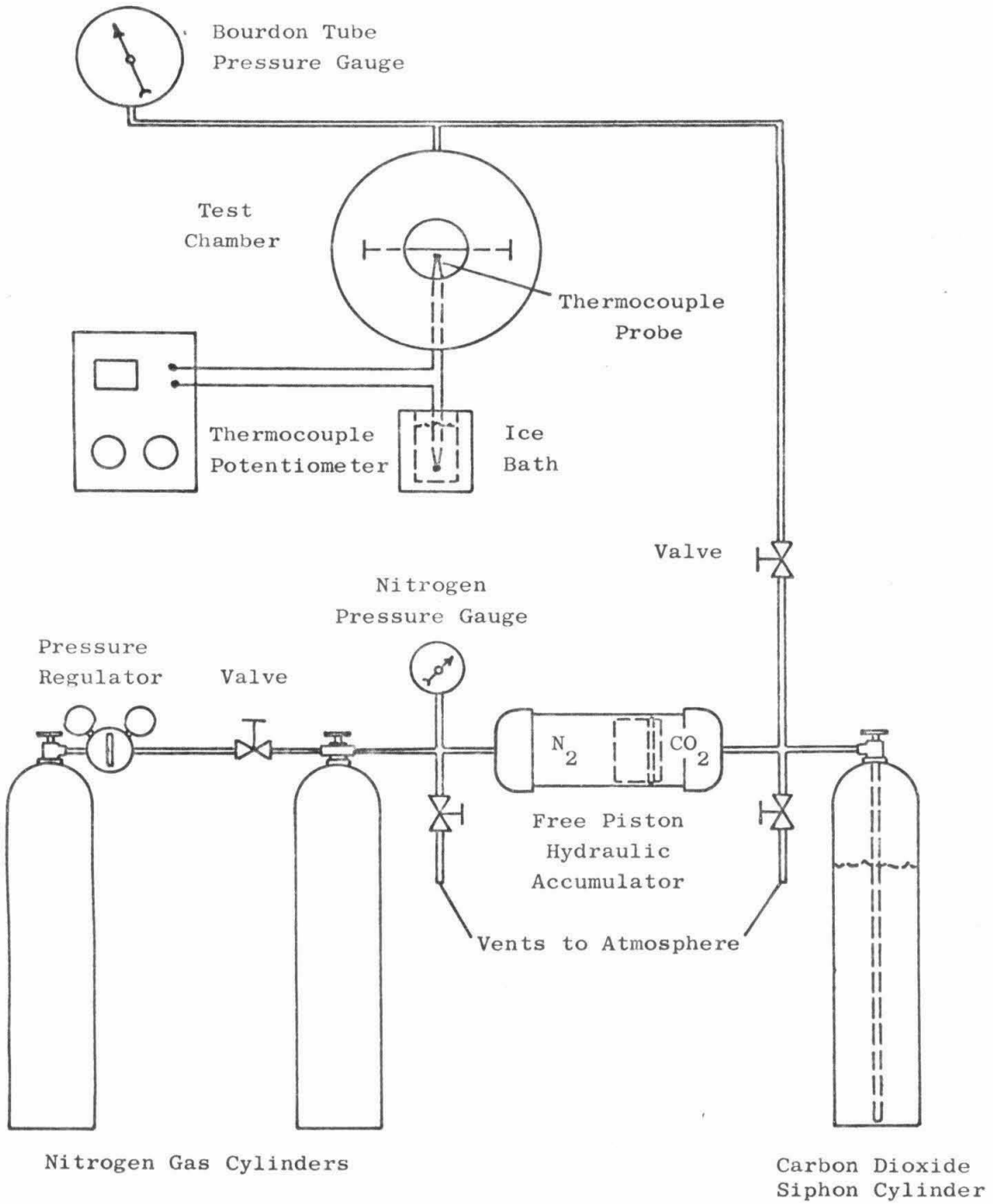


FIG. 40. SCHEMATIC DRAWING OF THE APPARATUS

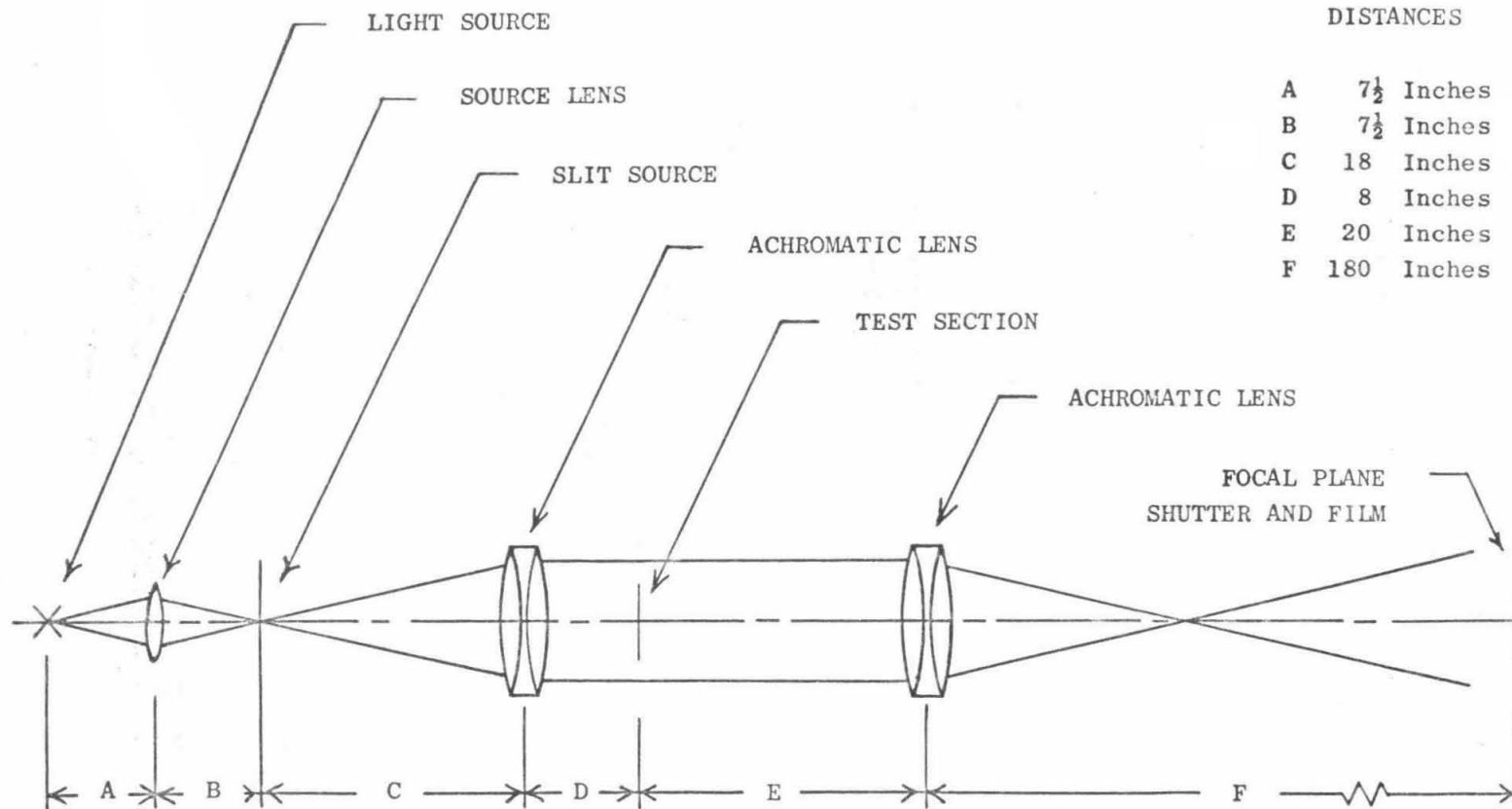


FIG. 41. SCHEMATIC DRAWING OF THE SHADOWGRAPH OPTICS

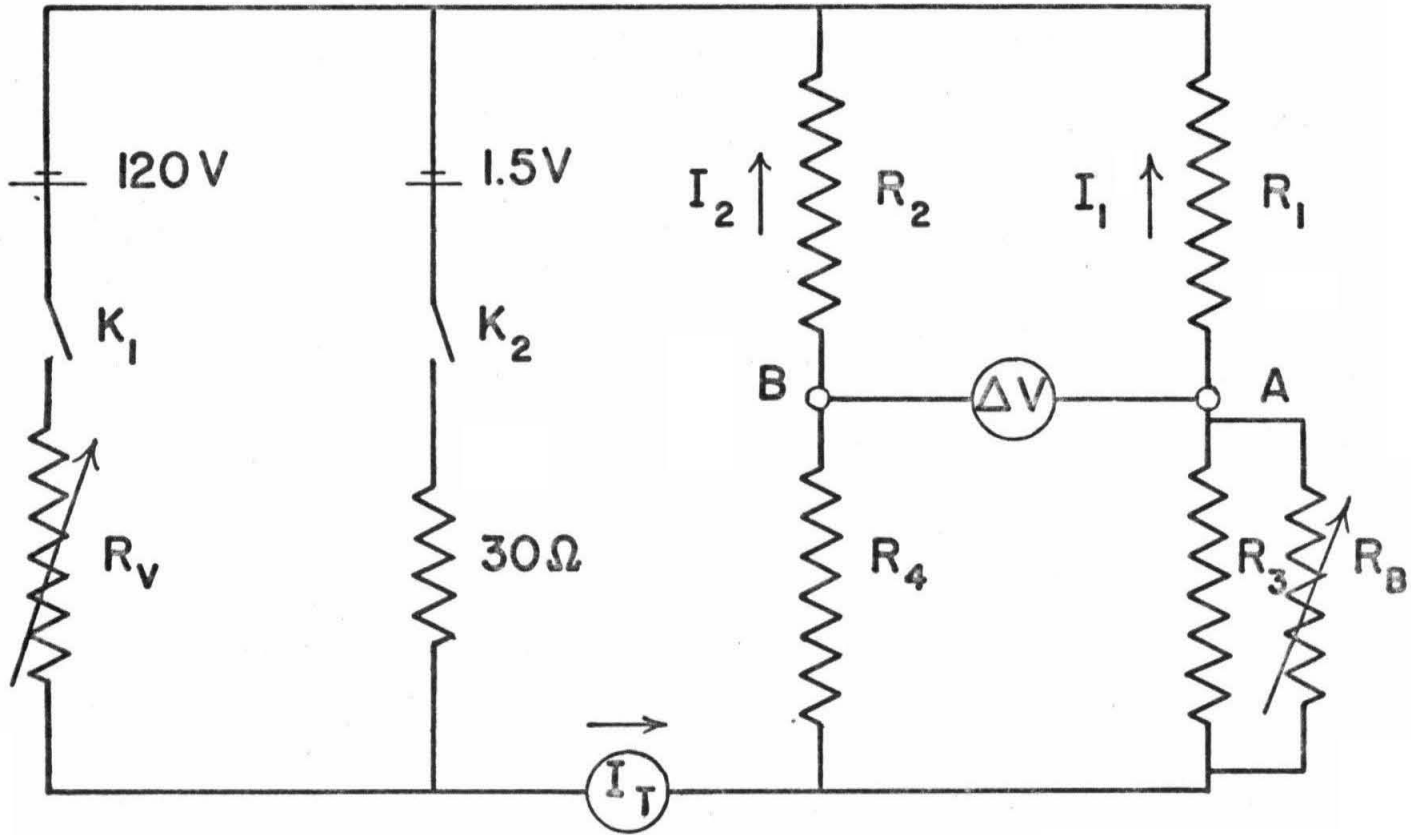


FIG. 42. WHEATSTONE BRIDGE CIRCUIT

Appendix E

WHEATSTONE BRIDGE CIRCUIT

Appendix E

WHEATSTONE BRIDGE CIRCUIT

A diagram of the Wheatstone bridge circuit employed in this investigation appears as Figure 42 in Appendix D. The value for the electrical resistance of each Wheatstone bridge leg in the tests with the 0.010-inch-diameter Nichrome wire is 1.258 ohms. In the tests with the Chromax strip the resistance leg values were each 0.827 ohm.

Three of the bridge's resistance legs remain constant in their resistance values while the fourth leg, the heat transfer test section, changes resistance as its temperature changes. For the range of temperatures used in this investigation, the resistance of the test section can be expressed by

$$R_1 = R_0 + \Delta R = R_0 (1 + \alpha \Delta T) \quad (1)$$

where α is the temperature coefficient of resistivity for the test section material, ΔT is the change in temperature of the test section, and R_0 is the resistance of the test section at the original temperature.

If the switch K_2 in Figure 42 is closed so that a small current, i , (0.05 amp) passes through the bridge, then the large variable resistor, R_B , which forms part of R_3 , can be adjusted until the voltages at A and B are equal (a null reading on the microvoltmeter). This current is so small that the temperature change of the test section is a small fraction of 1°F . This balancing procedure assures that

$$\frac{R_0}{R_3} = \frac{R_2}{R_4} \quad (2)$$

so that, if the test section remains at the temperature of the bulk fluid, there will be no voltage difference between A and B regardless of the current through the circuit. Any subsequent change in the temperature of the test section, ΔT , will now be identical to the temperature difference between the test section and the bulk fluid.

Consider now a situation where the switch K_1 is closed and an electrical current, I_t , controlled by the rheostat R_v , flows through the bridge. Assume that the test section resistance changes by an amount ΔR while a current I_1 passes through the test section and the resistance leg R_3 . If another current I_2 flows through the resistance

legs R_2 and R_4 then

$$I_1 + I_2 = I_t \quad (3)$$

Since these parallel resistance circuits have common junctions on each side, the voltage drop must be equal for both; therefore,

$$I_2 (R_2 + R_4) = I_1 (R_1 + R_3) \quad (4)$$

or

$$I_2 = I_1 \left(\frac{R_1 + R_3}{R_2 + R_4} \right)$$

The voltage difference between A and B is given by

$$\Delta V = V_A - V_B = I_1 R_1 - I_2 R_2 \quad (5)$$

Substituting for I_2 from equation (4)

$$\Delta V = \frac{I}{R_2 + R_4} (R_1 R_4 - R_3 R_2) \quad (6)$$

Substituting equations (1) and (2) for R_1 and $R_2 R_3$

$$\Delta V = \frac{I}{R_2 + R_4} (R_4 \Delta R) = \frac{I_1}{R_2 + R_4} (R_4 R_0 \alpha \Delta T) \quad (7)$$

Therefore, since $R_2 \cong R_4$

$$\Delta R = \frac{\Delta V}{I_1} \frac{R_2 + R_4}{R_4} \cong \frac{2\Delta V}{I_1} \quad (8a)$$

and

$$\Delta T = \frac{\Delta V}{I_2 \alpha} \frac{R_2 + R_4}{R_4 R_0} \cong \frac{2\Delta V}{I_2 \alpha R_0} \quad (8b)$$

This equation makes it possible to determine the temperature difference between the heated wire and the bulk fluid by measuring the voltage imbalance, ΔV , across the Wheatstone bridge.

Appendix F

CALCULATIONS AND ERROR ANALYSIS

Appendix F

CALCULATIONS AND ERROR ANALYSIS

A. Heat Flux Rate1. Nichrome Wire

	<u>Measurement</u>	<u>Minimum Accuracy</u>
Wire diameter, D	0.0100 inch	2.0%
Installed length, L	2.15 inches	1.0%
Installed resistance, R ₀	1.258 ohms	0.2%
Test section current, I ₁	(amperes)	0.5%

Heat flux rate,

$$q = \frac{R_0}{\pi LD} I_1^2 = 18.6 I_1^2 \text{ watts/in.}^2 = 0.0175 I_1^2 \text{ Btu/in.}^2\text{-sec.}$$

Maximum possible error in q,

$$\frac{\delta q}{q} = \frac{\delta R_0}{R_0} + \frac{\delta L}{L} + \frac{\delta D}{D} + \frac{2\delta I_1}{I_1} = 4.2\%$$

The 3.2% maximum possible error due to the measurement of the quantities D, L, and R₀ would be constant throughout the tests with the 0.010-inch-diameter Nichrome wire since the same test section was used for all the data presented. There is an additional error in the

heat flux rate calculation due to the change of resistance of the test section during heating. This correction can be calculated from the temperature difference, ΔT , between the wire and the bulk fluid:

$$\frac{\Delta q}{q} = \frac{\Delta R}{R_0} = \alpha \Delta T$$

where the temperature coefficient of resistance for Nichrome is

$$\alpha = 8.25 \times 10^{-5} \text{ } ^\circ\text{F}^{-1}$$

For a temperature difference of 120°F this correction, Δq , would be equal to 1% of the heat flux rate, q . About 15% of this correction is not required as the linear expansion of the wire slightly increases the heat transfer area.

2. Chromax Strip

	<u>Measurement</u>	<u>Minimum Accuracy</u>
Strip width, W	0.125 inch	1.0%
Installed length, L	2.08 inches	1.0%
Installed resistance, R_0	0.827 ohm	0.3%
Test section current, I_1	(amperes)	0.5%

Heat flux rate,

$$q = \frac{R_0}{2LW} I_1^2 = 1.59 I_1^2 \frac{\text{watt}}{\text{in.}^2} = 0.00149 I_1^2 \text{ Btu/in.}^2\text{-sec.}$$

Maximum possible error in q ,

$$\frac{\delta q}{q} = 3.3\%$$

Temperature coefficient of resistance for Chromax

$$\alpha = 2.12 \times 10^{-4} \text{ } ^\circ\text{F}^{-1}$$

For a temperature difference of 47°F the temperature correction, Δq , would be equal to 1% of the heat flux rate, q .

B. Temperature Difference

1. Nichrome Wire

	<u>Measurement</u>	<u>Minimum Accuracy</u>
Installed resistance, R_0	1.258 ohms	0.2%
Temperature coefficient of resistance, α	$8.25 \times 10^{-5} \text{ } ^\circ\text{F}^{-1}$	0.5%
Voltage difference, ΔV	(millivolts)	0.1%
Test section current, I_1	(amperes)	0.5%
Temperature difference,		

$$\Delta T = \frac{2\Delta V}{I_1 \alpha R_0} = 1.93 \left(\frac{\Delta V}{I_1} \right) ^\circ\text{F}$$

Maximum possible error in ΔT due to measurements,

$$\frac{\delta(\Delta T)}{\Delta T} = 2.2\%$$

The accuracy of the ΔV measurement is determined by the steadiness of the heat transfer process. Maximum error can be expected for measurements taken with the oscillating flow condition, where the recorded value of ΔV was averaged while fluctuations up to 15% of the average value were occurring. The accuracy of the Leeds & Northrup Speedomax millivolt potentiometer is 0.1% for a steady reading.

There is an additional possibility of error in ΔT resulting from any inaccuracy in the initial balance of the Wheatstone bridge. The bridge was balanced with a 0.05-ampere current while the large variable resistor across R_3 was adjusted until the electronic microvoltmeter shows less than 1 microvolt deflection from null. The maximum error which could result from this procedure would be

$$\delta(\Delta T) = \frac{1.93 \times 10^{-3}}{0.05} = 0.04^{\circ}\text{F}$$

which is negligibly small compared with the measurement errors and which is smaller than the allowed deviations of 0.1°F in the bulk temperature of the carbon dioxide. The bridge balance was checked after every three or four data points to adjust for small changes in the bulk temperature.

2. Chromax Strip

	<u>Measurement</u>	<u>Minimum Accuracy</u>
Installed resistance, R_0	0.827 ohm	0.3%
Temperature coefficient of resistance, α	2.12×10^{-4}	0.7%
Voltage difference, ΔV	(millivolts)	1.0%
Test section current, I_1	(amperes)	0.5%
Temperature difference,		

$$\Delta T = \frac{2\Delta V}{I_1 \alpha R_0} = 1.14 \left(\frac{\Delta V}{I_1} \right) \text{ } ^\circ \text{F}$$

Maximum possible error in ΔT ,

$$\frac{\delta(\Delta T)}{\Delta T} = 2.5\%$$

C. Interpretation of ΔT

The temperature difference, ΔT , has been described as the difference between the temperature of the wire and the bulk fluid temperature. No distinction has been made between the mean temperature of the wire, which is measured by the change of resistance of the test section, and the wire surface temperature. There is, in fact, a small difference between these two temperatures resulting from a radial temperature gradient in the wire.

An estimation of the difference between the mean wire temperature and the surface temperature can be made by solving the heat conduction equation for an infinitely long cylinder with uniform internal heat generation under the assumption of a uniform heat flux through the wire surface. The steady state heat conduction equation for this case can be written in the following form:

$$\frac{d^2\theta}{dr^2} + \frac{1}{r} \frac{d\theta}{dr} + \frac{Q}{k} = 0$$

where θ is the difference between the local temperature and the surface temperature, r is the radial distance measured from the center, k is the thermal conductivity of the material, and Q is the heat generation rate per unit volume.

The solution of this equation is given by:

$$\theta = \frac{Qr_0^2}{4k} \left(1 - \frac{r^2}{r_0^2} \right)$$

where r_0 is the radius of the wire.

Integrating over a cross section of the cylindrical wire we can obtain the difference between the mean temperature of the wire and the surface temperature:

$$\theta_m = T_m - T_s = \frac{Qr_0^2}{8k} = \frac{RI_1^2}{8\pi Lk}$$

For the Nichrome wire this temperature difference amounts to 3^oF for the maximum heat flux used in the experiments (0.44 Btu/in.²-sec). This temperature difference is proportionally smaller for lower heat fluxes.

Axial variations in the wire temperature due to heat conduction through the ends of the wire are very small, except near the electrodes, due to the high length-to-diameter ratio of the test section and the generally high heat transfer coefficients encountered in this investigation. A discussion and analysis of the axial temperature distribution in a similar test section appears as Appendix 3, p. 1849, of

Reference 23. Calculations for this investigation indicate that the difference between the temperature at the midpoint of the wire and the average temperature of the wire was always less than 0.1% of the temperature measurement.

D. Carbon Dioxide Pressure and Temperature

The accuracy of the Heise Bourdon tube gauge used in this investigation is 0.1% of full scale, or 1.5 psi as calibrated against a deadweight tester. The pressure was kept within a similar tolerance of each desired test pressure, so that the maximum error in the pressure would not exceed 3.0 psi, or about 0.25% of the test pressure.

The accuracy of the thermocouple potentiometer used with the copper-constantin thermocouple couples is better than 0.2°F for the temperatures measured in this investigation. Since the bulk temperature of the carbon dioxide, as measured by a probe $\frac{1}{4}$ inch below the test section, was allowed to vary as much as 0.1°F in the indicated reading, the total maximum error in the temperature at the probe would not exceed 0.3°F .

Since the tests were delayed every three or four data points to re-establish the bulk temperature and to check the balance of the Wheatstone bridge, the thermocouple probe measurements should give an accurate indication of the temperature of the bulk fluid for the horizontal test sections. In the case of the vertical wire experiment, however, the thermocouple probe measures a temperature at the center only, and there undoubtedly is a difference of several degrees between the bulk temperatures near the bottom and the top of the wire.

E. Expansion of the Test Section

At large temperature differences the change of length of the test section causes some bending along the length of the wire. This bending was usually symmetrical about the center of the test section, but somewhat random in direction. In cases where the bending occurred in the vertical plane, the center of the test section was observed to move several diameters above or below the original position. This would indicate that the wire was not exactly horizontal at higher temperature differences. The change in length of the Nichrome test section would be about 0.010 inch for a change of temperature of 500^o F. This change of length would correspond to a change in slope of less than 1% which would not be expected to have a major effect on the heat transfer.

F. Summary of Experimental Errors

The largest error in this investigation occurs in the heat flux calculation. The size of the maximum possible error in the values calculated for the heat flux varies from 4% at low temperature differences to 7% at high temperature differences. By comparison, the size of the maximum possible error in the temperature difference is about 3% including the error due to using the mean wire temperature instead of the surface temperature. Deviations from the desired bulk state conditions of the carbon dioxide, and changes due to the bending of the wire, do not appear to have a significant effect on the heat transfer results.

Appendix G

LIMIT CYCLE MODEL FOR OSCILLATING FLOW CONDITION

Appendix G

LIMIT CYCLE MODEL FOR OSCILLATING FLOW CONDITION

An oscillating flow condition, described and discussed in Sections VI and VII, was observed with heat transfer to supercritical carbon dioxide from horizontal wires of three different diameters. The oscillating flow condition occurs at intermediate heat flux rates between the laminar flow condition and the "bubble-like" flow condition, and consists of an oscillation between these two flow conditions with a frequency of 20 to 200 cycles per minute. These oscillations occur with a constant heat input into the wire, and they are accompanied by simultaneous oscillations in the wire temperature.

It appears that, for the range of heat flux rates in which the oscillating flow condition is observed, there is no single flow and heat transfer condition which will steadily balance the heat input into the wire. The "bubble-like" flow condition apparently results from a hydrodynamic instability in the laminar flow which it replaces. It appears that the agitation of the "bubble-like" flow results in much higher heat transfer rates than the preceding laminar flow.

Thus, if the average heat flux rate exceeds the value at which the laminar flow becomes unstable, but is still less than the value obtained by the existence of "bubble-like" flow, then the following sequence occurs: (1) First, the instability of the laminar flow develops into the "bubble-like" flow after the wire temperature has become high. With laminar flow the electrical heating is greater than the heat loss to the fluid. (2) The high heat transfer rate of the "bubble-like" flow reduces the wire temperature until the heat flux to the fluid is insufficient to support the "bubble-like" flow. (3) Laminar flow resumes and the wire heats up again until the cycle repeats itself.

It appears that the wire acts as a heat capacitor in an oscillation between the two heat transfer curves associated with the two different flow conditions, while the heat input remains essentially constant. Several equations can be written to help understand the characteristics of this process. Assume that the steady heat transfer rates for the laminar and "bubble-like" flow conditions are Q_1 and Q_2 , respectively. Let these be constant values averaged over the temperature range of the cycle. Let the heat input into the test wire, $I_1^2 R$, be expressed as Q_1 . The heat capacity, C_1 , of the wire

will be given by

$$C = \frac{cL\pi D^2}{4} \quad (1)$$

where c is the specific heat capacity of the wire material. An equation for the change of temperature of the wire can then be written as:

$$\frac{dT}{dt} = \frac{1}{C} (Q_2 - Q_1) > 0 \quad (2a)$$

when laminar flow exists, or as:

$$\frac{dT}{dt} = \frac{1}{C} (Q_1 - Q_2) < 0 \quad (2b)$$

when "bubble-like" flow exists, provided that $Q_2 > Q_1 > Q_1$

Let the maximum and minimum temperatures associated with the cycle at any given Q_i be denoted as T_m and T_l , respectively, and the difference between the two as ΔT . If the laminar part of the cycle exists for τ_1 seconds and the "bubble-like" flow for τ_2 seconds, then the total period of each complete cycle will be given by:

$$\tau = \tau_1 + \tau_2 \quad (3)$$

assuming that there are no delay times associated with the growth or collapse of the "bubble-like" flow condition.

Equations (2a) and (2b) can be integrated to obtain τ_1 and τ_2 :

$$\tau_1 = \frac{C\Delta T}{Q_2 - Q_1} \quad \tau_2 = \frac{C\Delta T}{Q_1 - Q_1} \quad (4)$$

Therefore,

$$\tau = C\Delta T \frac{Q_2 - Q_1}{(Q_2 - Q_1)(Q_2 - Q_1)} \quad (5)$$

and

$$\frac{\tau_2}{\tau_1} = \frac{Q_1 - Q_1}{Q_2 - Q_1} \quad (6)$$

If ΔT remains constant while Q_1 is varied, it would appear that the frequency would have a maximum when $Q_1 = \frac{(Q_1 + Q_2)}{2}$. In actuality, Figure 24 shows that the frequency of the oscillations continues to increase until "bubble-like" flow exists continuously. The implication is that ΔT decreases with increasing Q_1 .

The ratio of the two periods $\frac{\tau_2}{\tau_1}$ shows that, as Q_1 is increased, the flow spends an increasing proportion of the time in the "bubble-like" condition, as observed in the experiments.

Since the period of the oscillation is proportional to C , the frequency should be inversely proportional to the square of the wire diameter. Figure 24 tends to confirm this result, although it should be expected that the relationship between Q_1 and Q_2 as well as ΔT would change with the wire diameter.

Appendix H

EXPERIMENTAL DATA

TABLE 1. FREE CONVECTION HEAT TRANSFER DATA FOR A HORIZONTAL CYLINDER IN SUPERCRITICAL CARBON DIOXIDE AT 1500 psia AND 49.0°F (Nichrome Wire, 0.010-Inch Diameter)

I_1 (Amps)	q_2 (B/in. ² sec)	Test No. 98		Test No. 99		Flow Condition
		ΔV (Mv)	ΔT (°F)	ΔV (Mv)	ΔT (°F)	
0.52	0.0046	0.15	5.5	0.15	5.5	Laminar
1.00	0.0175	1.00	19.2	1.00	19.2	↓
1.50	0.0394	2.91	37.2	2.94	37.4	
1.75	0.0536	4.41	48.4	4.55	49.2	
2.00	0.070	7.03	67.5	7.35	69.1	
2.10	0.077	8.80	80	9.00	81	
2.20	0.085	10.6	93	10.7	93	
2.30	0.093	12.8	107	12.7	107	
2.40	0.101	15.0	120	15.4	122	
2.50	0.109	17.9	137	18.6	140	
2.60	0.118	21.2	157	20.9	156	
2.70	0.128	21.8*	155	21.7*	155	Oscil- lating
2.80	0.137	22.5*	154	22.6*	155	
2.90	0.147	24.3*	161	24.6*	162	
3.00	0.157	26.0*	166	26.2*	167	
3.10	0.168	27.7*	172	27.1*	170	
3.20	0.179	28.4*	170	28.0*	169	↓
3.30	0.190	29.6*	172	29.8*	173	
3.40	0.202	31.6*/27.6	178/156	30.6*/28.2	176/158	"Bubble- Like"
3.50	0.214	29.0	159	29.5	161	↓
3.60	0.227	29.8	159	29.8	159	
3.70	0.240	30.6	159	30.7	159	
3.80	0.253	31.6	160	31.7	160	
3.90	0.266	32.7	161	32.8	161	
4.00	0.280	35.5*	170	35.7*	171	
4.10	0.294	37.7	177	37.4	176	
4.20	0.308	41.4	189	41.5	190	
4.30	0.323	46.5	208	48.2	212	
4.40	0.338	50.6	221	50.8*	222	
4.50	0.354	54.7	233	54.5	233	
4.60	0.370	58.5	244	58.8	245	
4.70	0.386	61.5	251	62.5	253	
4.80	0.403	68*	272	66.0	268	
4.90	0.420	70.0	274	71.0	276	
5.00	0.437	74.6	286	74.5	286	

* Averaged reading

TABLE 2. FREE CONVECTION HEAT TRANSFER DATA FOR A HORIZONTAL CYLINDER IN SUPERCRITICAL CARBON DIOXIDE AT 1300 psia AND 49.0° F (Nichrome Wire, 0.010-Inch Diameter)

I_1 (Amps)	q_2 (B/in. ² sec)	Test No. 107		Test No. 110		Flow Condition	
		ΔV (Mv)	ΔT (°F)	ΔV (Mv)	ΔT (°F)		
0.52	0.0046	0.13	4.8	0.16	6.0	Laminar	
1.00	0.0175	0.97	18.6	1.00	19.2	↓	
1.50	0.0394	2.80	35.8	2.84	36.3		
1.75	0.0536	4.66	49.0	4.80	52.6		
2.00	0.070	8.20	79	7.92	76		
2.10	0.077	9.91	91	9.80	90		
2.20	0.085	12.0	105	11.8	103		
2.30	0.093	14.2	119	14.2	119		
2.40	0.101	17.9	143	17.0	136		
2.50	0.109	18.9/18.5*	145/142	18.8*	144		Oscil-
2.60	0.118	19.7*	145	19.3*	143		lating
2.70	0.128	21.4*/21.0	152/149	21.5*	153	↓	
2.80	0.137	23.0*	158	22.9*	157		
2.90	0.147	24.0*	159	24.0*	159		
3.00	0.157	25.1*	161	25.0*	160		
3.10	0.168	26.0*/23.3	161/144	25.9*/23.3	160/144		"Bubble-
3.20	0.179	24.5	147	24.5	147		Like"
3.30	0.190	25.3	147	26.3	153		↓
3.40	0.202	26.4	149	27.3	154		
3.50	0.214	30.3	166	30.3	166		
3.60	0.227	32.8	175	32.2	172		
3.70	0.240	35.5	184	35.3	183		
3.80	0.253	39.4	199	40.0	202		
3.90	0.266	43.8	216	43.0	212		
4.00	0.280	49.0	235	47.8	229		
4.10	0.294	54.1	253	53.5	251		
4.20	0.208	59.1	270	60.5	270		
4.30	0.323	63.0	281	64.0	286		
4.40	0.338	68.0 W	297	72.8 W	318		
4.50	0.354	74.5	318	75.1	320		
4.60	0.370	76.2	318	76.7	320		
4.70	0.386	78.8	322	78.5	321		
4.80	0.403	82.0	328	81.5	326		
4.90	0.420	86.0	337	85.5	335		
5.00	0.437	91.5	351	91.5	351		

* Averaged reading
W = whistle

TABLE 3. FREE CONVECTION HEAT TRANSFER DATA FOR A HORIZONTAL CYLINDER IN SUPERCRITICAL CARBON DIOXIDE AT 1200 psia AND 49.0°F (Nichrome Wire, 0.010-Inch Diameter)

I_1 (Amps)	q_2 (B/in. ² sec)	Test No. 108		Test No. 111		Flow Condition
		ΔV (Mv)	ΔT (°F)	ΔV (Mv)	ΔT (°F)	
0.52	0.0046	0.16	5.9	0.16	6.1	Laminar
1.00	0.0175	1.01	19.2	1.00	19.2	↓
1.50	0.0394	2.80	35.8	2.80	35.8	
1.75	0.0536	4.75	52.1	4.70	51.6	Oscil- lating
2.00	0.070	8.40	81	8.50	82	
2.10	0.077	10.4	95	10.5	96	↓
2.20	0.085	12.8	112	12.8	112	
2.30	0.093	15.3	128	15.6	130	"Bubble- Like"
2.40	0.101	17.7	142	17.5	140	
2.50	0.109	18.4*	141	18.1*	139	↓
2.60	0.118	19.8*	146	21.1*	156	
2.70	0.128	22.0*	156	22.2*	158	↓
2.80	0.137	23.0*	158	23.0*	158	
2.90	0.147	24.0*/21.5	159/142	24.0*/21.3	159/141	↓
3.00	0.157	22.6	145	22.7	145	
3.10	0.168	23.6	146	24.3	150	↓
3.20	0.179	27.0	162	26.8	161	
3.30	0.190	29.4	171	29.0	169	↓
3.40	0.202	31.8	180	31.6	178	
3.50	0.214	34.5	189	34.5	189	↓
3.60	0.227	38.0	203	37.9	202	
3.70	0.240	42.5	221	42.0	218	↓
3.80	0.253	47.2	238	46.7	236	
3.90	0.266	52.0	255	52.0	256	↓
4.00	0.280	57.5	276	57.5	276	
4.10	0.294	62.8	294	62.6	293	↓
4.20	0.308	68.4	313	68.3	312	
4.30	0.323	70.7	316	70.3	314	↓
4.40	0.338	73.5	321	75.0	327	
4.50	0.354	81.6	348	81.0	346	↓
4.60	0.370	88.0	367	85.0	355	
4.70	0.386	90.0	368	90.0	368	↓
4.80	0.403	94.0	376	93.0	372	
4.90	0.420	98.5	376	98.0	384	↓
5.00	0.437	105.0	386	103.0	396	

* Averaged measurement

TABLE 4. FREE CONVECTION HEAT TRANSFER DATA FOR A HORIZONTAL CYLINDER IN SUPERCRITICAL CARBON DIOXIDE AT 1100 psia AND 49.0°F (Nichrome Wire, 0.010-Inch Diameter)

I_1 (Amps)	q_2 (B/in. ² sec)	Test No. 104		Test No. 109		Flow Condition
		ΔV (Mv)	ΔT (°F)	ΔV (Mv)	ΔT (°F)	
0.52	0.0046	0.14	5.2	0.14	5.3	Laminar
1.00	0.0175	0.95	18.2	0.96	18.4	↓ Oscil- lating ↓ "Bubble- Like" ↓
1.50	0.0394	2.79	35.7	2.89	37.0	
1.75	0.0536	4.80	52.6	5.15	54.5	
2.00	0.070	9.15	88	9.25	89	
2.10	0.077	11.1	101	11.37	104	
2.20	0.085	14.0	122	14.1	123	
2.30	0.093	15.6	130	16.3	136	
2.40	0.101	16.5	132	17.2	138	
2.50	0.109	17.8*	137	18.3	141	
2.60	0.118	20.3*	150	19.0	140	
2.70	0.128	21.3*	151	22.5*	160	
2.80	0.137	21.3*	146	22.2*	152	
2.90	0.147	23.4	155	23.5	156	
3.00	0.157	26.5	170	26.1	167	
3.10	0.168	28.9	179	29.1	180	
3.20	0.179	31.6	190	31.3	188	
3.30	0.190	34.5	201	35.0	204	
3.40	0.202	37.5	212	38.7	218	
3.50	0.214	41.7	229	43.2	237	
3.60	0.227	45.8	244	46.5	248	
3.70	0.240	51.0	265	50.7	263	
3.80	0.253	54.6	276	55.3	279	
3.90	0.266	62.0	305	63.0	310	
4.00	0.280	65.0	312	65.8	316	
4.10	0.294	67.0	314	67.8	318	
4.20	0.308	73.5	336	73.7	337	
4.30	0.323	80.0	357	81.0	362	
4.40	0.338	89.0	388	89.0	388	
4.50	0.354	97.0	414	96.0	410	
4.60	0.370	102.0	426	102	426	
4.70	0.386	112.0	457	113*	462	

* Averaged measurement

TABLE 5. FREE CONVECTION HEAT TRANSFER DATA FOR A HORIZONTAL CYLINDER IN SUPERCRITICAL CARBON DIOXIDE AT 1500 psia AND 77.0°F (Nichrome Wire, 0.010-Inch Diameter)

I_1 (Amps)	q_2 (B/in. ² sec)	Test No. 89		Test No. 100		Flow Condition
		ΔV (Mv)	ΔT (°F)	ΔV (Mv)	ΔT (°F)	
0.52	0.0046	0.16	5.9	0.16	5.9	Laminar
1.00	0.0175	0.85	16.3	1.00	19.3	
1.50	0.0394	2.80	35.9	2.99	38.4	
1.75	0.0536	4.85	53.4	5.08	55.9	
2.00	0.070	8.56	82	8.58	83	
2.10	0.077	10.2	94	10.5	96	
2.20	0.085	13.3	116	12.5	109	
2.30	0.093	14.8	124	15.0	126	
2.40	0.101	16.8	135	16.6*	133	
2.50	0.109	17.7*	136	17.3*	133	Oscil- lating
2.60	0.118	18.6*	138	17.8	132	
2.70	0.128	20.4*	145	18.5	132	
2.80	0.137	22.3*	154	21.0*	144	
2.90	0.147	24.0*/20.2	160/134	22.5*	149	
3.00	0.157	25.9*/21.4	166/137	24.4*/20.9	157/134	"Bubble- Like"
3.10	0.168	26.8*/22.9	167/142	22.2	146	
3.20	0.179	23.6	142	22.9	138	
3.30	0.190	25.2	146	24.1	140	
3.40	0.202	26.3	149	28.3	160	
3.50	0.214	27.0	149	29.9	162	
3.60	0.227	29.0	155	30.7	164	
3.70	0.240	31.6	165	32.1	167	
3.80	0.253	35.1	178	35.8	181	
3.90	0.266	39.0 W	192	40.5	200	
4.00	0.280	41.5	200	44.8 W	216	
4.10	0.294	45.0	212	47.0	221	
4.20	0.308	48.0	220	50.6	232	
4.30	0.323	51.8	232	54.3	243	
4.40	0.338	55.5	243	58.5	256	
4.50	0.354	59.0	253	60.2*	258	
4.60	0.370	61.0	255	63.0	264	
4.70	0.386	65.5	269	70.5	289	
4.80	0.403	71.0	284	75.0	301	
4.90	0.420	76.5	300	77.5	305	
5.00	0.437	80.5	310	81.5	319	

* Averaged measurement

W = whistle

TABLE 6. FREE CONVECTION HEAT TRANSFER DATA FOR A HORIZONTAL CYLINDER IN SUPERCRITICAL CARBON DIOXIDE AT 1300 psia AND 77.0° F (Nichrome Wire, 0.010-Inch Diameter)

I_1 (Amps)	q_2 (B/in. ² sec)	Test No. 90		Test No. 106		Flow Condition
		ΔV (Mv)	ΔT (°F)	ΔV (Mv)	ΔT (°F)	
0.52	0.0046	0.15	5.6	0.15	5.5	Laminar
1.00	0.0175	0.88	16.9	0.87	16.7	↓
1.50	0.0394	2.85	36.5	2.97	38.1	
1.75	0.0536	5.30	58	5.35	58.8	Oscil- lating
2.00	0.070	9.35	90	9.95	96	
2.10	0.077	11.35	104	11.6	106	↓
2.20	0.085	19.2	124	13.6*	119	
2.30	0.093	14.9*	125	14.3*	120	"Bubble- Like"
2.40	0.101	15.7*	126	15.0	120	
2.50	0.109	17.7*/16.7	136/129	17.0*	131	↓
2.60	0.118	18.4*	136	18.3*	135	
2.70	0.128	21.1*	150	19.3*	138	"Bubble- Like"
2.80	0.137	22.5*/19.1	155/135	21.3*/18.2	146/125	
2.90	0.147	23.6*/20.1	157/133	19.1	127	↓
3.00	0.157	21.1	135	21.4	137	
3.10	0.168	22.4	139	23.5	146	↓
3.20	0.179	23.1	139	25.5	153	
3.30	0.190	27.0	157	28.0	163	↓
3.40	0.202	30.5	173	30.0	170	
3.50	0.214	33.0	182	33.0	182	↓
3.60	0.227	37.5	201	36.5	195	
3.70	0.240	40.0	208	40.2	209	↓
3.80	0.253	43.8	221	44.3	224	
3.90	0.266	49.2	243	49.5	244	↓
4.00	0.280	55.0	265	52.5	253	
4.10	0.294	57.0	267	59.0	277	↓
4.20	0.308	63.0	289	63.1	289	
4.30	0.323	64.7	289	64.5	289	↓
4.40	0.338	66.3	290	66.5	291	
4.50	0.354	68.7	294	69.9	299	↓
4.60	0.370	72.0	301	73.8	309	
4.70	0.386	76.5	313	78.2	320	↓
4.80	0.403	82.0	329	84.1	337	
4.90	0.420	87.5	344	90.2	354	↓
5.00	0.437	95.2	367	97.5	375	

* Averaged measurement

TABLE 7. FREE CONVECTION HEAT TRANSFER DATA FOR A HORIZONTAL CYLINDER IN SUPERCRITICAL CARBON DIOXIDE AT 1200 psia AND 77.0 °F (Nichrome Wire, 0.010-Inch Diameter)

I_1 (Amps)	q_2 (B/in. ² sec)	Test No. 91		Test No. 101		Flow Condition
		ΔV (Mv)	ΔT (°F)	ΔV (Mv)	ΔT (°F)	
0.52	0.0046	0.15	5.6	0.14	5.2	Laminar
1.00	0.0175	0.80	15.4	0.75	14.4	
1.50	0.0394	3.05	39.2	3.05	39.1	
1.75	0.0536	5.72	63.1	5.72	63	
2.00	0.070	10.1	97	10.5	101	
2.10	0.077	12.5	115	12.6	116	
2.20	0.085	13.9	122	13.5*	118	
2.30	0.093	14.7*	123	14.3	120	
2.40	0.101	16.3*/15.5	131/124	16.3*	131	Oscil- lating
2.50	0.109	18.3*	141	17.6*	136	
2.60	0.118	20.0*	148	18.7*	138	
2.70	0.128	21.2*	151	20.1*/17.1	143/122	"Bubble- Like"
2.80	0.137	20.1	138	18.3	126	
2.90	0.147	22.4	149	20.3	135	
3.00	0.157	23.9	153	22.3	143	
3.10	0.168	26.5	165	24.0	149	
3.20	0.179	28.1	169	25.8	155	
3.30	0.190	30.2	176	28.2	164	
3.40	0.202	33.1	187	33.5	190	
3.50	0.214	38.0	209	37.2	204	
3.60	0.227	41.7	223	41.0	219	
3.70	0.240	45.0	234	45.3	236	
3.80	0.253	50.5	256	49.4	250	
3.90	0.266	55.5	274	51.4	254	
4.00	0.280	60.0	289	59.7	287	
4.10	0.294	61.3	288	61.7	290	
4.20	0.308	63.5	291	63.4	291	
4.30	0.323	67.5	302	67.4*	302	
4.40	0.338	74.0	324	74.5	326	
4.50	0.354	77.0	329	79.0	338	
4.60	0.370	80.0	335	81.6	341	
4.70	0.386	87.0	356	86.0	352	
4.80	0.403	93.0	373	92.6	371	
4.90	0.420	101.0	397	99.5	391	
5.00	0.437	110.0	424	110.0	424	

* Averaged measurement

TABLE 8. FREE CONVECTION HEAT TRANSFER DATA FOR A HORIZONTAL CYLINDER IN SUPERCRITICAL CARBON DIOXIDE AT 1100 psia AND 77.0°F (Nichrome Wire, 0.010-Inch Diameter)

I_1 (Amps)	q_2 (B/in. ² sec)	Test No. 92		Test No. 105		Flow Condition
		ΔV (Mv)	ΔT (°F)	ΔV (Mv)	ΔT (°F)	
0.52	0.0046	0.14	5.1	0.135	5.0	Laminar
1.00	0.0175	0.73	14.1	0.72	13.9	↓
1.50	0.0394	3.37	43.3	3.30	42.4	
1.75	0.0536	6.50	71.5	6.37	70.1	Oscil- lating
2.00	0.070	11.3	109	11.0	106	
2.10	0.077	12.9*	118	11.8	108	↓
2.20	0.085	13.5*	118	13.5	118	
2.30	0.093	15.2*/14.6	127/122	13.5/15.1*	113/126	"Bubble- Like"
2.40	0.101	17.4*	140	16.2*	130	
2.50	0.109	18.8*	145	16.5*	127	↓
2.60	0.118	19.4*/17.2	144/127	17.8	132	
2.70	0.128	21.2	150	20.0	143	↓
2.80	0.137	23.9	164	21.7	149	
2.90	0.147	25.2	167	23.5	157	↓
3.00	0.157	27.6	177	25.6	164	
3.10	0.168	29.3	182	27.3	170	↓
3.20	0.179	31.7	191	32.7	197	
3.30	0.190	36.1	211	34.6	202	↓
3.40	0.202	39.8	225	37.3	211	
3.50	0.214	43.3	238	42.4	233	↓
3.60	0.227	48.0	257	46.0	246	
3.70	0.240	53.0	276	53.0	276	↓
3.80	0.253	57.0	289	55.1	279	
3.90	0.266	58.0	286	57.3	283	↓
4.00	0.280	62.1	299	63.0	303	
4.10	0.294	68.5	322	69.8	328	↓
4.20	0.308	76.0	348	75.0	344	
4.30	0.323	82.0	368	79.5	356	↓
4.40	0.338	85.0	372	82.5	361	
4.50	0.354	91.0	389	88.5	379	↓
4.60	0.370	95.0	398	92.5	387	
4.70	0.386	101.0	414	104.0	426	↓
4.80	0.403	110.0*	441	107.0*	429	
4.90	0.420	116.0*	456			↓
5.00	0.437	117.0	450			

* Averaged measurement

TABLE 9. FREE CONVECTION HEAT TRANSFER DATA FOR A HORIZONTAL CYLINDER IN SUPERCRITICAL CARBON DIOXIDE AT 1500 psia AND 107.0°F (Nichrome Wire, 0.010-Inch Diameter)

I_1 (Amps)	q_2 (B/in. ² sec)	Test No. 86		Test No. 97		Flow Condition
		ΔV (Mv)	ΔT (°F)	ΔV (Mv)	ΔT (°F)	
0.52	0.0046	0.14	5.2	0.14	5.2	Laminar
1.00	0.0175	0.95	18.4	0.97	18.8	↓
1.50	0.0394	3.76	48.5	4.00	51.8	
1.75	0.0536	6.85	75	7.15	79.3	Oscil-
2.00	0.070	11.6	113	11.0*	107	lating
2.10	0.077	12.2*	113	11.4*	105	↓
2.20	0.085	13.0*	115	12.1	107	
2.30	0.093	13.7	116	13.1	110	"Bubble-
2.40	0.101	15.6*	126	13.6	110	Like"
2.50	0.109	17.4*/15.0	135/116	14.3	111	↓
2.60	0.118	18.8*/16.0	140/119	16.6	124	
2.70	0.128	17.2	124	16.8	121	↓
2.80	0.137	18.4	127	20.1	139	
2.90	0.147	20.5	137	23.0	154	↓
3.00	0.157	23.4	151	24.8	160	
3.10	0.168	24.4	153	26.3	165	↓
3.20	0.179	26.1	158	28.0	170	
3.30	0.190	27.6	163	30.2	178	↓
3.40	0.202	29.6	169	32.1	183	
3.50	0.214	32.0	177	36.2 W	201	↓
3.60	0.227	34.8	188	38.2	206	
3.70	0.240	38.5 W	202	41.5	218	↓
3.80	0.253	40.8	209	44.0	225	
3.90	0.266	45.1	225	46.0	229	↓
4.00	0.280	48.0	234	49.5	240	
4.10	0.294	50.5	240	53.5	253	↓
4.20	0.308	53.2	246	58.0	268	
4.30	0.323	57.2	259	61.5	277	↓
4.40	0.338	62.3	276	64.5	284	
4.50	0.354	66.1	287	68.0	243	↓
4.60	0.370			72.1	304	
4.70	0.386			76.7	317	↓
4.80	0.403			82.0	331	
4.90	0.420			88.0	348	↓
5.00	0.437			73.0	361	

W = whistle
* Averaged measurement

TABLE 10. FREE CONVECTION HEAT TRANSFER DATA FOR A HORIZONTAL CYLINDER IN SUPERCRITICAL CARBON DIOXIDE AT 1300 psia AND 107.0 °F (Nichrome Wire, 0.010-Inch Diameter)

I_1 (Amps)	q_2 (B/in. ² sec)	Test No. 95		Test No. 96		Flow Condition
		ΔV (Mv)	ΔT (°F)	ΔV (Mv)	ΔT (°F)	
0.52	0.0046	0.17	6.3	0.16	6.0	Laminar
1.00	0.0175	1.50	29.1	1.53	29.7	↓
1.50	0.0394	6.30	82	6.70	87	
1.75	0.0536	8.8*	98	8.90*	99	
2.00	0.070	11.2*	109	11.8*	114	Oscil.
2.10	0.077	11.9	110	12.2	113	↓
2.20	0.085	13.4	118	14.0	123	"Bubble- Like"
2.30	0.093	17.8	150	17.3	146	
2.40	0.101	21.0	170	20.1	162	
2.50	0.109	24.5	190	24.0	186	
2.60	0.118	27.0	201	26.0	194	
2.70	0.128	29.1	209	29.3	210	
2.80	0.137	35.0	243	31.2	216	
2.90	0.147	39.0	261	38.8	260	
3.00	0.157	42.3	274	43.0	278	
3.10	0.168	44.8*W	280	45.0* W	281	
3.20	0.179	45.0*	273	44.8*	272	
3.30	0.190	46.7	275	46.0	270	
3.40	0.202	49.5	282	49.0	280	
3.50	0.214	53.5	297	52.0	288	
3.60	0.227	58.0	313	57.5	310	
3.70	0.240	61.8	324	61.5	322	
3.80	0.253	66.5	340	66.2	338	
3.90	0.266	68.6	341	69.0	343	
4.00	0.280	70.7	343	71.0	344	
4.10	0.294	74.0	350	-	-	
4.20	0.308	70.0	323	75.7	350	
4.30	0.323	70.3	344	77.2	348	
4.40	0.338	78.5	345	81.2	358	
4.50	0.354	85.0*	366	88.0	379	
4.60	0.370	92.4	390	95.0	401	
4.70	0.386	99.0	409			↓

W = whistle
* Averaged measurement

TABLE 11. FREE CONVECTION HEAT TRANSFER DATA FOR A HORIZONTAL CYLINDER IN SUPERCRITICAL CARBON DIOXIDE AT 1200 psia AND 107.0° F (Nichrome Wire, 0.010-Inch Diameter)

I_1 (Amps)	q_2 (B/in. ² sec)	Test No. 94		Test No. 102		Flow Condition
		ΔV (Mv)	ΔT (°F)	ΔV (Mv)	ΔT (°F)	
0.52	0.0046	0.30	11.2	0.31	11.6	Laminar
1.00	0.0175	2.40	46.6	2.44	47.3	↓
1.50	0.0394	7.45	96	8.00*	109	"Bubble- Like"
1.75	0.0536	11.0*	122	10.2	113	↓
2.00	0.070	13.7	133	15.0	146	↓
2.10	0.077	16.1	149	17.3	160	↓
2.20	0.085	19.7	174	20.4	180	↓
2.30	0.093	22.7	191	23.7	200	↓
2.40	0.101	26.4	213	27.0	218	↓
2.50	0.109	30.1	234	30.9	240	↓
2.60	0.118	34.5*	257	35.0	261	↓
2.70	0.128	37.1	267	37.5	269	↓
2.80	0.137	39.3	272	39.6	274	↓
2.90	0.147	40.7	272	41.5	278	↓
3.00	0.157	42.9	277	43.3	280	↓
3.10	0.168	46.0	287	47.3	296	↓
3.20	0.179	51.5	312	52.3	317	↓
3.30	0.190	56.2	330	57.0	335	↓
3.40	0.202	61.0	348	63.0	359	↓
3.50	0.214	67.0	371	68.4	379	↓
3.60	0.227	72.0	388	73.2	394	↓
3.70	0.240	79.5	417	79.0	414	↓

* Averaged measurement

TABLE 12. FREE CONVECTION HEAT TRANSFER DATA FOR A HORIZONTAL CYLINDER IN SUPERCRITICAL CARBON DIOXIDE AT 1100 psia AND 107.0°F (Nichrome Wire, 0.010-Inch Diameter)

I_1 (Amps)	q_2 (B/in. ² sec)	Test No. 93		Test No. 103		Flow Condition
		ΔV (Mv)	ΔT (°F)	ΔV (Mv)	ΔT (°F)	
0.52	0.0046	0.41	15.3	0.39	14.6	Laminar
1.00	0.0175	3.11	60.3	3.17	61.5	↓
1.50	0.0394	9.8	127	9.8	127	"Bubble- Like"
1.75	0.0536	12.4	138	12.9	143	
2.00	0.070	18.4	178	18.4	178	
2.10	0.077	21.0	194	21.2	196	
2.20	0.085	23.5	207	24.5	216	
2.30	0.093	28.1	237	28.3	239	
2.40	0.101	31.9	258	32.2	260	
2.50	0.109	35.6	276	36.7	285	
2.60	0.118	39.0	291	39.6	295	
2.70	0.128	41.8	301	42.0	302	
2.80	0.137	44.8	310	44.9	311	
2.90	0.147	46.9	314	47.9	320	
3.00	0.157	50.6	327	51.9	336	
3.10	0.168	55.0	344	55.5	347	
3.20	0.179	60.2	365	60.7	369	
3.30	0.190	64.6	380	66.0	388	
3.40	0.202	70.3	401	71.8	410	
3.50	0.214	76.5	424	76.0	421	↓

TABLE 13. FREE CONVECTION HEAT TRANSFER DATA FOR A HORIZONTAL CYLINDER IN SUPERCRITICAL CARBON DIOXIDE AT 1500 psia AND 137.0° F (Nichrome Wire, 0.010-Inch Diameter)

I_1 (Amps)	q_2 (B/in. ² sec)	Test No. 112		Test No. 116		Flow Condition
		ΔV (Mv)	ΔT (°F)	ΔV (Mv)	ΔT (°F)	
0.52	0.0046	0.31	12.0	0.32	12.4	Laminar
1.00	0.0175	2.30	64.0	2.35	45.6	↓
1.50	0.0394	7.70	100	7.8*	101	"Bubble-
1.75	0.0536	9.85	109	10.2	113	Like"
2.00	0.070	14.0	136	14.7	143	↓
2.10	0.077	16.3	151	16.7	154	↓
2.20	0.085	18.7	165	19.0	168	↓
2.30	0.093	21.4	180	22.3	188	↓
2.40	0.101	24.7	200	25.4	205	↓
2.50	0.109	28.6	222	28.9	224	↓
2.60	0.118	32.0	239	32.0	239	↓
2.70	0.128	35.2	253	36.0	259	↓
2.80	0.137	37.2	258	38.8	269	↓
2.90	0.147	40.3	270	41.1	275	↓
3.00	0.157	42.3	274	44.0	281	↓
3.10	0.168	44.4	278	46.5	291	↓
3.20	0.179	47.8	290	48.5	294	↓
3.30	0.190	51.5	303	52.5	309	↓
3.40	0.202	54.5	311	56.7	324	↓
3.50	0.214	61.0	338	62.1	344	↓
3.60	0.227	66.0	356	65.1	351	↓
3.70	0.240	72.0	378	73.1	383	↓
3.80	0.253	77.0	393	76.0	388	↓
3.90	0.266	73.0* W	363	76.7 W	382	↓
4.00	0.280	73.5 ↓	357	77.8 ↓	377	↓
4.10	0.294	76.8 ↓	363	80.6 ↓	381	↓
4.20	0.308	82.5 ↓	381	85.0 ↓	393	↓
4.30	0.323	88.0 ↓	397			↓

* Averaged measurement

W = whistle

TABLE 14. FREE CONVECTION HEAT TRANSFER DATA FOR A HORIZONTAL CYLINDER IN SUPERCRITICAL CARBON DIOXIDE AT 1300 psia AND 137.0° F (Nichrome Wire, 0.010-Inch Diameter)

I_1 (Amps)	q_2 (B/in. ² sec)	Test No. 113		Test No. 115		Flow Condition
		ΔV (Mv)	ΔT (°F)	ΔV (Mv)	ΔT (°F)	
0.52	0.0046	0.42	16.3	0.42	16.3	Laminar
1.00	0.0175	3.31	64.2	3.25	63.1	↓
1.50	0.0394	9.6	124	9.7	125	"Bubble- Like"
1.75	0.0536	13.0	144	13.3	147	↓
2.00	0.070	19.0	184	19.3	187	↓
2.10	0.077	22.5	208	21.7	200	↓
2.20	0.085	25.0	220	25.2	222	↓
2.30	0.093	28.6	241	28.7	242	↓
2.40	0.101	32.5	263	32.1	260	↓
2.50	0.109	36.2	281	36.1	280	↓
2.60	0.118	39.0	291	39.2	293	↓
2.70	0.128	41.8	301	42.7	307	↓
2.80	0.137	45.1	312	46.1	320	↓
2.90	0.147	48.3	323	48.9	327	↓
3.00	0.157	51.7	334	52.7	341	↓
3.10	0.168	55.2	345	55.5	347	↓
3.20	0.179	59.0	358	59.8	363	↓
3.30	0.190	64.7	380	64.5	379	↓
3.40	0.202	70.0	399	70.0	399	↓

TABLE 15. FREE CONVECTION HEAT TRANSFER DATA FOR A HORIZONTAL CYLINDER IN SUPERCRITICAL CARBON DIOXIDE AT 1200 psia AND 137.0° F (Nichrome Wire, 0.010-Inch Diameter)

I_1 (Amps)	q_2 (B/in. ² sec)	Test No. 114		Test No. 117		Flow Condition
		ΔV (Mv)	ΔT (°F)	ΔV (Mv)	ΔT (°F)	
0.52	0.0046	0.48	18.6	0.52	20.2	Laminar
1.00	0.0175	4.1	79.5	4.18	81.1	↓
1.50	0.0394	10.5	136	11.0	142	"Bubble- Like"
1.75	0.0536	15.2	168	15.3	170	↓
2.00	0.070	22.0	213	22.0	213	↓
2.10	0.077	25.0	217	25.2	233	↓
2.20	0.085	28.2	249	29.1	257	↓
2.30	0.093	32.5	274	32.6	275	↓
2.40	0.101	36.2	293	36.5	295	↓
2.50	0.109	39.8	309	40.7	316	↓
2.60	0.118	43.8	327	45.0	336	↓
2.70	0.128	47.5	341	47.9	344	↓
2.80	0.137	50.6	351	51.5	357	↓
2.90	0.147	54.1	362	54.3	363	↓
3.00	0.157	57.5	377	58.0	375	↓
3.10	0.168	60.8	380	61.0	382	↓

TABLE 16. FILM BOILING HEAT TRANSFER DATA FOR A HORIZONTAL CYLINDER
 IN SUBCRITICAL CARBON DIOXIDE AT 1000 psia, 49.0° AND 77.0° F
 (Nichrome Wire, 0.010-Inch Diameter)

I_1 (Amps)	q_2 (B/in. ² sec)	Test No. 119, 77.0° F		Test No. 120, 49.0° F		Flow Condition
		ΔV (Mv)	ΔT (°F)	ΔV (Mv)	ΔT (°F)	
2.00	0.070	11.6	109			Film Boiling 
2.10	0.077	12.8	117	12.1	111	
2.20	0.085	15.0	131	15.3	134	
2.30	0.093	17.0	142	16.9	141	
2.40	0.101	20.2	162	18.7	150	
2.50	0.109	22.0	169	21.0	161	
2.60	0.118	24.1	178	24.2	179	
2.70	0.128	26.4	188	27.2	193	
2.80	0.137	29.0	199	28.7	197	
2.90	0.147	32.3	214	31.5	208	
3.00	0.157	36.2	232	34.0	218	
3.10	0.168	40.0	248	37.4	232	
3.20	0.179	49.0	294	41.2	247	
3.30	0.190	51.9	302	45.0	262	
3.40	0.202	55.4	313	50.0	282	
3.50	0.214	60.2	330	55.1	302	
3.60	0.227	65.5	350	58.5	312	
3.70	0.240	71.7	372	60.3W	313	
3.80	0.253	77.0	389	71.8	362	
3.90	0.266	84.5	416	78.0	384	
4.00	0.280	9.10	437	85.4	410	

W = whistle

TABLE 17. FREE CONVECTION HEAT TRANSFER DATA FOR A VERTICAL CYLINDER IN SUPERCRITICAL CARBON DIOXIDE AT 1200 psia AND 77.0° F (Nichrome Wire, 2.15-Inch Height)

I_1 (Amps)	q_2 (B/in. ² sec)	Test No. 121		Test No. 122		Flow Condition
		ΔV (Mv)	ΔT (°F)	ΔV (Mv)	ΔT (°F)	
0.52	0.0046	0.15	5.8	0.19	7.2	
1.00	0.0175	1.00	19.3	1.28	25	
1.50	0.0394	3.80	49	4.2*	54	
1.75	0.0536	6.60	73	7.3	80	
2.00	0.1070	10.80	104	10.4	100	
2.10	0.077	11.4	104	10.7	98	
2.20	0.085	12.9	109	11.9	104	
2.30	0.093	13.5	113	12.5	105	
2.40	0.101	14.3*	115	13.2	106	
2.50	0.109	16.8*	129	13.8	107	
2.60	0.118	17.6*	130	14.5	108	
2.70	0.128	18.1	131	17.3	124	
2.80	0.137	20.2	139	19.7	134	
2.90	0.147	22.6	150	21.5	143	
3.00	0.157	25.0	158	24.8	160	
3.10	0.168	27.0	168	26.0	161	
3.20	0.179	30.0	181	27.5	166	
3.30	0.190	33.0	193	29.5	172	
3.40	0.202	35.0	198	32.4	184	
3.50	0.214	38.7	213	35.8	197	
3.60	0.227	42.3	228	39.1	210	
3.70	0.240	47.0	245	43.8	228	
3.80	0.253	53.5	272	48.4	246	
3.90	0.266	55.7	276	50.7	251	
4.00	0.280	59.0	285	54.4	262	
4.10	0.294	63.5	299	58.5	276	
4.20	0.308	68.0	312	63.5	291	
4.30	0.323			67.0	300	

* Averaged reading

TABLE 18. FREE CONVECTION HEAT TRANSFER DATA FOR A HORIZONTAL STRIP IN SUPERCRITICAL CARBON DIOXIDE AT 1200 psia AND 77.0°F (Chromax Strip, 0.125-Inch Width)

I_1 (Amps)	q_2 (B/in. ² sec)	Test No. 127		ΔV (Mv)	ΔT (°F)	Flow Condition
		ΔV (Mv)	ΔT (°F)			
1.00	0.0015	0.215	2.5			
2.00	0.0060	2.00	11.4			
2.60	0.0101	4.11	17.9			
3.00	0.0134	6.25	23.8			
3.40	0.0172	9.35	32.5			
3.80	0.0215	14.1	42.3			
4.20	0.0263	17.2	46.8			
4.60	0.0316	27.5	68			
5.00	0.0373	41.5	95			
5.40	0.0436	60.0	127			
5.80	0.0503	90	177			
6.20	0.0574	111	204			
6.60	0.0650	132	228			
7.00	0.0731	158	258			
7.40	0.0820	190	293			
7.80	0.091	220	322			
8.20	0.101	260	362			
8.60	0.110	290	385			
9.00	0.121	350	444			
9.40	0.132	400	486			
9.80	0.143					
10.20	0.155					

TABLE 19. FREE CONVECTION HEAT TRANSFER DATA FOR A SHORT VERTICAL WALL IN SUPERCRITICAL CARBON DIOXIDE AT 1200 psia AND 77.0°F (Chromax Strip, 0.125-Inch Height)

I_1 (Amps)	q_2 (B/in. ² sec)	Test No. 124		Test No. 125		Flow Condition
		ΔV (Mv)	ΔT (°F)	ΔV (Mv)	ΔT (°F)	
1.00	0.0015	0.33	3.8	0.37	4.2	Laminar
2.00	0.0060	2.22	12.7	2.07	11.8	↓ Trans- ition ↓
2.60	0.0101	3.81	16.6	3.61	15.8	
3.00	0.0134	5.65	21.4	5.29	20.1	
3.40	0.0172	8.62	28.9	7.65	25.6	
3.80	0.0215	12.1	36.3	11.7	35.1	
4.20	0.0263	17.6	47.8	17.1	46.4	
4.60	0.0316	26.5	66	25.1	62	
5.00	0.0373	38.5	88	36.3	83	
5.40	0.0436	53.2	112	50.0	105	
5.80	0.0503	71.0	139	68.7	118	
6.20	0.0574	93.1	171	90.5	146	
6.60	0.0650	117	202	118	204	
7.00	0.0731	148	242	139	226	
7.40	0.0820	173	267	170	262	
7.80	0.091	202	295	204	298	
8.20	0.101	238	331	231	322	
8.60	0.110	271	360	267	354	
9.00	0.121	310	393	306	388	
9.40	0.132	345	419	330	400	
9.80	0.143	375	436	370	431	
10.20	0.155	420	470	425	475	